Mechanisms of neuronal degeneration and clearance: from caspases to chemokines

Jennifer Dana Sokolowski
Charlottesville, Virginia

B.A. Neuroscience, University of Virginia, 2007

A Dissertation presented to the Graduate Faculty
of the University of Virginia in Candidacy for the Degree of
Doctor of Philosophy

Graduate Program in Neuroscience

University of Virginia
December, 2013

Abstract

Neuronal death and axon degeneration occur during brain development, during physiological turnover of neurons, and after injury. Degeneration is not a passive phenomenon, but an ordered, active process. Apoptosis, or programmed cell death, leads to activation of proteolytic enzymes known as caspases which are responsible for degrading proteins and preparing the apoptotic cell for clearance. Degeneration is not a passive phenomenon, but an ordered, active process. Apoptosis, or programmed cell death, leads to activation of proteolytic enzymes known as caspases which are responsible for degrading proteins and preparing the apoptotic cell for clearance. We studied the features of axon degeneration and confirmed that apoptotic machinery is involved. We detected caspase-mediated cytoskeletal degradation a) *in vitro*, in neuronal cultures induced to undergo axonal degeneration via nerve growth factor deprivation, b) *in vivo*, after alcohol-induced apoptosis as well as during developmental pruning and physiological turnover of neurons, and c) in degenerating neurites in human hypoxic-ischemic injury. In addition to examining degeneration, we also studied mechanisms involved in clearance. We showed that the chemokine fractalkine is released after alcohol-induced apoptosis and that fractalkine modulates the recruitment of microglia to promote clearance of apoptotic cells. In mice lacking fractalkine or its receptor, CX3CR1, injury leads to increased apoptotic debris and altered cytokine production. We also studied an engulfment receptor, Brain-specific angiogenesis inhibitor-1 (BAI1), to determine whether it plays a role in clearance in the brain. Immunolocalization data and analysis of the BAI1-deficient mouse suggested that while it may subserve astrocytic engulfment, it is unlikely to play a critical role in microglial engulfment. We found BAI1 was predominantly neuronal and localized to neuropil, suggesting a synaptic function, and we found no evidence of a defect in clearance in the BAI1-knockout mouse after alcohol-induced apoptosis. Further work should aim to identify receptors required for glial engulfment during apoptotic cell clearance in the brain.

Acknowledgements

Many people contributed to my success and I want to thank them…

My mentor, Dr. Jim Mandell, and lab mate, Dan Heffron, for creating a great work environment and providing advice and direction as well their ears. The Ravichandran lab members, for providing feedback and making me feel welcome at their lab meetings. My co-mentor Kodi Ravichandran, for his generosity and example. My committee, Kodi Ravichandran, Jonathan Kipnis, Peter Brunjes, Alev Erisir, Vesna Jevtovic-Todorovic, for their time and counsel. Undergraduate students, Suzanne Nobles, Kimberly Monks, Kelly Voltz, Ana Tucker, Usnish Majumdar, and especially Samantha Hale, Aleks Janjic, and Chloe Chabanon-Hicks for their contributions to the projects in the lab. Nicole Brimer for her technical advice and cheer. Kendra Simpson, for her camaraderie. Dr. Jaya Panicker, for her kindness. My MSTP classmates and their spouses, Ali and Kaitlyn Dhanaliwala, Aaron Fond and Elizabeth Molacek, Jeremy and Elise Rubinstein, Jamie Walsh and Claudia Han, Elizabeth Ames and Josh Meisner, and Dan Matson, for the sense of solidarity and good times. My parents, Jerry and Eileen Eudy, for getting me here and for their ongoing support throughout. My in-laws, Frank and Rosanne Sokolowski, for their eagerness to help and step in when needed. My husband Paul, for his patience, moral support, and being a great Papa and partner. My daughter, Avery, for smiling and brightening every day.

I would also like to acknowledge people and labs for their assistance and contributions during the course of this work…
The Roth lab (University of Alabama) supplied tissue from ethanol-treated BAX, PUMA and p53 knockouts. The LeBlanc lab (McGill University) supplied the TubulinΔCsp6 antibody and recombinant caspases. Hannelore Asmussen from the Horowitz lab (University of Virginia) provided primary cortical neuron cultures. Kanchana Gamage from the Deppmann lab (University of Virginia) prepared sympathetic neuron cultures. The Ravichandran lab (University of Virginia): Claudia Han performed in vitro phagocytosis assays, Daeho Park supplied stably-transfected HA-BAI1 LR73 cells, Chang Sup Lee generated and provided BAI1 knockout mice.

Contents

INTRODUCTION TO CELL DEATH AND CLEARANCE IN THE BRAIN

Cell Death in the Nervous System

Cell death in the nervous system occurs in a variety of scenarios, and there is much to learn about how neurons degenerate and are cleared from the CNS. Neuronal death occurs in contexts ranging from stroke and injury, to cancer, neurodegeneration and development (Madden, Cotter 2008), as well as during normal homeostasis.

Apoptosis is one form of programmed cell death. In general, debris from apoptotic cells must be cleared a) to prevent inflammation, as material present in dead or dying cells has the potential to evoke autoimmunity and inflammatory cascades that can create damage to tissue (Lleo, Selmi et al. 2008), and b) to make room for the incoming replacement neurons (Mouret, Lepousez et al. 2009). However, how the brain clears apoptotic cells and their different compartments is largely unknown.

The apoptotic cascade and neuronal degeneration

The cascades of events that occur during apoptosis are well described for non-neural cells. There are two main pathways that can lead to apoptosis. First, the intrinsic pathway initiates via mitochondrial-dependent processes whereby mitochondrial permeabilization leads to cytochrome c release and subsequent formation of a complex known as the apoptosome, which leads to caspase activation. In contrast, the extrinsic pathway is activated via ligand-receptor interactions and downstream signaling that leads to formation of the death-inducing signaling complex. Ultimately, both converge on activation of caspases. Caspase activation is a central feature of apoptosis and caspases are the main executioner enzymes responsible for mediating the DNA fragmentation, protein degradation, and blebbing that occurs (Earnshaw, Martins et al. 1999, Coleman, Sahai et al. 2001). As a cell undergoes apoptosis, biochemical reactions occur that allow the cell to process its contents and prepare to be 'eaten' by surrounding cells (Kinchen, Ravichandran 2007). As far as we know, similar processes and signals occur during degeneration of apoptotic neuronal bodies (Olney, Tenkova et al. 2002); however, we do not know whether axons and dendrites undergo 'apoptosis-like' cascades of events, and whether they undergo specific changes that allow them to be eaten by surrounding cells. In particular, whether the apoptotic pathways and caspases are involved in axon degeneration has been controversial and is an area requiring more research (Finn, Weil et al. 2000, Simon, Weimer et al. 2012). Until our studies, there has been a paucity of markers available that are able to highlight degenerating axons.

Cell death during development

Neuronal apoptosis and pruning occur as elaborately orchestrated processes during development of the nervous system. During development, there is an overproliferation of neurons and it is estimated that as many as 70% of neurons die (Blaschke, Staley et al. 1996). This extensive cell death is necessary to remove superfluous neurons; wiring the brain is an exquisite process and not all neurons end up at the right place at the right time. The nervous system eliminates aberrant cells and connections in order to mold itself into a working network, and this is essential for proper development and function (Vanderhaeghen, Cheng 2010). Defects in apoptotic pathways can lead to aberrations in brain development. For example, caspase-3 and caspase-9 deficient mice have neuronal hyperplasia (Degterev, Boyce et al. 2003). In addition, animals deficient in caspase-3 or caspase-6 display delayed retinocollicular pruning (Simon, Weimer et al. 2012). It is only recently that these genetic models have been used to show that caspases are involved in pruning, and not many studies actually examine the degenerating neuronal processes during pruning, largely due to the lack of good markers to highlight degenerating neurons and their neurites. Our studies characterize new markers that will be useful for studying pruning during development.

Models to study degeneration and clearance

Studies in animal models have shown that the balance between expression of pro- and anti-apoptotic factors changes as the brain develops (Harris, Hardie et al. 2005). During embryonic and early postnatal ages, expression of pro-apoptotic factors is at a peak, which helps explain why immature neurons are more susceptible to death. As

neurons wire into circuits, they are able to persist if they acquire sufficient pro-survival signals. One such target-derived growth factor is nerve growth factor (NGF). We and other researchers have used NGF-deprivation as an *in vitro* assay to induce apoptosis and as a model that parallels apoptosis that occurs during development (Deshmukh, Johnson 1997). An advantage of this *in vitro* model is that it provides a simplified system with which to study apoptosis and perform manipulations that are not possible *in vivo*.

While *in vitro* studies are a useful tool, it is also important to study neuronal apoptosis and clearance *in vivo*. The developing brain undergoes physiological apoptosis, and in addition, is particularly susceptible to certain insults that induce cell death. Alcohol exposure during embryonic and early postnatal ages induces substantial neuronal apoptosis (Ikonomidou, Bittigau et al. 2000). Because substantial brain development (and a period of susceptibility to ethanol injury) occurs postnatally in mice, ethanol exposure at postnatal day 7 is an accepted model of fetal alcohol exposure in humans and has been widely used to study neuronal apoptosis (Ikonomidou, Bittigau et al. 2000, Olney, Wozniak et al. 2001, Olney, Tenkova et al. 2002, Young, Klocke et al. 2003, Ghosh, Walls et al. 2009). Therefore, we use this model to study neuronal degeneration and clearance *in vivo*.

Recognition of apoptotic cells and debris by phagocytes

Phagocytosis [from Greek, phago- "eating", -cyte "vessel", -osis a process] is the mechanism by which cells engulf and internalize particles such as apoptotic cells; cells that engulf debris are known as phagocytes.

In order for clearance to take place, a dying cell or material must be recognized as a target. In other words, the debris must induce recruitment and activation of phagocytic cells. Much work has been done describing the general process by which apoptotic cells are recognized and removed (Ravichandran, Lorenz 2007). Briefly, apoptotic cells release factors such as fractalkine and ATP, which create a homing gradient to attract phagocytes (Elliott, Chekeni et al. 2009, Truman, Ford et al. 2008). In addition, they may display specific cell-surface 'eat me' signals such as phosphatidylserine on their outer membranes or may be targeted for removal through opsonization (Ravichandran, Lorenz 2007). Opsonins such as complement and MFGE8 bind apoptotic cells or debris, enhance recognition and target the apoptotic cell for clearance (Mevorach 2000).

There are specific receptors on phagocytes that allow direct recognition of material to be cleared. For example, phosphatidylserine becomes exposed on the cell surface of apoptotic cells and acts as an 'eat me' signal' which is recognized by phagocytes through receptors such as BAI1, as well as scavenger receptors, LRP1, MerTK and others (Ravichandran, Lorenz 2007). These signals 'activate' the phagocytic cell and stimulate signal transduction through multiple pathways. Depending on the context, this may lead not only to phagocytosis, but also to changes in cell morphology,

induction of migration, and secretion of cytokines. Engulfment may be mediated by neighboring cells or by phagocytes that are recruited to the site.

Fractalkine, a potential 'find me' signal, and BAI1, an engulfment receptor, are both expressed in the brain, but before our studies, their role in recognition and clearance of apoptotic neurons in the brain had not been established.

Engulfment

Recognition of debris or apoptotic cells stimulates phagocytosis. Cytoskeletal rearrangement leads first to formation of a phagocytic cup and then a phagosome, or vacuole around the material. Actin dynamics modulate the changes in cell shape required for engulfment, and the small GTPase Rac1 has been implicated as the downstream player responsible for regulating these cytoskeletal alterations. There are at least two potential signaling modules upstream of Rac1 that could be involved in modulating engulfment: first, a complex of ELMO-Dock180 functions as a GEF for Rac1; second, LRP1 is a potential engulfment receptor that interacts with GULP, an adaptor protein that has been linked to engulfment through Rac1 activation (Kinchen, Ravichandran 2007). Once the cell engulfs material, the phagosome fuses with lysosomal compartments, forming what is known as the phagolysosome and degradation occurs (Yu, Lu et al. 2008).

'Activated' Phagocytes – A Phenotypic Spectrum

'Activation' of a glial cell in response to debris not only stimulates phagocytosis, but also results in other downstream effects, such as secretion of cytokines and production of reactive oxygen species (Cook, Chen et al. 2001, Noda, Doi et al. 2011). An issue that complicates analysis of the literature is that researchers refer to 'activation' of glia without acknowledging or accounting for the ambiguity of that label. This is problematic because there is a continuum of activation for microglia that entails a range of phenotypes, and the expression of 'activation markers' can vary (Saxena, Caroni 2007). The terms *classical activation*, also known as *M1*, hallmarked by production of pro-inflammatory cytokines and free radicals, and *alternate activation*, also known as *M2*, a less well defined anti-inflammatory phenotype, have been described for macrophages, and these are largely defined based on cytokine and receptor expression profiles (Kotilinek, Bacskai et al. 2002). However, the immunomodulatory milieu in the CNS differs and activation phenotypes may not mimic those in the periphery (Koldamova, Fitz et al. 2010) Future studies should aim to generate functional delineations so that researchers can better categorize the spectrum of glial activation phenotypes.

Regulation of phagocytosis

Cell-cell interactions and the cytokine environment determine whether phagocytes are in the mood for clearance. Several studies have shown that astrocytes modulate microglial phagocytic activity *in vitro* (Noda, Doi et al. 2011, Olney, Wozniak et al. 2001) Neuronal signals also appear to influence the activation of glia. For example,

in culture, neuronal activity modulates IFNγ-induced MHCII expression on astrocytes and microglia, ultimately dampening inflammatory activity (Alliot, Godin et al. 1999). Thus, neurons may influence the overall activation phenotype and phagocytic properties of surrounding glia.

Phagocytic clearance in the brain

Most research on phagocytosis has been done in the context of the peripheral immune system, and there is much to learn about the specific pathways that are activated during phagocyte activation and engulfment in the nervous system. Engulfment may play a role not only in clearance of apoptotic neurons and their processes, but may also be critical for pruning superfluous neuritic branches that do not find their correct targets during development.

There are multiple lines of evidence suggesting that phagocytes play an active role in mediating developmental pruning. Studies in drosophila have shown that disrupting glial phagocytic activity by knocking out engulfment receptors results in defective pruning of axons in the mushroom body (Awasaki, Tatsumi et al. 2006). In addition, studies in rodents have shown that animals deficient for complement proteins C1q and C3 have defects in developmental pruning (Fourgeaud, Boulanger 2007, Stevens, Allen et al. 2007, Schafer, Lehrman et al. 2012).

Interestingly, genome association studies have implicated an association between schizophrenia and genes involved in engulfment pathways (Chen, Sun et al. 2009),

supporting the idea that engulfment may be relevant with regards to human neurodevelopmental defects.

While infiltrating macrophages and their CNS-resident counterparts, microglia, are considered the 'professional phagocytes' in the brain, there are other populations of potential phagocytes in the CNS, including neural progenitors and astrocytes.

There have been studies showing a role for engulfment by neural progenitors, and one study showed that neural progenitors deficient for the engulfment pathway protein ELMO1 had defects in engulfment (Lu, Elliott et al. 2011). Also, a microarray study on acutely isolated mouse brain astrocytes unexpectedly revealed that these cells express many components of evolutionarily conserved phagocytic pathways and numerous receptors involved in innate immunity, including Toll-like receptors, scavenger receptors and mannose receptors, as well as components of the complement system (Braak, Ghebremedhin et al. 2004). Astrocytes highly express a known phagocytic receptor, BAI1 (Park, Tosello-Trampont et al. 2007); therefore one of the goals of our work was to determine whether astrocytes and BAI1 play a role in engulfment.

Microglia perform typical immune cell functions much like macrophages, including phagocytosis and antigen presentation, as well as production of inflammatory mediators and modulation of the general immune response (Klein, Kaeser et al. 2001). Microglia have been identified as critical players in synaptic remodeling, and use factors such as complement (Stevens, Allen et al. 2007, Stephan, Barres et al. 2012) to direct pruning of synapses during development. Neurons communicate with microglia to

mediate these events, and one pathway of particular interest is the fractalkine pathway. Neurons express fractalkine and microglia express the receptor, CX3CR1. Studies have shown that animals deficient for fractalkine signaling have defects in pruning during development (Hoshiko, Arnoux et al. 2012, Paolicelli, Bolasco et al. 2011). It is possible that the mechanisms involved in synaptic pruning are similar to those involved in clearance of apoptotic neurons and that fractalkine also plays a role in clearance of apoptotic cells.

Microglia clear dead and dying neurons after injury, and a goal of our study was to identify factors that mediate the recognition of apoptotic debris. A study has shown that apoptotic cells release fractalkine, which acts as a 'find me' signal (Truman, Ford et al. 2008), and as microglia express the fractalkine receptor, CX3CR1, this pathway may be critical for proper clearance of apoptotic neurons. Fractalkine signaling is known to be an important neuronal-microglial communication tool (Mizuno, Kawanokuchi et al. 2003); however, the role of fractalkine specifically in the context of apoptosis in the brain has not been explored until our study.

Our studies

There are three main obstacles in that field that we attempted to address in our studies. First, there is a paucity of markers available to highlight dying neurons in order to study degeneration and clearance. Second, the mechanism underlying recognition of apoptotic neurons have not been fully established, including the signals released by dying cells and the receptors involved in clearance. Third, we do not know the ultimate

consequences of lack of clearance and persistence of apoptotic cells after developmental apoptotic injury.

We aimed to address these gaps in knowledge through:

1. Discovery and characterization of markers that highlight degenerating neurons and their neurites during development and after injury.
2. Identification of 'find me' signals involved in recognition of apoptotic neurons and receptors responsible for modulating clearance after alcohol injury.
3. Assessment of the consequences of lack of clearance by measuring inflammation after alcohol injury.

We discovered that antibodies against the caspase-cleaved cytoskeletal proteins actin and tubulin are useful markers that highlight axon degeneration. Our extensive characterization of these antibodies demonstrates that these tools are useful for studying neuronal degeneration in *in vitro* as well as *in vivo* models, and for rodent or human tissue. An advantage of these markers is that they also indicate the mechanisms underlying degeneration. We anticipate that these tools will be useful for studying developmental defects in pruning as well as axon degeneration in a variety of injury models.

Fractalkine and BAI1 are both expressed in the brain, but before our studies, their role in recognition and clearance of apoptotic neurons in the brain had not been established. We identify fractalkine as a 'find me' cue that recruits microglia toward apoptotic debris and show that lack of fractalkine signaling leads to increased apoptotic

debris after alcohol-induced injury. We show that this increase in debris is associated with increased inflammation, suggesting that one consequence of defective clearance may be an exaggerated immune response. BAI1, on the other hand, does not play a critical role in clearance after alcohol-induced apoptosis, and there are likely other receptors involved in promoting phagocytosis of apoptotic neurons. These findings show although BAI1 has been shown to promote phagocytosis *in vitro*, it is not required in the brain.

CHAPTER 1: Caspase-mediated cleavage of actin and tubulin is a common feature and sensitive marker of axonal degeneration in neural development and injury

Axon degeneration occurs after neuronal injury and during developmental pruning. Here we confirm that apoptotic machinery is involved in axon degeneration and caspase-mediated cytoskeletal degradation is a common convergence point. Using antibodies against caspase-generated neoepitopes of beta-actin and alpha-tubulin, we demonstrate that axon degeneration involves caspase-mediated cleavage of these cytoskeletal elements. These cleavage events are conserved and seen in a variety of contexts, including a) *in vitro* in neuronal cultures induced to undergo axonal degeneration via nerve growth factor deprivation and b) *in vivo* after ethanol-induced apoptosis as well as during developmental pruning and physiological turnover of neurons. Finally, these markers may have clinical utility, as they highlight degenerating neurites in human hypoxic-ischemic injury. These findings not only confirm a common downstream mechanism involved in axon degeneration, but also emphasize the broad utility of antibodies to caspase-cleavage-specific epitopes as markers of degenerating neurons.

INTRODUCTION

Axon degeneration occurs not only after injury but also during normal central nervous system development. Degeneration may be initiated due to lack of trophic signals, presence of toxins, or trauma. The upstream factors involved in axonal degeneration are different depending on the context or the mode of injury, but regardless of the instigating stimulus the process is an active, orchestrated event as opposed to a passive phenomenon.

There are many parallels between programmed cell death, or apoptosis, and the process of axon degeneration. Apoptotic signals may arise from a variety of stimuli, but both the extrinsic and intrinsic pathways converge to activate caspases, a group of proteolytic enzymes that cleave their substrates at specific residues. An ordered set of events follows that includes degradation of proteins and cytoskeletal elements, morphological changes such as blebbing of the membrane, and the release of apoptotic bodies, or membrane-bound vesicles, that are phagocytosed by neighboring cells (Bishop, Misgeld et al. 2004). Whether similar processes are involved in axon

degeneration has been controversial (Finn, Weil et al. 2000, Simon, Weimer et al. 2012).

Recent work using genetic deletion of caspase-3 and caspase-6 has indicated that they are required for nerve growth factor (NGF) deprivation induced axon degeneration. These studies also showed that these caspases are important for proper developmental pruning of retinocollicular axons in mice (Simon, Weimer et al. 2012).

In order to study whether apoptosis-related pathways and caspases are involved in cytoskeletal degradation during axon degeneration, we have used both *in vitro* and *in vivo* models. *In vitro*, axon degeneration can be induced in cultured sympathetic neurons via NGF-deprivation. NGF deprivation has been widely used as an *in vitro* model to induce axon degeneration and is thought to model many aspects of developmental pruning. During degeneration, the axon blebs and fragments. This blebbing and fragmentation is dependent on cytoskeletal disassembly and has been hypothesized to be controlled by factors that regulate microtubule stability, such as microtubule-associated proteins (Saxena, Caroni 2007). The mechanisms underlying cytoskeletal degradation are unclear, but it is known to be a convergence point for axon degeneration induced by a variety of mechanisms.

Here we investigate this common convergence point using experimental models and human specimens. We demonstrate that antibodies against caspase-generated neoepitopes of beta-actin and alpha-tubulin are sensitive and specific indicators of caspase-mediated cytoskeletal degradation. These markers indicate that axonal degeneration involves caspase-mediated cleavage of the actin and tubulin.

These cleavage events occur in a variety of contexts involving axon degeneration, including a) *in vitro* in neuronal cultures induced to undergo apoptosis via nerve growth factor deprivation, b) *in vivo* after ethanol-induced apoptosis as well as during developmental apoptosis and physiological turnover of neurons, and c) in human brain after acute or subacute hypoxic-ischemic injury.

METHODS

Tissue processing

All animal procedures were approved by the University of Virginia Animal Care and Use Committee. Mice used were C57/bl6 (Charles River). Animals were anesthetized with a lethal dose of pentobarbital. Whole embryos harvested at E14.5 were post-fixed overnight in 4% paraformaldehyde. Brains from postnatal and adult mice were harvested and fixed in either paraformaldehyde or 70% ethanol. Tissue was processed into paraffin by standard methods. Tissue from BAX knockout and PUMA knockout animals was provided by the Roth lab (University of Alabama). For analysis of human specimens, archival paraffin-embedded brain tissue was obtained from autopsies from 5 patients who had been diagnosed with acute or subacute brain infarct.

Caspase enzymatic assay and western blot

To prepare synaptosomes, cortex was homogenized in Locke's buffer with ten strokes of a tight-fitting glass Dounce tissue grinder. The homogenate was centrifuged at 500*g* for 10 min and the resulting supernatant was centrifuged at 12,000*g* for 15 min. The

pellet was resuspended in Locke's buffer and centrifuged at 12,000*g* for 15 min to obtain the final pellet containing the synaptosome-enriched fraction. The caspase enzymatic assay was performed as previously described (LeBlanc, Liu et al. 1999). Laemmli sample buffer was added to synaptosomes and 50ug of protein was loaded into each lane and separated by electrophoresis using standard procedures. Gels were transferred to a PVDF membrane for 90 min with a semidry transfer apparatus and treated with blocking reagent (LI-COR block; LI-COR, Lincoln NE) for 1 hour and then probed with primary antibodies overnight. Antibodies used were the following: TubulinΔCsp6 (LeBlanc lab, 1:20,000), alpha-tubulin (clone DM1A, 1:10,000), fractin (Millipore, 1:1000). For visualization, blots were incubated with fluorescent secondary antibodies (LI-COR, 1:2000) for 1-2 hours and imaged on a LI-COR Odyssey infrared scanner.

Cell Culture

Neurons for nerve growth factor (NGF) deprivation were obtained by acute dissection and enzymatic dissociation of postnatal rat (P0-P3) superior cervical ganglia. Neurons were plated in Poly-D-Lysine/Laminin-coated coverslips with compartmentalized microfluidic devices with DMEM supplemented with 10% FBS, penicillin/streptomycin (1 U/ml), and 40ng/ml NGF purified from mouse salivary glands (Kuruvilla, Zweifel et al. 2004). After 24–48 hours, 5μM Ara-C was added to the culture media for 48 hours to reduce glial contamination. For microfluidic devices, neurons were given time to project their axons to the outer chamber (5-7 days *in vitro*). Neurons were either maintained in NGF or for NGF deprivation, cultures were

rinsed three times with medium lacking NGF and then maintained in NGF- deficient media containing a neutralizing antibody to NGF (Millipore). For pan-caspase inhibition, neurons were treated with 100μM of ZVAD (Enzo Life Sciences) concurrent with NGF deprivation. Neurons were fixed by incubating in 4% paraformaldehyde for 15 minutes, washing with PBS twice. Cells were then stained.

Ethanol injury

Ethanol was injected subcutaneously into postnatal day 7 (P7) pups as a 20% solution in 0.9% saline at 15.9μL/g body weight. It was administered twice, 2 hours apart (as described by (Ghosh, Walls et al. 2009)). Brain tissue was harvested 6 or 24 hours after the first injection.

Immunostaining

For immunocytochemistry, cells were fixed for 15 minutes in 4% paraformaldehyde, rinsed in PBS then blocked (1 hour, 2% horse serum, .1% Tween in PBS) prior to incubation with primary (overnight at 4°C, diluted in block). For tissue staining, paraffin-embedded sections were dewaxed, rehydrated, underwent antigen retrieval (Tris-EDTA pH 9, 12 min over a boiling water bath), were quenched (15 min, .6% H_2O_2 in dH_2O) and blocked (1 hour, 2% horse serum, .1% Tween in PBS) prior to incubation with primary (overnight at 4°C, diluted in block). Primary antibodies: TubulinΔCsp6 (LeBlanc lab, 1:2000), fractin (Millipore, 1:1000), CC3 (Cell Signaling, 1:100), NFM (DSHB, clone 2H3, 1:2000), β3-tubulin (Tuj1, 1:500), iba1 (Wako, 1:500).

Immunoperoxidase detection was performed using the ImmPress polymeric peroxidase reagents (Vector). Diaminobenzidine (Dako) 1 mg/ml plus 0.02% hydrogen peroxide was applied for 3–5 min. Immunofluorescence detection was performed using secondary antibodies conjugated to Alexa-488 and Alexa-546 dyes (Invitrogen, 1:2000) and DAPI (1μg/mL).

Automated image analysis

Cell profiler (Broad Institute, (Lamprecht, Sabatini et al. 2007)) was used for automated analysis of staining. Pipelines were set up to identify axons via Tuj1 and those regions of interest were used to quantify fluorescence intensity of fractin and TubulinΔCsp6 staining within axons. Data was graphed and analyzed using Graphpad Prism (La Jolla, CA).

RESULTS

Recombinant caspases are sufficient to generate fractin and cleaved tubulin

The fractin and TubulinΔCsp6 antibodies are specific to the caspase-cleaved fragments of beta-actin (cleaved by caspase-3 at D244 (Yang, Sun et al. 1998) and alpha-tubulin (cleaved by caspase 6 at D438 (Klaiman, Petzke et al. 2008), respectively. We performed an *in vitro* enzymatic assay in order to test whether caspases are sufficient to generate the neoepitopes and we found that both caspase-3 and caspase-6 are capable of generating the epitope recognized by TubulinΔCsp6, whereas fractin is only produced

by caspase-3 (Fig. 1a). Also the no enzyme control shows the antibodies are specific to the caspase-cleaved products and do not detect intact protein.

Cleavage of actin and tubulin occurs after induction of apoptosis

We used an animal model of fetal alcohol syndrome in order to visualize axonal degeneration after induction of neuronal apoptosis *in vivo*. We injected postnatal day 7 (P7) mice with ethanol and harvested the brain 6 or 24 hours post injury. BAX and PUMA deficient animals are known to be protected from caspase activation in this model (Ghosh, Walls et al. 2009); therefore we quantified cleaved-caspase-3, fractin and TubulinΔCsp6 staining in these mice after ethanol-induced apoptosis. We found that along with cleaved-caspase-3 staining, fractin and TubulinΔCsp6 staining is abrogated in these animals (Fig. 1b). This confirms that axon degeneration and production of these epitopes is downstream of an active, apoptosis-related process.

After ethanol-induced apoptosis, cleaved caspase-3 is readily visible in apoptotic cell bodies (corpses); however, it is difficult to find staining in axons. Rare, isolated degenerating axon fibers are detected (Fig 1c, arrowhead), but overall, CC3 is not readily visible in degenerating axon tracts via standard staining techniques. Tyramide signal amplification (TSA) is required to detect caspase-3 activity in degenerating axons. CC3 signal amplified with TSA localizes to axon tracts labeled with neurofilament in a pattern that mimics fractin and TubulinΔCsp6 (Fig. 1c, Fig. 2).

Unlike cleaved caspase-3, fractin and TubulinΔCsp6 readily highlight not only cell bodies, but also degenerating axons (Fig. 2). This suggests that while caspase

activity is present in degenerating axons, the concentration of cleaved caspases may be below the threshold of detection via standard immunostaining techniques. Staining for caspase-substrate neoepitopes via fractin and TubulinΔCsp6 may be a more sensitive indicator of caspase activity in axons.

NGF-withdrawal-induced apoptosis leads to cleavage of actin and tubulin in axons

We used NGF-deprivation to induce axon degeneration in cultured sympathetic neurons. The neurons were grown in a microfluidic devices in order to separately visualize the axons and the cell bodies. NGF-replete neurons had little fractin or TubulinΔCsp6 labeling. However, 12 hours of NGF-deprivation leads to fractin (Fig. 3a) and cleaved tubulin (Fig. 3b) production. As expected, this staining corresponded with an increase in blebbing and fragmentation of the axons, visible with β_3-tubulin (Tuj1) staining.

Caspase activity is sufficient cleave actin and tubulin (Fig.1 a); however, this does not indicate whether caspase activity is necessary. In order to test this, we performed NGF-deprivation in the presence of a pan-caspase inhibitor (ZVAD). We quantified the fluorescence intensity of staining within axons. We found that 12 hours of NGF-deprivation leads to significant fractin production and incubation with ZVAD prevents the increase in staining (Fig. 3c). TubulinΔCsp6 staining trended in the same directions (Fig. 3d). Overall, this indicates that caspases are involved in axon degeneration secondary to trophic-factor-withdrawal.

Physiological axon pruning *in vivo* during nervous system development involves caspase-cleavage of actin and tubulin

Axonal degeneration occurs during developmental pruning, and we were interested in determining whether this degeneration also involved caspase-mediated cleavage of actin and tubulin. We harvested embryonic day 14.5 (E14.5) animals and stained for cleaved caspase-3, fractin and TubulinΔCsp6. We found prominent labeling in ganglia in a subset of corpses with all the markers. Fractin and most notably TubulinΔCsp6 also highlighted axons emanating from the dorsal root ganglion (Fig. 4).

Olfactory neurons are one of the few populations of neurons known to undergo continuous turnover throughout life. Olfactory sensory neurons (OSNs) send projections to the olfactory bulb, and upon apoptosis of the OSNs, their axons also degenerate. Both fractin and TubulinΔCsp6 also highlight degenerating axons in the glomeruli of the adult olfactory bulb (data not shown).

This suggests that caspase-cleavage of actin and tubulin also occurs during physiological degeneration of axons and this provides novel insights into the potential mechanism of axon pruning.

These markers highlight degenerating axons in human pathological specimens

To determine whether these antibodies may be useful as markers of neuronal apoptosis and axon degeneration in human pathological specimens, we obtained autopsy tissue from five patients who had been diagnosed with acute or subacute infarcts of the CNS (Table 1). We show representative images from an adult case (Fig.

5a) and an infant case (Fig. 5b). Histology showed areas of gliosis, and these regions were chosen for analysis of axon degeneration. We identified gliosis via iba1 staining, which highlighted ameboid microglia in areas of injury. These areas often showed evidence of axon degeneration via our cleavage-specific antibodies (Fig. 5a, to the right of the arrowhead). We found evidence of fractin and TubulinΔCsp6 staining in all five cases. We found that fractin and TubulinΔCsp6 antibodies highlight apoptotic corpses as well as degenerating axons (Fig. 5b). We compared fractin and TubulinΔCsp6 staining to CC3 and to SMI32, another marker widely used to highlight axon degeneration. We found that fractin and TubulinΔCsp6 were more specific and provided a higher signal-to-noise ratio for staining degenerating axons as compared to either CC3 or SMI32.

The utility of these markers is not limited to hypoxic-ischemic injury, as we also saw staining in a sample of an active multiple sclerosis lesion (data not shown). Of note, we also stained tissue from multiple patients with a variety of chronic neurodegenerative diseases, including Alzheimer's disease, Parkinson's disease, and epilepsy, but did not see evidence that these markers specifically highlighted a significant amount of axonal debris in these tissues (data not shown). We also stained tissue from patients with psychiatric diseases such as schizophrenia and saw no evidence of staining (data not shown).

The absence of staining in chronic neurodegenerative disease cases suggests either that these markers may preferentially highlight acute processes or that there is not

a significant amount of caspase-mediated axonal degeneration occurring in these cases at the time of autopsy.

DISCUSSION

The apoptotic cascade has been well-enumerated and has been shown to be dependent on caspases as executioners. However, whether axon degeneration similarly involves caspase activity has been somewhat controversial. Axon degeneration involves cytoskeletal degradation and morphological changes such as prominent blebbing and fragmentation. These are also hallmark features of apoptosis and, in that context, modulated by caspase activity (Coleman, Sahai et al. 2001). Due to the parallels between apoptosis and axon degeneration, we hypothesized that cytoskeletal degradation in axon degeneration would similarly involve caspase activity.

Initial studies were unable to detect caspase activation in degenerating axons and suggested they had no role (Finn, Weil et al. 2000). However, this is likely due to a lack of sensitive markers and a low threshold of caspase activation required. Indeed, our experience with cleaved-caspase-3 staining suggests activity may be below the threshold for detection via standard staining techniques. However, we find that tyramide signal amplification enables more sensitive detection of activated caspase-3 and allows for detection in degenerating axons.

Studies also ruled out a role for caspases in axon degeneration because they found that caspase inhibitors were unable to prevent degeneration (Finn, Weil et al.

2000, Lirk, Haller et al. 2007, Lirk, Haller et al. 2008). However, under normal circumstances inhibitors may not be potent enough, especially if there is a low threshold of caspase activation required to initiate the downstream cascade. A recent study showed that inhibitors were able to delay NGF-induced axon degeneration, however, only in caspase-3 heterozygous neurons, not wild type neurons (Simon, Weimer et al. 2012).

We aimed to look further at the role of caspases in axon degeneration, and we focused on the role of caspases in cytoskeletal degradation. In order to examine whether caspase-mediated cleavage of cytoskeletal elements was involved, we used antibodies that are specific to the caspase-cleaved forms of actin and tubulin. We show via *in vitro* assays that caspases are sufficient to cleave actin and tubulin, and our cleavage-specific antibodies recognize a neoepitope generated by cleavage.

In order to determine whether apoptosis-induced axon degeneration involves caspase-mediated cytoskeletal degradation, we used an animal model of fetal alcohol syndrome. Ethanol exposure during development results in robust neuronal apoptosis (Ikonomidou, Bittigau et al. 2000). Ethanol-induced neuronal death has been shown to be dependent on the intrinsic apoptotic pathway, as animals deficient in the pro-apoptotic mitochondrial proteins BAX and PUMA are resistant to ethanol-induced caspase-3 activation and apoptosis (Young, Klocke et al. 2003, Ghosh, Walls et al. 2009). We found that ethanol-induced apoptosis led to extensive degeneration that was detectable via the fractin and TubulinΔCsp6 antibodies. As expected, animals deficient

in BAX or PUMA (which are protected from caspase activation) lacked staining for fractin and TubulinΔCsp6.

In addition, we show that antibodies against caspase-cleaved substrates not only provide specific markers that indicate caspase activity but also allow enhanced visualization of degenerating axons compared to cleaved caspase-3. Antibodies specific to caspase-cleaved actin and tubulin prove to be very useful for detecting caspase activation in axon degeneration. This is likely because a) one activated caspase molecule is able to cleave multiple substrate molecules, leading to amplified signal, and b) cytoskeletal elements are an abundant substrate in axons.

This further supports the idea that apoptosis-related mechanisms are involved in cytoskeletal degradation during axonal degeneration. Our results support a recent study that showed caspases are involved in certain types of axon degeneration (Simon, Weimer et al. 2012). They used caspase-3 and caspase-6-deficient neurons and showed that they are protected from NGF-deprivation induced axon degeneration. Our findings similarly suggest that caspases are involved in apoptosis-induced degeneration. We find caspase-cleaved tubulin and fractin in axons degenerating due to NGF-deprivation or ethanol-induced apoptosis. Overall these findings solidify a role for caspase-3 and caspase-6 as mediators of cytoskeletal degradation during axon degeneration.

We show that caspases are responsible for generating the specific cleavage products. Caspase-3 generates fractin whereas caspase-3 and caspase-6 can both generate cleaved tubulin. This specificity is useful for evaluating which caspases are involved in axon degeneration in different contexts, such as during apoptosis versus

during pruning. Our staining in the embryo sheds light on processes that occur during developmental pruning. There are some previous studies that suggest a role for caspases in pruning. A study in *Drosophila* showed that caspases are involved in developmental dendrite pruning (Williams, Kondo et al. 2006). A more recent study showed that caspase-3 and caspase-6 are necessary for proper retinocollicular pruning in mice (Simon, Weimer et al. 2012). Not surprisingly, we see that many neurons are undergoing apoptosis at E14.5, particularly in the ganglia. As expected, cleaved-caspase-3, fractin, and TubulinΔCsp6 staining highlight the apoptotic bodies. However, the emanating fibers are preferentially highlighted by TubulinΔCsp6. This is in contrast to what we see after apoptosis –induced degeneration, where there are comparable levels of fractin and cleaved tubulin. The predominance of cleaved tubulin (produced by both caspase-3 caspase-6) and lack of fractin (produced by caspase-3) suggests that caspase-6 is the major mediator of cytoskeletal degeneration during pruning. This validates other studies that suggest that caspase-3 and caspase-6 may have unique roles in cell body versus axon degeneration (Nikolaev, McLaughlin et al. 2009, Cusack, Swahari et al. 2013). In addition to illuminating details about caspase activity during pruning, our finding also sheds light on the role of microtubule versus actin degradation and adds information about the role cytoskeletal degeneration during pruning.

Pruning can occur via a combination of retraction and degeneration, both of which have been well-visualized in the peripheral nervous system at the neuromuscular junction (Bishop, Misgeld et al. 2004). However, the relative importance of each in other contexts is a bit unclear as it has been difficult to study via static techniques. While

retraction may be important for modest local remodeling, removal of larger fragments appears to involve degeneration (Bishop, Misgeld et al. 2004, Hoopfer, McLaughlin et al. 2006). Retraction is speculated to depend largely on actin dynamics, whereas degeneration involves microtubules (Saxena, Caroni 2007). The fact that we predominantly see cleaved tubulin in the fibers supports the idea that a) caspase-6-mediated tubulin cleavage occurs pruning and b) that degeneration is occurring as opposed to just retraction.

We were interested in determining whether these antibodies may be useful as markers of neuronal apoptosis and axon degeneration in human pathological specimens. We found that fractin and TubulinΔCsp6 antibodies highlight acute axonal degeneration in neonatal, infant, and adult hypoxic-ischemic injury in the area of infarct as well as in a sample of an active multiple sclerosis lesion. Another paper showed fractin in hypoxic-ischemic injury, and they do mention finding positive axon segments (Rossiter, Anderson et al. 2002) We also stained tissue from patients with a variety of chronic neurodegenerative diseases, including Alzheimer's disease, Parkinson's disease and epilepsy, and did not see evidence that these markers specifically highlighted a significant amount of axonal debris in these tissues. Others have shown fractin and TubulinΔCsp6 staining in tissue from Alzheimer's disease (Klaiman, Petzke et al. 2008, Rossiter, Anderson et al. 2000)in Hirano bodies and neuronal bodies respectively, but they do not note labeling of axon degeneration. The mechanisms of axon degeneration in these other diseases have not been well elucidated, and it is difficult to conclude precisely why these cases are negative for these markers. It is possible that the

degeneration is not caspase-dependent, but it is also possible that there are not enough simultaneously-degenerating neurons to detect significant signal at an isolated time point. Ultimately, we conclude that that fractin and TubulinΔCsp6 antibodies are best used as markers of acute degeneration.

There are other limitations of these markers. While fractin and cleaved tubulin staining can serve as readouts of caspase-3 versus caspase-6 activity, one must keep in mind the limitations of these markers. First of all, staining is dependent on whether the proteins localize to and are abundant in the compartment of interest as well as whether the specific caspases are activated. Axons are rich in actin and tubulin, therefore these are ideal caspase substrates to use to study caspase-mediated cytoskeletal degradation in axons. Secondly, as degeneration progresses, these epitopes may be degraded and no longer recognized by these markers, i.e. the lifespan of the epitope may be limited. Despite these limitations, we have found these markers to be very useful.

There are still questions that remain unanswered. Is caspase-mediated degradation of the cytoskeleton directly involved in mediating blebbing and fragmentation? There is support for this hypothesis, as one study showed that exogenous expression of actin fragments (caspase-cleaved size fragments) was sufficient to induce morphological changes of apoptosis downstream of caspase activation (Mashima, Naito et al. 1999). This could also be examined by testing whether mutation of the caspase-cleavage sites on actin and tubulin confers resistance to blebbing and fragmentation of degenerating axons.

What alternative pathways mediate cytoskeletal degradation and axonal degeneration when caspases are not the executioners, as in Wallerian degeneration? Calpains are likely candidates, as they have been shown to be activated after axotomy and inhibiting calpains confers resistance to axotomy-induced degeneration (George, Glass et al. 1995, Ma, Ferguson et al. 2013).

In conclusion, caspase-mediated cleavage of actin and tubulin is a common feature in some forms of axon degeneration. We show that antibodies against caspase-generated neoepitopes provide useful tools to demonstrate caspase activity. We show that caspases are involved in cleaving cytoskeletal elements actin and tubulin during degeneration following apoptosis and during pruning. In addition to serving as useful markers of caspase activity, these markers inform about features of degeneration. Design of additional antibodies targeting specific caspase-generated epitopes would provide valuable tools for the field. In particular, it would be useful to identify substrates from specific glial and neuronal cells and from subcellular compartments, such as dendrites, axons or synapses. Identification of synapse-specific caspase substrates is an ongoing project in the lab.

FIGURES

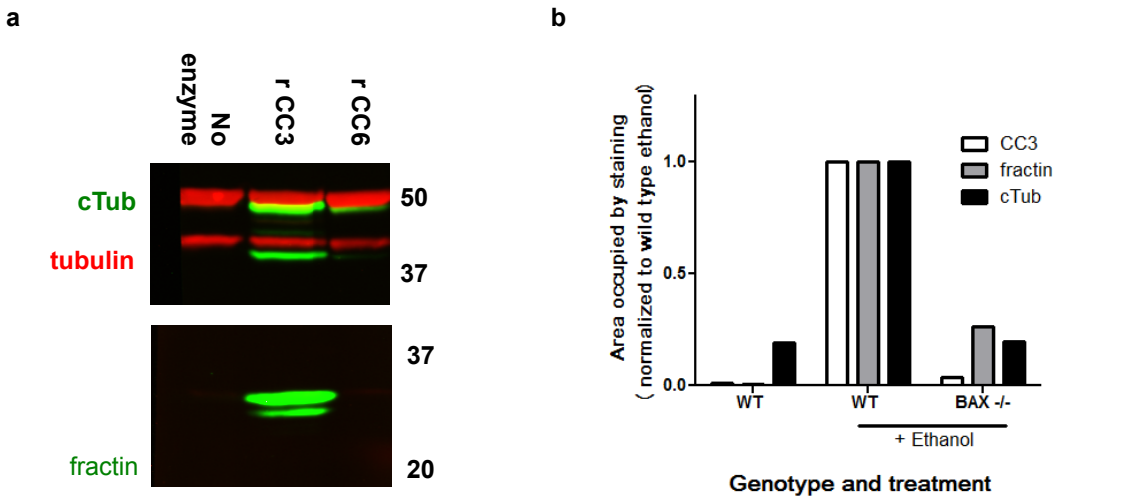
a
No enzyme
r CC3
r CC6
cTub
tubulin
50
37
37
fractin
20
b
Area occupied by staining
(normalized to wild type ethanol)
1.0
0.5
0.0
CC3
fractin
cTub
WT
WT
BAX -/-
+ Ethanol
Genotype and treatment
c
Ethanol
Control
CC3
CC3 + TSA amplification

Figure 1

Figure 1: Generation of fractin and cleaved-tubulin is downstream of the apoptotic cascade and caspases. An *in vitro* enzymatic assay using recombinant caspases and brain-derived synaptosomes is sufficient to generate cleavage of actin and tubulin. The cleavage-specific epitopes recognized by fractin and TubulinΔCsp6 (cTub) are identified via western blot. Recombinant cleaved-caspase-3 (rCC3) generates both fractin and cleaved tubulin whereas recombinant cleaved-caspase-6 only generates cleaved tubulin (a). P7 pups were injected with ethanol in order to induce neuronal apoptosis. The amount of CC3, fractin and TubulinΔCsp6 staining was quantified 6 hours after injury via Cell profiler. Data was normalized to the value calculated from the wild type ethanol-treated tissue in order to represent relative levels in each genotype and treatment. BAX deficiency protected neurons from ethanol-induced caspase-3 activity and prevented generation of fractin and cleaved tubulin (b). While ethanol-induced apoptosis led to CC3-positive cell bodies, CC3 was not usually seen in axon fibers via conventional staining techniques, and fibers such as the one shown (c, arrowhead) were rarely detected. Tyramide signal amplification (TSA) was required for visualization of CC3 in axon fibers after ethanol-induced apoptosis (shown are striatal pencil fibers). CC3 with TSA (CC3 + TSA) was only detected in tissue after ethanol-induced apoptosis, and CC3 staining was not seen in control tissue (c). Scale 50μm.

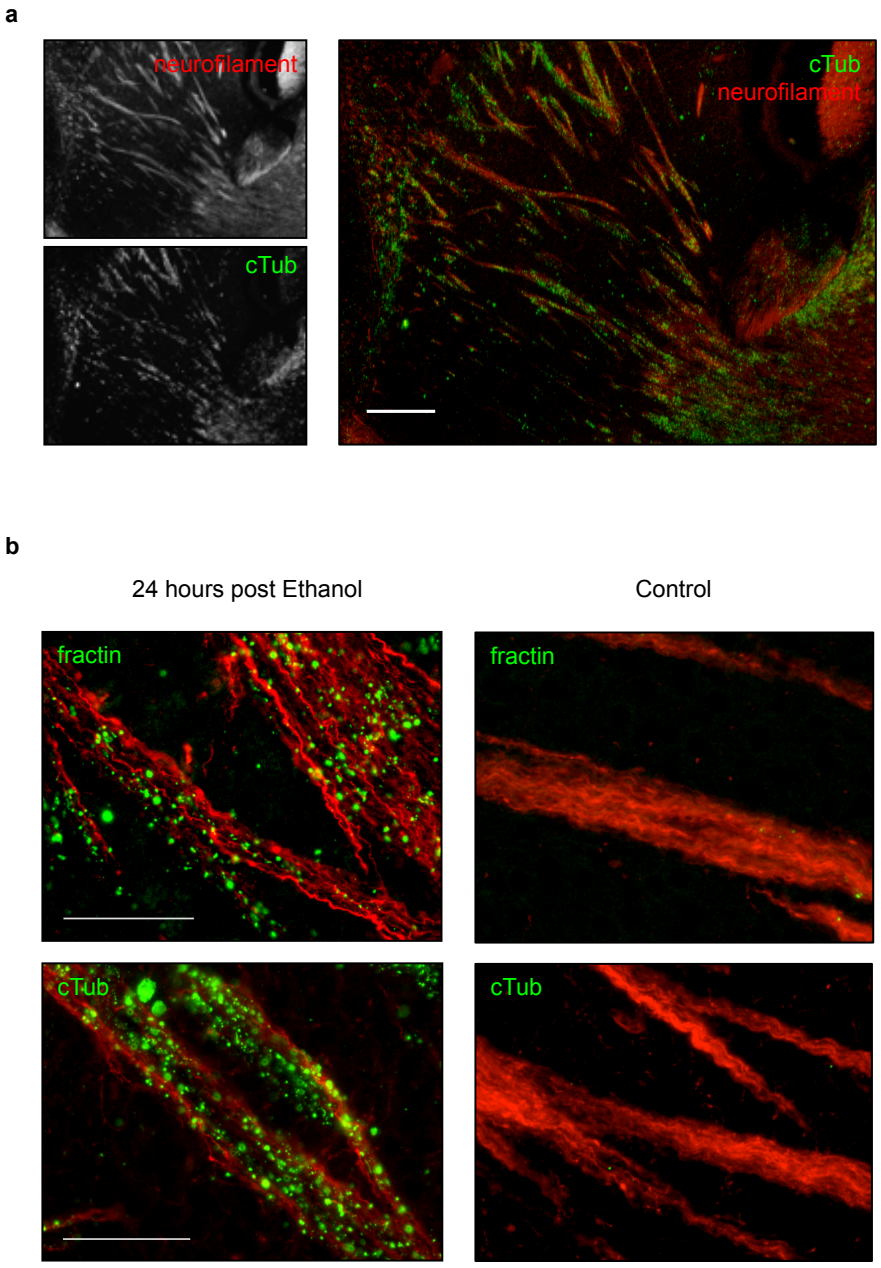
a
neurofilament
cTub
cTub
neurofilament
b
24 hours post Ethanol
Control
fractin
fractin
cTub
cTub

Figure 2

Figure 2: Fractin and TubulinΔCsp6 highlight degenerating axon tracts after ethanol-induced apoptosis. Co-labeling in the striatum using TubulinΔCsp6 (cTub) (green) along with a marker for neurofilaments (red) reveals that TubulinΔCsp6 localizes to axon tracts after ethanol treatment. Shown here is 24 hours after ethanol treatment (a). Co-labeling in the striatum using fractin or TubulinΔCsp6 (green) along with a marker for neurofilaments (red) reveals that both of these markers highlight degenerating axon tracts after ethanol-induced apoptosis and are absent in control tissue (b). Scale in (a) is 200 μm. Scale in (b) is 50 μm.

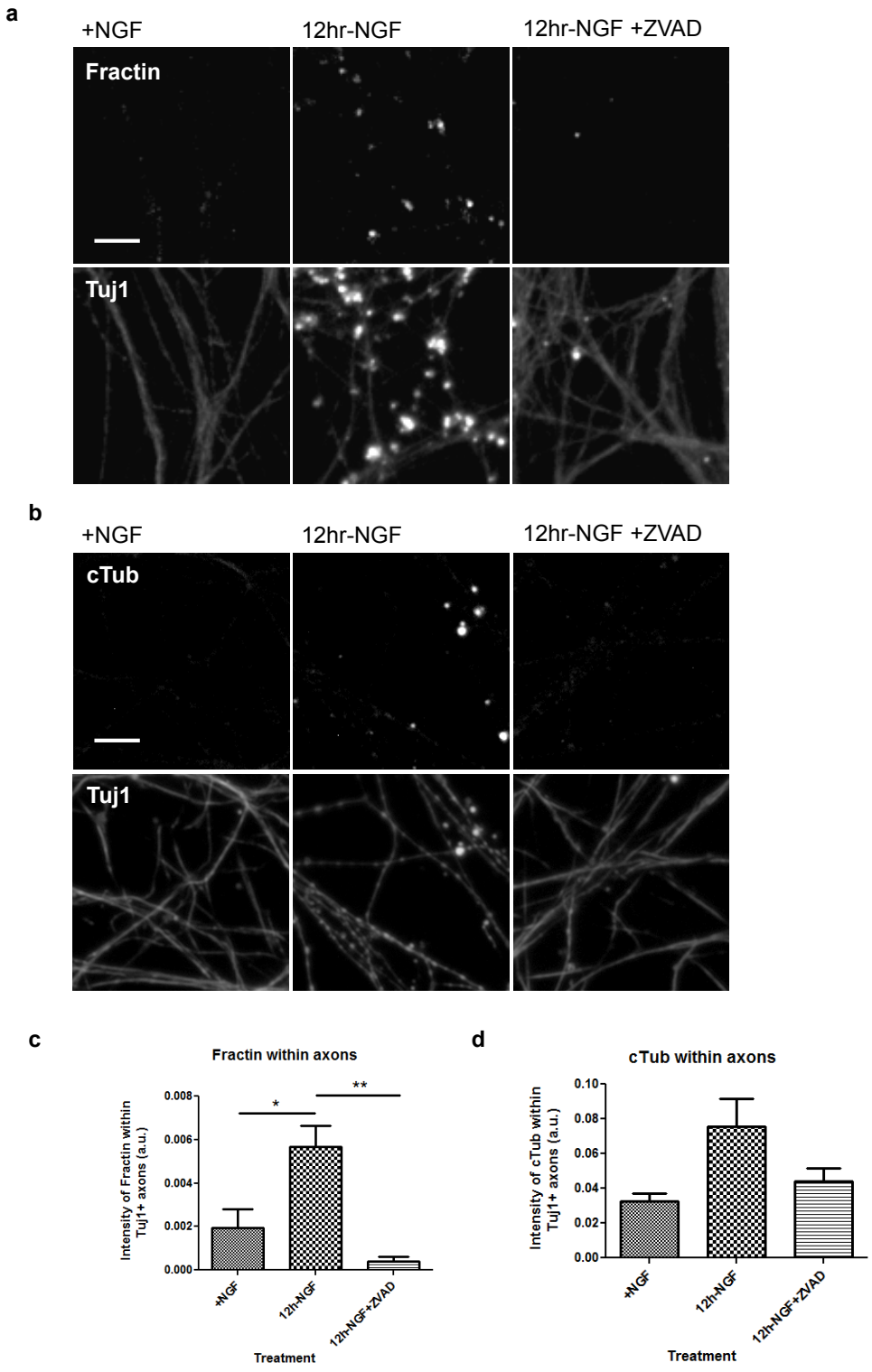
a
+NGF
12hr-NGF
12hr-NGF +ZVAD
Fractin
Tuj1
b
+NGF
12hr-NGF
12hr-NGF +ZVAD
cTub
Tuj1
c
Fractin within axons
Intensity of Fractin within Tuj1+ axons (a.u.)
0.008
0.006
0.004
0.002
0.000
*
**
+NGF
12hr-NGF
12hr-NGF+ZVAD
Treatment
d
cTub within axons
Intensity of cTub within Tuj1+ axons (a.u.)
0.10
0.08
0.06
0.04
0.02
0.00
+NGF
12hr-NGF
12hr-NGF+ZVAD
Treatment

Figure 3

Figure 3: NGF-deprivation induces caspase-mediated cleavage of actin and tubulin. NGF-replete (+NGF) cultured sympathetic neurons are viable and axons are intact, as visible with β_3 tubulin (Tuj1) staining. NGF-withdrawal-induced apoptosis causes axon degeneration by 12 hours that is marked with antibodies against cleaved actin (fractin) (a) or TubulinΔCsp6 (cTub) (b) and appears to be blocked by caspase inhibition using ZVAD. Intensity of fractin (c) and TubulinΔCsp6 (d) staining in axons was measured in arbitrary fluorescence units (a.u.). Data represents multiple experiments. (c) One-way ANOVA, *$p<.05$, **$p<.01$. Scale bar = 10μm.

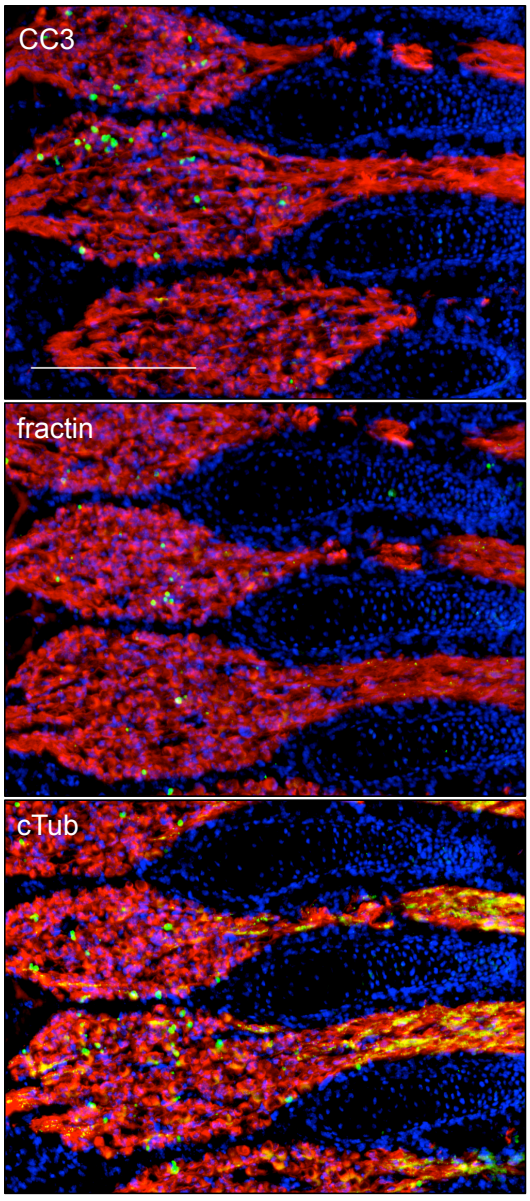

Figure 4

Figure 4: Fractin and cTub highlight degenerating axon tracts during developmental pruning. Adjacent sections from embryonic day 14.5 mice were stained with CC3, fractin and cTub (green) along with neurofilament (red) and the dorsal root ganglia were imaged. Fractin and cTub highlight a subset of cell bodies and axons emanating from the ganglia, likely representing neurons undergoing physiological developmental pruning. Scale 200μm.

Table 1: Cases used in analysis of axon degeneration after infarct injury		
Age	**Diagnosis**	**Approximate stage of injury**
Prenatal (33 weeks)	Placental infarction	Subacute
Newborn	Acute hypoxic injury	Acute
6 day old	Cardiomyopathy, multifocal acute and subacute ischemic injury	Subacute
6 month old	Small and large intestine necrosis; sepsis, watershed infarcts	Acute, 5-7 days
35 year old	Sepsis, cerebral infarction	Acute, 2-5 days

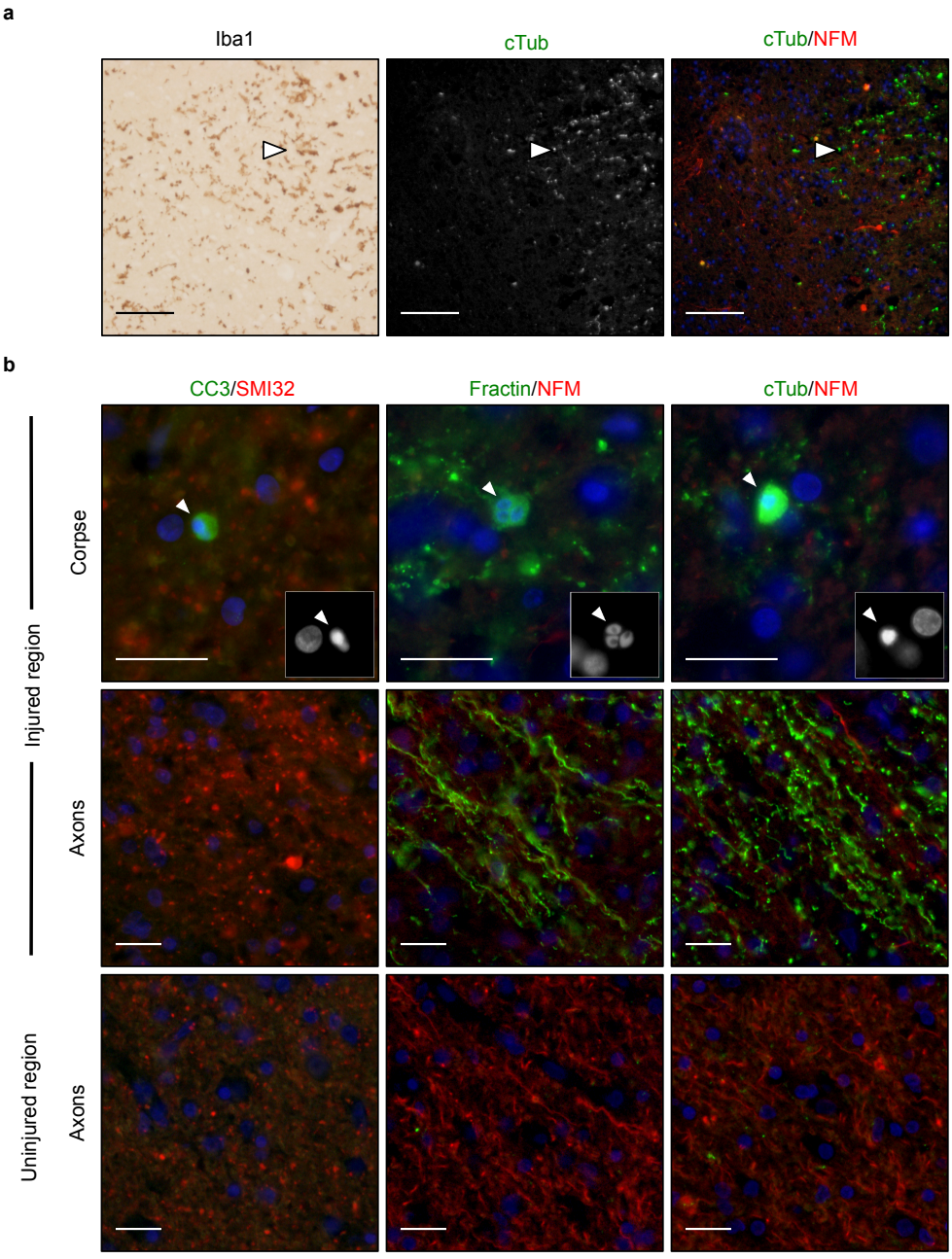
a
Iba1
cTub
cTub/NFM
b
CC3/SMI32
Fractin/NFM
cTub/NFM
Injured region
Corpse
Axons
Uninjured region
Axons

Figure 5: Fractin and cleaved tubulin highlight degenerating neurons and neurites in areas of infarct damage in human brain. Histology showed areas of gliosis via staining with a microglial marker (iba1), which highlighted ameboid microglia in areas of injury (a, to the right of the arrowhead). These areas showed evidence of axon degeneration via TubulinΔCsp6 (cTub) staining in an adjacent section. Adjacent sections from a different case were labeled with CC3 (green) and SMI32 (red), or TubulinΔCsp6 and neurofilament (red), or fractin (green) and neurofilament (red) (b). (Row 1) Insets show DAPI-labeled pyknotic nuclei (arrowhead) in apoptotic corpses that are labeled with CC3, fractin and TubulinΔCsp6. (Row 2) Fractin and TubulinΔCsp6 antibodies highlight degenerating axons, whereas CC3 fails to label degenerating axons via conventional staining techniques. (Row 3) Uninjured areas have decreased SMI32 staining and no fractin or TubulinΔCsp6 -labeled axons (b). Scale = 25 μm.

CHAPTER 2: Fractalkine signaling plays a role in ethanol-induced developmental apoptosis

In the context of the central nervous system, fractalkine is generally known as a neuron-microglial communication factor. However, its precise function in the context of *in vivo* neuronal apoptosis has not been described. We used an animal model of fetal alcohol syndrome to induce neuronal apoptosis and show that this leads to release of soluble, extracellular fractalkine. The extracellular media harvested from these apoptotic brains induces microglial migration in a fractalkine-dependent manner that is prevented by neutralization of fractalkine with a blocking antibody or by deficiency in the receptor, CX3CR1. This suggests that fractalkine acts as a chemoattractant to recruit microglia toward apoptotic cells and may be involved in promoting their clearance. We used the fetal alcohol syndrome model to determine whether fractalkine signaling plays a role in clearance of apoptotic neurons. We examined fractalkine-knockout and CX3CR1-knockout mice after ethanol-induced apoptosis and found increased apoptotic debris and altered cytokine production in the brains of these knockouts by 6 hours after ethanol treatment. Collectively, this suggests that fractalkine acts as a 'find me' signal for apoptotic neurons and plays a critical role in modulating clearance and the inflammatory response after ethanol-induced apoptosis.

INTRODUCTION

There is still much to learn about the process of neuronal death and how neurons help orchestrate the response of the surrounding cells when undergoing apoptosis. Clearance of apoptotic neurons is vital as cells that are not cleared may undergo secondary necrosis, become leaky, and release intracellular contents that are toxic and inflammatory. Efficient clearance is thought to be critical in order to avoid an adverse immune reaction and secondary degeneration (Ravichandran, Lorenz 2007). However, the precise mechanisms by which apoptotic neurons mediate their clearance have yet to be elucidated. Most of the work on apoptotic cell clearance has been done in the context of peripheral systems or in invertebrate animal models (Truman, Ford et al. 2008, Elliott, Chekeni et al. 2009, Gronski, Kinchen et al. 2009). Elucidation of mechanisms used for clearance of apoptotic cells in the mammalian brain is an important next step.

Studies have shown that as cells undergo apoptosis, they release soluble signals that attract phagocytes and modulate their clearance (Ravichandran, Lorenz 2007), and the chemokine fractalkine has been described as one of many 'find me' signals released by apoptotic cells (Truman, Ford et al. 2008). The finding that a cytokine is involved in

apoptotic cell clearance ran counter to the general dogma that apoptotic cell death is immunologically silent (Ravichandran 2003), and was a novel function to be ascribed to a cytokine until a recent paper suggested that other cytokines can also act as 'find me' signals to recruit phagocytes toward apoptotic cells (Cullen, Henry et al. 2013).

Fractalkine is a transmembrane chemokine that is cleaved constitutively by matrix metalloprotease ADAM10 and inducibly by ADAM 17 (also known as the TNFα-converting enzyme, TACE) to release an extracellular soluble fragment. Inducible cleavage occurs following cell stress or injury, and the soluble fragment acts as a chemotactic factor for T cells, monocytes, and microglia (Bazan, Bacon et al. 1997, Harrison, Jiang et al. 1998).

The study describing fractalkine as a 'find me' signal showed that it is released following induction of apoptosis and that the fractalkine receptor, CX3CR1, modulates recruitment of phagocytes to apoptotic germinal center B cells (Truman, Ford et al. 2008). Whether these processes are relevant *in vivo* in a physiologically relevant central nervous system (CNS) injury has yet to be determined, but it seems plausible that fractalkine signaling could play an important role in recognition and clearance of apoptotic neurons in the brain.

In the context of the CNS, fractalkine has been described in general terms as a 'neuron-microglia communication factor.' Fractalkine is expressed by neurons and cleaved by matrix metalloproteases to release a soluble fragment after neuronal stress. Neurons express high amounts of fractalkine and microglia express the fractalkine receptor, CX3CR1 (Harrison, Jiang et al. 1998). Studies in CNS models have largely

focused on the role of fractalkine in neurotoxicity and have shown that fractalkine signaling modulates the inflammatory response of microglia (Noda, Doi et al. 2011, Mizuno, Kawanokuchi et al. 2003); however, whether fractalkine signaling promotes a beneficial versus a detrimental response has been unclear, as studies have come to different conclusions depending on the injury model and the outcomes measured (Noda, Doi et al. 2011, Fuller, Van Eldik 2008, Mizuno, Kawanokuchi et al. 2003, Staniland, Clark et al. 2010). An interesting paper showed that CX3CR1 deficiency leads to delayed development of the barrel cortex, suggesting that fractalkine plays a role in developmental pruning(Hoshiko, Arnoux et al. 2012). However, as far as we know, no one has looked at the role of fractalkine signaling in a developmental apoptotic injury.

An animal model of fetal alcohol syndrome is a useful tool with which to study developmental neuronal apoptosis. Ethanol exposure at postnatal day 7 causes robust apoptosis (as opposed to other forms of cell death such as necrosis) and the dose required and time course have been well characterized (Ikonomidou, Bittigau et al. 2000). This model has been extensively used to study factors involved in the neuronal apoptotic cascade (Young, Klocke et al. 2003, Ghosh, Walls et al. 2009). However, this model has not been widely used to assess what factors may be involved in orchestrating clearance of apoptotic neurons or the response of neighboring glia.

Up to this point, there had been no evidence that acute ethanol exposure and subsequent neuronal apoptosis involves inflammatory factors; however, our data provide strong evidence for a function of inflammatory mediators. We show that ethanol-induced apoptosis leads to production of soluble fractalkine and expression of

inflammatory cytokines, and we demonstrate that fractalkine signaling plays a role in the injury response. Deficiency in fractalkine or the receptor leads to increased apoptotic debris and an altered inflammatory response. This suggests that fractalkine release from apoptotic neurons may act as a 'find me' signal to recruit microglia and promote clearance after ethanol-induced apoptosis.

METHODS

Tissue processing

All animal procedures were approved by the University of Virginia Animal Care and Use Committee. Mice used were C57/bl6 (Charles River), $CX3CR1^{eGFP/+}$ and $CX3CR1^{eGFP/eGFP}$ (Jung, Aliberti et al. 2000) or fractalkine knockout (Cook, Chen et al. 2001) on C57/bl6 background. $CX3CR1^{eGFP}$ mice have GFP inserted into the CX3CR1 locus, therefore $CX3CR1^{eGFP/eGFP}$ animals are functional knockouts. Brains were harvested and fixed in either paraformaldehyde or 70% ethanol.

Ethanol injury and brain-conditioned media

Ethanol was injected subcutaneously in postnatal day 7 pups as a 20% solution in 0.9% saline at 15.9μL/g body weight. It was administered twice, 2 hours apart (as described by (Ghosh, Walls et al. 2009)). Brain tissue was harvested 4 or 6 hours after the first injection. Brain-conditioned media was prepared as follows: brains harvested at 6 hours were hemisected and three coronal cuts were made. These tissue chunks were

incubated in DMEM (no antibiotics, 1 mL per brain) in a 15mL conical tube for 2 hours on a rocker on ice. The media was then isolated, excluding the tissue, and filtered through a .4μm filter and stored at -20°C until use.

Western Blotting

Brain-conditioned media from 2 brains (2mLs) was collected and a BCA protein assay (Pierce) was performed. Protein (2mg) was precipitated in 15% TCA at 4°C for 2 hours. The precipitate was spun down at 12k rpm for 15 minutes at 4°C. The resulting pellet was washed 3 times with ice-cold acetone. The pellet was resuspended in 2X alkaline sample buffer (100mM Tris pH 8.0, 4% SDS, 200mM DTT, 20% glycerol). A NuPAGE gel (Life Technologies) was loaded with 50ug of protein per lane and separated by electrophoresis using standard procedures. Gels were transferred to a PVDF membrane (Immobilon) for 90 min with a semidry transfer apparatus and treated with blocking reagent (LI-COR block; LI-COR, Lincoln NE) for 1 hour and then probed with primary antibodies overnight. Antibodies used were the following: rat monoclonal anti-fractalkine (1:500, R&D systems). For visualization, blots were incubated with fluorescent secondary antibodies (1:2000, LI-COR) for 2 hours and imaged on a LI-COR Odyssey infrared scanner.

Cell Culture

Glia were harvested from the forebrain of newborn pups (postnatal day 1-3). Briefly, meninges were removed from the brain and tissue was dissociated in 0.05%

trypsin EDTA for 10 min at 37 °C. Following trituration, cells were suspended in DMEM supplemented with 10% fetal bovine serum and plated into flasks. Cells were grown in an incubator at 37°C, 5% CO_2. Media was replaced twice per week for 2 weeks to obtain mixed glial culture. To harvest glia-conditioned media, media on mixed-glial cultures was changed to fresh growth media (DMEM with 10% FBS), then this media was collected after 24-48 hours. Microglia were isolated via the shake-off method. Briefly, flasks were shaken for 2-4 hours at 37 °C and the resultant detached microglia were spun down and resuspended at desired cell density.

Bone marrow-derived macrophages were prepared from mice by flushing the femurs with 1% FBS in PBS and then cultured in RPMI containing 10% L929 media for 7 days. Resident peritoneal macrophages were collected from mice by flushing the peritoneal cavity with 1% FBS in PBS and then plating collected cells in XVIVO-10 supplemented with 1% PSQ. Cells were allowed to adhere overnight and floaters were washed off; remaining cells were used in the phagocytosis assay a day later.

Migration assay

Chemoattractants included soluble fractalkine (.1nM-10nM, chemokine domain, R&D systems), CXCL12 (100ng/mL, R&D systems), and brain-conditioned media harvested from control or ethanol-treated pups. An anti-fractalkine antibody (3.5ug/mL, rat monoclonal, R&D systems) was used in some experiments to neutralize fractalkine. Chemokines were prepared in .1% BSA in DMEM and brain-conditioned media was used neat. Chemoattractants were added to 12-well plates at a volume of 600uL per well

and allowed to equilibrate in the incubator for 30 minutes prior to addition of transwell inserts (Millicell-PCF inserts, 8um pore size, Millipore) and microglia. Microglia were isolated via the shake-off method, resuspended in .1% BSA in DMEM, and $5x10^4$ cells were added in 400uL to the upper chamber, according to transwell instructions. Plates were placed in the incubator for the duration of migration. After 3 hours, transwells were placed in 4% PFA with DAPI for 20 minutes in order to fix cells and stain nuclei. The top of the inserts was wiped clean and only migrated cells remained on the membrane. The membrane was imaged (6-8 fields), and the number of cells per field was averaged for each transwell. Replicates were biological replicates, that is, each replicate data point represents microglia harvested from a different animal.

Immunostaining

For cleaved-caspase-3 and fractin staining, tissue was processed into paraffin by standard methods. Paraffin-embedded sections were dewaxed, rehydrated, underwent antigen retrieval (Tris-EDTA pH 9, 12 min over a boiling water bath), were quenched (15 min, .6% H2O2 in dH2O) and blocked (1 hour, 2% horse serum, .1% Tween in PBS) prior to incubation with primary (overnight at 4°C, diluted in block). Primary antibodies: fractin (Millipore, 1:1000), CC3 (Cell Signaling, 1:100). Immunoperoxidase detection was performed using the ImmPress polymeric peroxidase reagents (Vector). Diaminobenzidine (Dako) 1 mg/ml plus 0.02% hydrogen peroxide was applied for 3–5 min. Immunofluorescence detection was performed using secondary antibodies conjugated to Alexa-488 and Alexa-546 dyes (Invitrogen, 1:2000).

Confocal Imaging

Free-floating sections were cut to a thickness of 40μm and stained with DAPI. Confocal imaging was performed using a Leica SP5 X. Images in stacks were .5μm apart and the depth collected was 20μm. Images were acquired from the cortex and data represents the average of 3-6 fields per animal. Microglia were visualized with endogenous GFP expression and apoptotic cells were identified via their DAPI-stained pyknotic nuclei.

Phagocytosis

Thymocytes from 6-8 week old mice were incubated with 50μM of dexamethasone for 4 hours and then labeled with CypHer 5e. Stained thymocytes were resuspended in glia-conditioned medium and added to phagocytes. The cells were then spun down and incubated at 37°C, 5% CO2 for 1 hour. After completion of the engulfment assay, the wells were washed three times with PBS, trypsinized, and resuspended in glia-conditioned medium and analyzed by two-color flow cytometry. The microglial cells were recognized by their GFP fluorescence. For each point, 10,000 GFP-positive events were collected and the data was analyzed using FlowJo software.

Quantitative PCR

For quantitative PCR using brain tissue, pieces of lateral cortex were isolated and stored at -80°C until RNA isolation. RNA was isolated using RNeasy Lipid Mini kit (Qiagen). Reverse transcription was performed using 1000ng of RNA according to manufacturer's instructions (High Capacity cDNA kit, Applied biosystems). Quantitative PCR was performed with Sybr green according to manufacturer's instructions (Platinum Sybr kit, Life Technologies) with annealing temperatures of 60°C. Primers used were: actin, forward CCCAGAGCAAGAGAGGTGTC, reverse AGAGCATAGCCCTCGTAGAT; IL-6, forward GAGGATACCACTCCCAACAGACC, reverse AAGTGCATCATCGTTGTTCATACA; IL-10, forward CCCTGGGTGAGAAGCTGAAG, reverse CACTGCCTTGCTCTTATTTTCACA; TNFα, forward GGCAGGTCTACTTTGGAGTCATTGC, reverse ACATTCGAGGCTCCAGTGAATTCGG; CX3CL1, forward CTCACGAATCCCAGTGGCTT, reverse TTTCTCCTTCGGGTCAGCAC; CX3CR1, forward TGCAGAAGTTCCCTTCCCATC, reverse GGCCTCAGCAGAATCGTCATA; CXCR1eGFP, forward (same as CX3CR1) TGCAGAAGTTCCCTTCCCATC, GFP reverse CTGAACTTGTGGCCGTTTAC. Specificity of CX3CR1, CX3CR1eGFP and CX3CL1 was confirmed by lack of amplification in respective knockout tissues.

RESULTS

In vivo ethanol-induced neuronal apoptosis leads to release of soluble fractalkine

We hypothesized that fractalkine signaling may play a role in the microglial response to apoptotic neurons. Therefore, we used an animal model of fetal alcohol syndrome in order to induce neuronal apoptosis *in vivo* and tested whether soluble fractalkine was released. We harvested brains after ethanol-induced apoptosis and incubated them in media to isolate diffusible extracellular factors and tested whether fractalkine was present. We detected soluble fractalkine in brain-conditioned media from animals treated with ethanol, but not in saline-treated controls (Fig. 1a). This shows that fractalkine is released as a soluble fragment in response to ethanol-induced injury.

Microglia migrate toward apoptotic brain-conditioned media in a fractalkine and CX3CR1-dependent manner

Microglia are the only cells in the brain that express appreciable levels of the fractalkine receptor, CX3CR1, and are the cell most likely to respond to fractalkine released by injured neurons. Fractalkine is a known chemotactic factor, and we aimed to determine whether fractalkine released from apoptotic neural cells was necessary and sufficient to induce microglial chemotaxis.

We found that microglia migrate towards soluble fractalkine, and there was no difference in migration between wild type versus CX3CR1 heterozygous microglia (Fig. 1b); therefore heterozygous microglia were used in subsequent experiments. We found that migration toward fractalkine was dose-dependent, and as expected, CX3CR1-knockout microglia did not migrate toward fractalkine (Fig. 1c). CX3CR1 deficiency

does not lead to a general migration defect as knockout microglia are still able to migrate toward another chemokine, CXCL12 (Fig. 1d). A fractalkine-neutralizing antibody blocks migration toward fractalkine, and this antibody is not a general inhibitor of migration, as it has no effect on migration toward CXCL12 (Fig. 1e).

Next, we tested whether microglia respond to brain-conditioned media. The apoptotic brain-conditioned media from ethanol-treated animals was sufficient to induce migration (Fig. 2a). Microglia did not migrate toward the non-apoptotic brain-conditioned media from the control saline-treated animals. Fractalkine signaling was absolutely required to stimulate migration toward the apoptotic brain-conditioned media. Neutralizing fractalkine blocked migration toward the apoptotic brain-conditioned media (Fig. 2a), and CX3CR1-deficient microglia failed to migrate toward it (Fig. 2b). This data shows that in the context of ethanol-induced injury, soluble fractalkine signals to microglia in a CX3CR1-dependent manner. Our data suggests that this signaling could help microglia hone in to apoptotic neurons.

Fractalkine or CX3CR1 deficiency leads to an increase or persistence of apoptotic debris in the brain after ethanol-induced apoptosis

Fractalkine signaling to microglia appears to play a role in the response to apoptotic stimuli, and we hypothesized that deficiency in fractalkine signaling may lead to an increase or persistence of apoptotic debris in our fetal alcohol syndrome model. We quantified the amount of apoptotic debris after ethanol-induced apoptosis and found that the fractalkine and CX3CR1-knockout mice had increased apoptotic debris

compared to wild type animals by 6 hours after injury (Fig.3a-b). Of note, CX3CR1 heterozygous mice had levels of debris comparable to wild type animals (Fig 3c). We hypothesized that this increase in debris could be due to a defect in microglial recruitment to apoptotic cells. Brain tissue from CX3CR1-knockout or CX3CR1 heterozygous pups was collected at 4 hours and 6 hours after ethanol treatment and confocal images were acquired. There was no difference in microglial cell density between the heterozygous or the knockout animals (Fig. 4a). Therefore the increase in debris in the CX3CR1-knockout brain is not attributable to a difference in density of microglia. Microglia are normally ubiquitous throughout brain tissue, therefore long distance migration may not be required for the microglial response. Instead, apoptotic signals may signal for local 'recruitment' of microglia, and this could manifest as movement of the entire cell or just the arms or processes of the cell. An association index was calculated by quantifying the fraction of microglia touching apoptotic cell bodies. CX3CR1-knockout microglia had a lower association index at 6 hours (Fig. 4b). It is possible that an early difference in recruitment or association could contribute to the increased debris seen at 6 hours after injury. Therefore, recruitment was also assessed at 4 hours by measuring the distance between each apoptotic corpse (highlighted by its DAPI-stained pyknotic nucleus) and the nearest microglial process (highlighted by eGFP). However, there was no difference in recruitment or association index at the earlier 4-hour time point (Fig. 4c-d).

An increase in apoptotic debris could be due to defects in microglial recruitment, but could also be due to a defect in microglial phagocytosis and clearance. We used the

same confocal images to determine whether CX3CR1-deficient microglia had an *in vivo* defect in phagocytosis (Fig. 5a). The fraction of apoptotic debris engulfed within microglia was quantified and the microglial phagocytic index was quantified by measuring the fraction of microglia containing engulfed apoptotic cells (Fig. 5b-c). We found no change in the fraction of debris engulfed or the phagocytic index at either 4 or 6 hours after ethanol treatment.

We also performed *in vitro* phagocytosis assays to determine whether fractalkine signaling modulates phagocytosis. We tested whether soluble fractalkine promotes phagocytosis and whether CX3CR1-knockout cells have a defect in phagocytosis. We utilized multiple approaches. We used apoptotic thymocytes as targets and tested macrophages pretreated with fractalkine or treated concurrent with addition of apoptotic cells (Fig 5a-d). Addition of exogenous fractalkine had no effect and CX3CR1-deficient macrophages had a comparable phagocytic index. Next, we tried microglia isolated from CX3CR1 heterozygous or knockout glial cultures, but found no effect of fractalkine or CX3CR1 deficiency (Fig. 5e). Finally, we speculated that perhaps astrocytes produce fractalkine and could have an effect on the microglial phenotype and response. We added apoptotic thymocytes to mixed glial cultures from CX3CR1 heterozygous or knockout animals treated with or without fractalkine and quantified the microglial phagocytic index and found that neither exogenous fractalkine nor CX3CR1-deficiency had an effect (Fig. 5f). The combination of *in vitro* and *in vivo* data suggest that fractalkine signaling does not have a prominent role in regulating phagocytosis.

We have not ruled out the possibility that CX3CR1- knockout microglia have a defect in their ability to digest apoptotic cells, which could also lead to a persistence of debris after ethanol-induced apoptosis.

Fractalkine or CX3CR1 deficiency leads to an altered inflammatory response to ethanol-induced apoptosis

Apoptotic cells and fractalkine are both known to modulate inflammatory responses. Therefore, we hypothesized that the increased apoptotic load and/or defective fractalkine signaling would lead to an altered inflammatory response in the brain after ethanol injury. We quantified mRNA expression of factors associated with microglial activation and cytokines, including arginase 1 (Arg1), cyclooxygenase-2 (COX-2), the interleukins IL-6 and IL-10, and TNFα as well as fractalkine and CX3CR1. We found increased IL-6 mRNA at 6 hours after ethanol treatment in wild type animals. In addition we found an altered expression profile in the brain of CX3CR1 knockouts and fractalkine knockouts compared to wild type animals after ethanol treatment (Fig. 8,9,10). We began our analyses comparing the inflammatory response in wild type and CX3CR1 knockout after ethanol treatment (Fig. 7,8). We then tested to see whether the fractalkine knockout phenocopied the CX3CR1 knockout (Fig. 9). We quantified IL-6 and TNFα mRNA expression 6 hours after ethanol treatment. At 6hrs after ethanol treatment, IL-6 expression in the brain of both fractalkine and CX3CR1-knockout mice was increased compared to wild type. Baseline levels of TNFα did not vary between wild type and CX3CR1 mice, and only CX3CR1-knockouts upregulated TNFα at 6 hours

after ethanol injury. In contrast, fractalkine-knockout mice had increased TNFα expression at baseline, at levels comparable to the levels seen in ethanol-treated CX3CR1 mice, and the level did not change with ethanol treatment.

We also tested whether fractalkine or CX3CR1 expression was modulated by ethanol-induced apoptosis. We found no difference in mRNA expression in the brain of wild type animals after ethanol treatment. We also analyzed expression in the knockout animals. We found an increase in fractalkine mRNA expression in the CX3CR1-knockout animals after ethanol treatment. We assessed expression of transcript for the receptor and we found increased CX3CR1 in the fractalkine knockout. The CX3CR1 knockout does not express functional CX3CR1, however GFP transcript can be used as a reporter for gene expression. We used a primer set designed to amplify CX3CR1-eGFP transcript and we found increased production of this transcript in the CX3CR1 knockout after ethanol treatment.

DISCUSSION

Fractalkine has been previously described as a neuron-microglia communication factor and is known to be a chemokine that can modulate migration of immune cells (Ransohoff, Liu et al. 2007). Our data illuminate the importance of fractalkine signaling in the response to apoptotic neuronal cells. In addition, we show that ethanol exposure not only induces apoptosis, but also induces an inflammatory response in the developing brain that appears to be modulated by fractalkine signaling.

Only one previous study has looked at fractalkine after ethanol injury. They showed that the quantity of fractalkine protein increases after prenatal ethanol injury in mice (Roberson, Kuddo et al. 2011). Using our model, we did not detect mRNA expression changes in wild type mice after postnatal ethanol injury Fig. 9b). However, when we isolated brain-conditioned media, that is, the extracellular soluble components from the brain, we detected an increase in cleaved soluble fractalkine after ethanol injury (Fig. 1a). This cleaved fractalkine released from apoptotic neurons may create a gradient that allows microglia to hone in on apoptotic neurons.

A previous study showed that fractalkine acts as a 'find me' signal to guide phagocytes such as macrophages to apoptotic cells (Truman, Ford et al. 2008), and others have shown that fractalkine can modulate chemotaxis of microglia (Maciejewski-Lenoir, Chen et al. 1999). However, these studies predominantly used *in vitro* models or peripheral systems. We show that fractalkine acts as an important 'find me' signal to modulate microglial recruitment in order to help clear apoptotic neurons in *in vivo* brain injury.

Apoptosis may result in the release of many factors, and fractalkine is only one of many possible chemoattractants (Ravichandran 2003, Ravichandran, Lorenz 2007). However, we show that fractalkine signaling is critical for migration toward apoptotic brain-conditioned media: blocking fractalkine signaling by neutralizing fractalkine or through CX3CR1 deficiency prevents migration (Fig. 2). Does this suggest other 'find me' signals are irrelevant?

Other signals such as ATP and UDP have been shown to modulate microglial movement and phagocytosis (Davalos, Grutzendler et al. 2005, Koizumi, Shigemoto-Mogami et al. 2007). ATP and UDP are unstable in the extracellular space due to the presence of ubiquitous ATPases (Zimmermann 2000). It seems possible that fractalkine may have a longer half-life than other potential 'find-me' signals and therefore fractalkine may just be the dominant chemoattractant remaining in apoptotic brain-conditioned media. These other signals may still be relevant in other conditions.

Our *in vitro* data suggests that fractalkine 'find me' signaling is the critical factor for recruitment of microglia; however, *in vivo*, other signals are probably also involved. Although we found that microglia from CX3CR1-knockout mice did not associate with apoptotic debris as well as wild type microglia, the *in vivo* defect in recruitment and association after ethanol injury was not large (Fig. 4). This suggests two possibilities: a) microglia are ubiquitous and motile enough that in the absence of fractalkine signaling they are still able to encounter apoptotic debris by chance, or b) perhaps there are other factors that can act to recruit microglia in the absence of fractalkine signaling. For example cell surface 'eat me' signals are likely involved.

A defect in recruitment or the association of microglia with apoptotic neurons would lead to failed or slowed clearance of debris. We speculate that this explains why the fractalkine and CX3CR1-knockout brains have more apoptotic debris after ethanol injury compared to wild type animals (Fig.3).

The increased apoptotic debris could be attributable to a defect in recruitment, but could also be due to a defect in phagocytosis. However, we could not find any

evidence for an *in vivo* defect in phagocytosis, as the microglial phagocytic index was similar in wild type and CX3CR1-knockout animals (Fig. 5). In addition, we tested *in vitro* phagocytosis and found no effect of fractalkine and no defect in the CX3CR1-deficient microglia (Fig. 6). Another factor that would influence the amount of debris is the rate of degradation of apoptotic material, and we have not ruled out the possibility that CX3CR1-knockout microglia could have a defect in the ability to digest corpses. This could be tested by following the fate of apoptotic cells in time lapse imaging experiments both *in vitro* and perhaps *in vivo* using slice cultures of alcohol-injured brain.

We do not know if other glia are also playing a role in clearance of apoptotic cells. Astrocytes are capable of engulfment (Noda, Doi et al. 2011), and it is possible that they may engulf debris after alcohol injury. However, we were unable to identify astrocytes via conventional astrocyte markers such as glial fibrillary aidic protein (GFAP) or S100β at this age in development. Therefore, we were unable to determine whether astrocytic engulfment contributed to clearance. Astrocytes do not express appreciable levels of CX3CR1 *in vivo*; therefore they are unlikely to be responding to fractalkine in this injury.

A common dogma in the field of apoptotic cell clearance is that cells must be cleared in order to prevent an exaggerated immune response (Ravichandran, Lorenz 2007). Interestingly, we find that in conjunction with the increased apoptotic cell load, we see an exaggerated immune response in the fractalkine and CX3CR1-knockout animals. It would be interesting if this exaggerated inflammatory response were due to

persistence of apoptotic debris and secondary necrosis. However, we cannot tease apart whether this altered immune response is due the persistence of apoptotic cells or due to the defect in fractalkine signaling, as both apoptotic cells and fractalkine have been shown to modulate inflammatory responses (Mizuno, Kawanokuchi et al. 2003, Griffiths, Gasque et al. 2009).

Interestingly, there are common signaling pathways induced by fractalkine and apoptotic cells. Both have been shown to lead to an influx in calcium in phagocytic cells (Harrison, Jiang et al. 1998, Gronski, Kinchen et al. 2009). One study showed that the influx in calcium was critical for an anti-inflammatory response in phagocytes (Gronski, Kinchen et al. 2009). It is possible that an increase in intracellular calcium could be a common signal used to generate an anti-inflammatory response in phagocytes in response to both fractalkine and apoptotic cells.

Related to this, another possibility we have not ruled out is that the increase in apoptotic debris could be due to increased neurotoxicity because of an adverse inflammatory response. Fractalkine may be important for immunomodulation (perhaps suppression). Fractalkine has been shown to downregulate production of proinflammatory factors in response to LPS (Mizuno, Kawanokuchi et al. 2003). Avoiding the exaggerated immune response may be critical to avoid secondary degeneration.

Another goal of this study was to determine whether there is an inflammatory response after acute ethanol injury. *In vitro* studies have suggested that ethanol leads to TLR4 signaling (Blanco, Guerri 2007, Fernandez-Lizarbe, Pascual et al. 2009, Alfonso-

Loeches, Pascual-Lucas et al. 2010, Fernandez-Lizarbe, Montesinos et al. 2013), and this suggests that ethanol may be a pro-inflammatory stimulus. Previous studies using different ethanol injury models have indicated that chronic alcohol exposure leads to inflammation (Alfonso-Loeches, Pascual-Lucas et al. 2010). To our knowledge, we are the first to show that acute *in vivo* ethanol injury is sufficient to induce increased expression of cytokines as early as 4 hours. Ultimately *in vivo* we cannot tease apart whether the ethanol or the apoptotic cells are signaling for the production of cytokines.

Future directions

In vitro or *ex vivo* experiments using time lapse imaging would allow monitoring of migration, phagocytosis, and the fate of debris once engulfed. This may illuminate defects that are not seen via the other assays we have used. For example, we would like to determine whether degradation of apoptotic cells is affected by fractalkine signaling.

Future experiments would aim to establish which downstream signaling pathways are involved in modulating the response to ethanol, fractalkine, and apoptotic cells. Not many specific details are known about downstream mediators involved in fractalkine signaling, and based on our expression data, we speculate that it involves regulation of transcription factors or repressors that modulate expression of inflammatory factors.

It is interesting that the ligand and receptor knockout phenocopied with respect to increased apoptotic debris after injury, but had differences in mRNA expression of TNFα. It is possible that intact fractalkine has other important functions distinct from its

role in CX3CR1-receptor signaling that would explain baseline (pre-injury) differences in TNFα expression in the fractalkine-knockout brain. Fractalkine is known as an adhesion molecule. Perhaps it also associates with and modulates other signaling molecules or has an (as of yet unidentified) intracellular signaling component. It is also interesting that fractalkine and TNFα are both cleaved by ADAM 17 (also known as the TNF*α*-converting enzyme, TACE). Perhaps fractalkine deficiency somehow leads to dysregulation of TNF*α* due to this shared relationship with ADAM 17.

Finally, we show that there is an immune response after ethanol injury. It would be of interest to establish whether TLR 4 is involved in this acute *in vivo* response to ethanol by exposing TLR4 deficient mice to this injury. Quantifying apoptosis and characterizing the cytokine production may help tease apart the relative contribution of ethanol versus apoptotic cells in regulation of the inflammatory response.

FIGURES

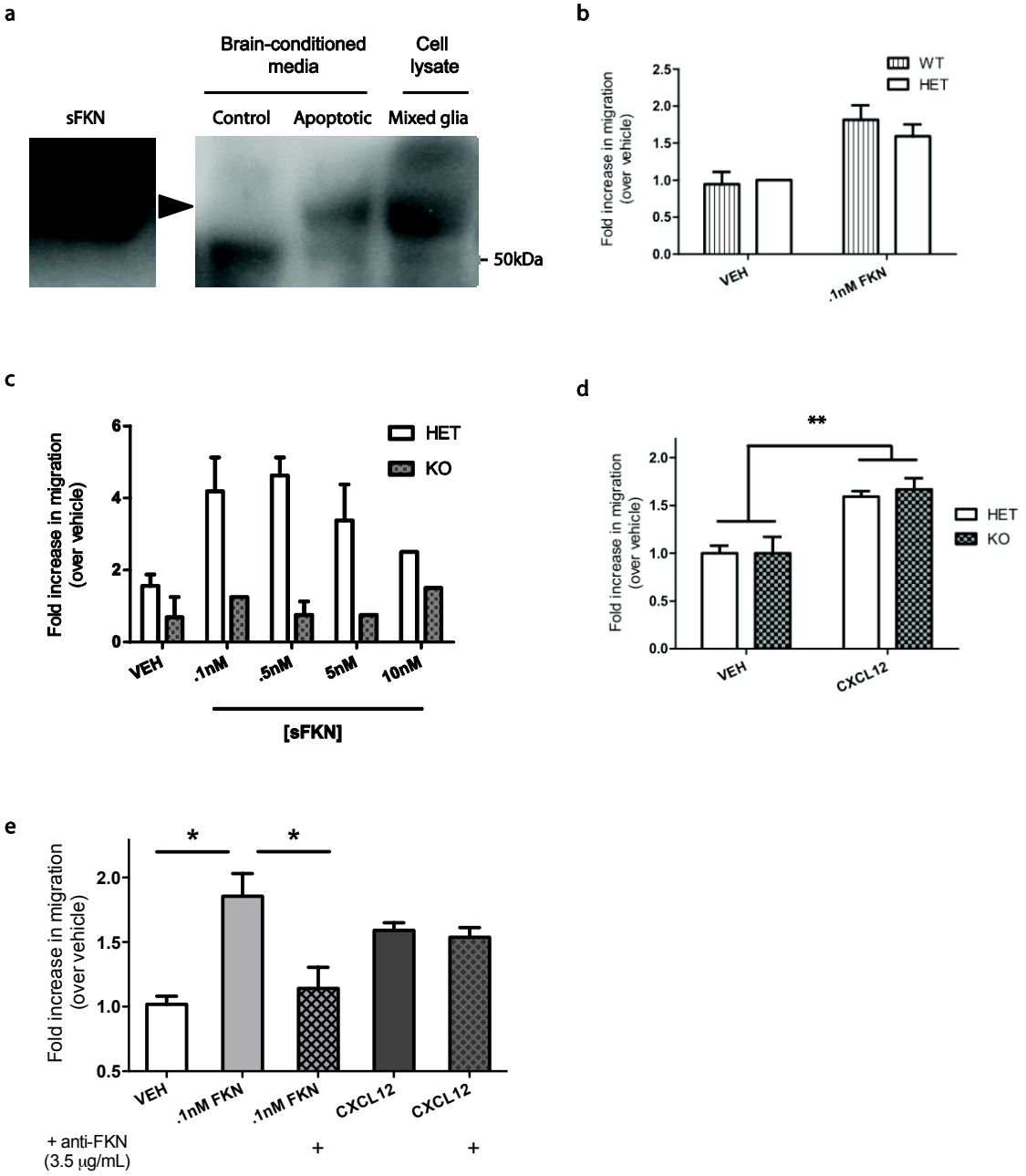
a
Brain-conditioned media
Cell lysate
sFKN
Control
Apoptotic
Mixed glia
50kDa
b
WT
HET
Fold increase in migration (over vehicle)
VEH
.1nM FKN
c
HET
KO
Fold increase in migration (over vehicle)
VEH
.1nM
.5nM
5nM
10nM
[sFKN]
d
**
HET
KO
Fold increase in migration (over vehicle)
VEH
CXCL12
e
*
*
Fold increase in migration (over vehicle)
VEH
.1nM FKN
.1nM FKN
CXCL12
CXCL12
+ anti-FKN (3.5 μg/mL)
+
+

Figure 1

Figure 1: Soluble fractalkine is released into the extracellular space after injury and acts as a chemotactic factor for microglia. P7 mice were treated with saline (control) or ethanol to induce neuronal apoptosis (apoptotic), and the brains were incubated in DMEM on ice for 2 hours to isolate brain-conditioned media (BCM). 2mg of protein were TCA precipitated, run on a gel, and probed with anti-fractalkine via western blot. Soluble fractalkine (sFKN) and lysate from mixed astrocyte-microglial cultures were used for comparison. We found fractalkine in brain-conditioned media from apoptotic, but not control brain (a, arrowhead points to band of interest). Transwell migration assays were performed to determine whether microglia transmigrate toward fractalkine. Microglia were isolated from mixed glial cultures via the shake-off method and added to the upper chamber of a transwell insert. After 3 hours of migration, the cells that had migrated to the bottom surface of the transwell were fixed, stained with DAPI, and counted. Wild type and CX3CR1-heterozygous microglia migrated toward .1nM sFKN to a comparable degree and CX3CR1-heterozygous were subsequently used to compare to CX3CR1-knockout (b). A dose-response curve was done using CX3CR1-heterozygous and CX3CR1-knockout microglia with soluble fractalkine concentrations ([sFKN]) ranging from .1nM to 10nM. This showed that .1nM was sufficient to induce migration and that CX3CR1-knockout microglia fail to migrate toward fractalkine (c). CX3CR1-knockout microglia were tested for a general migration defect using CXCL12 (100ng/mL) as a chemoattractant (d). CX3CR1-heterozygous and knockout microglia migrated toward CXCL12 to a comparable degree. A fractalkine-neutralizing antibody

(3.5ug/mL) was pre-incubated with .1nM of sFKN to neutralize it and block fractalkine-induced migration. This antibody specifically blocked fractalkine-induced migration, as CXCL12-induced migration was not inhibited (e). Data is representative of repeated experiments. (d) 2-way ANOVA, **p<.01; (e) One-way ANOVA, *p<.05.

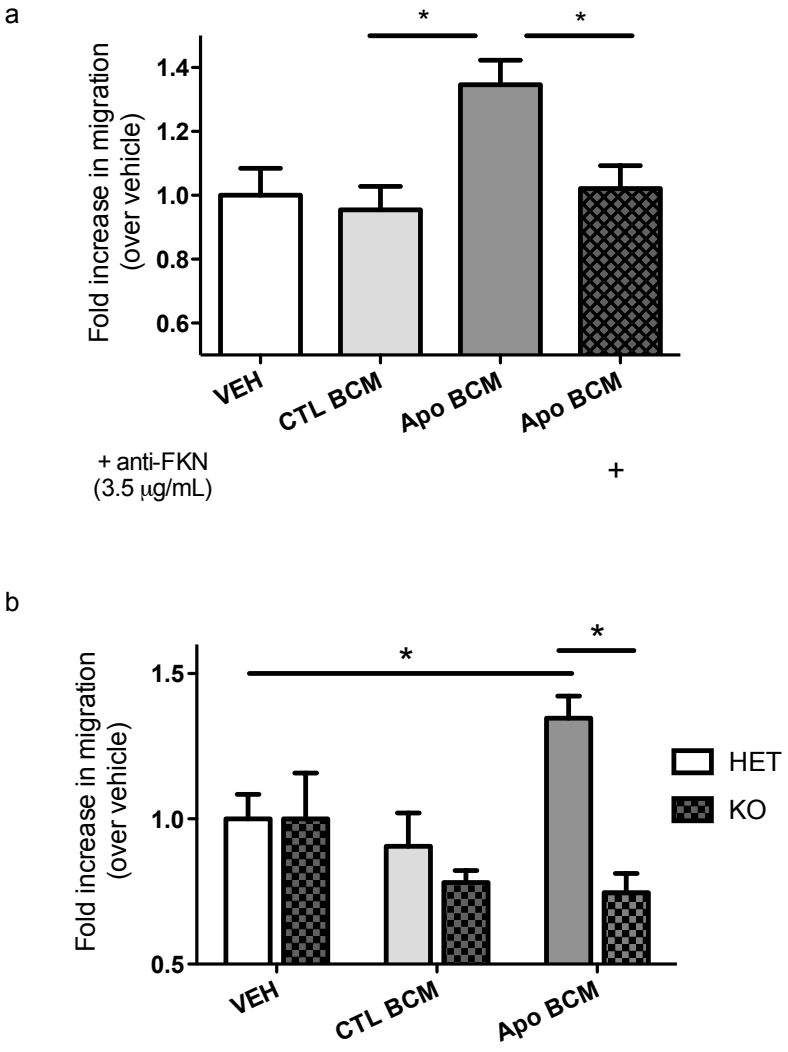
a
*
*
Fold increase in migration (over vehicle)
1.4
1.2
1.0
0.8
0.6
VEH
CTL BCM
Apo BCM
Apo BCM
+ anti-FKN (3.5 μg/mL)
+
b
*
*
Fold increase in migration (over vehicle)
1.5
1.0
0.5
VEH
CTL BCM
Apo BCM
HET
KO

Figure 2

Figure 2: Microglia migrate toward apoptotic brain-conditioned media in a fractalkine-dependent manner. P7 mice were treated with saline or ethanol to induce neuronal apoptosis, and the brains were incubated in DMEM on ice for 2 hours to isolate brain-conditioned media (BCM) from saline-treated control (CTL BCM) or apoptotic brain (Apo BCM). BCM was used as a chemoattractant in the lower chamber for transwell migration assays. Microglia were isolated from mixed glial cultures via the shake-off method and added to the upper chamber of a transwell insert. After 3 hours of migration, the cells that had migrated to the bottom surface of the transwell were fixed, stained with DAPI, and counted. Microglia migrate toward apoptotic BCM but not control BCM. A fractalkine-neutralizing antibody (3.5ug/mL) was pre-incubated with apoptotic BCM (indicated by (+)) to block fractalkine-dependent migration and this prevented migration toward the apoptotic BCM (a). Migration toward brain-conditioned media was quantified in CX3CR1 heterozygous (HET) versus knockout (KO) microglia (b). CX3CR1 deficient microglia fail to migrate toward brain-conditioned media. Data is representative of repeated experiments. Replicates are biological replicates (microglia harvested from different animals). (a,b) One-way ANOVA, *$p<.05$.

a

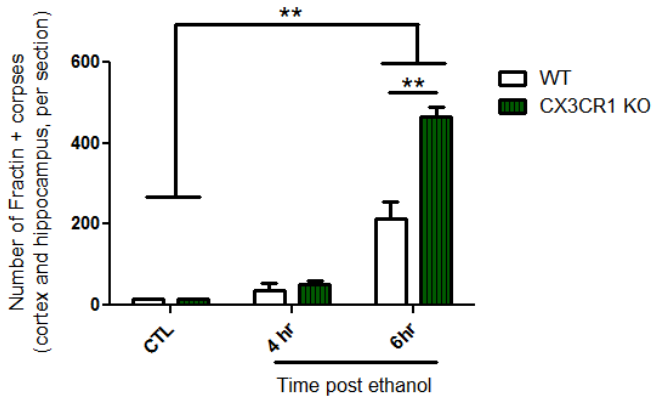
**
**
600
400
200
0
Number of Fractin + corpses
(cortex and hippocampus, per section)
WT
CX3CR1 KO
CTL
4 hr
6hr
Time post ethanol

b

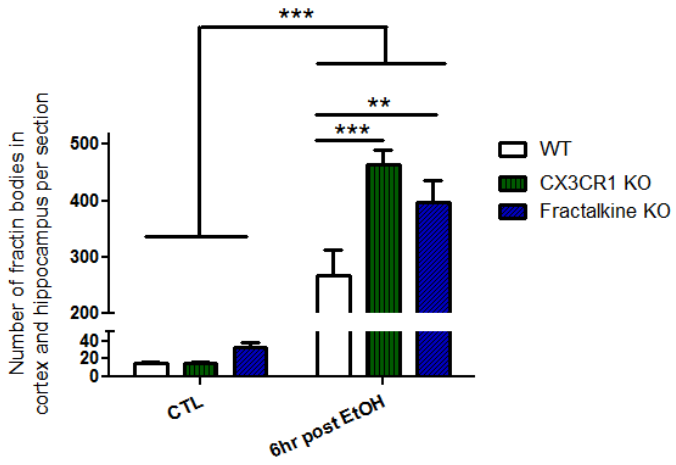
***
**
***
500
400
300
200
40
20
0
Number of fractin bodies in
cortex and hippocampus per section
WT
CX3CR1 KO
Fractalkine KO
CTL
6hr post EtOH

c

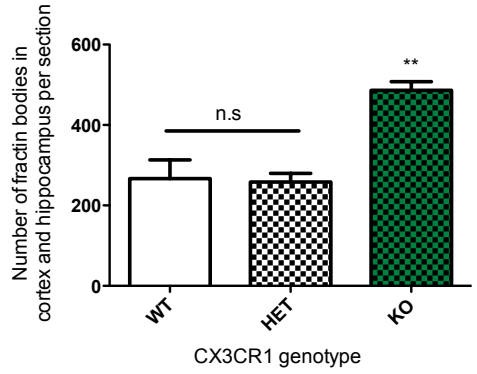
600
400
200
0
**
n.s
Number of fractin bodies in
cortex and hippocampus per section
WT
HET
KO
CX3CR1 genotype

Figure 3

Figure 3: Deficiency in fractalkine signaling leads to increased apoptotic debris at 6 hours after ethanol-induced apoptosis. Pups were injected with saline (CTL) or ethanol to induce neuronal apoptosis. Brain tissue was harvested at 4 or 6 hours after the initial injection and the number of fractin-positive apoptotic corpses in the cortex and hippocampus was counted (3 sections averaged per animal). Wild type (WT) pups were compared to CX3CR1 knockout (KO) pups at 4 and 6 hours, and by 6 hours, CX3CR1-knockout brains had increased debris compared to wild type (a). Wild type, CX3CR1-knockout, and fractalkine-knockout pups were compared at 6 hours and the number of fractin-positive apoptotic corpses in the cortex and hippocampus was counted (b). Wild type, CX3CR1 heterozygous, and CX3CR1-knockout pups were compared at 6 hours and the number of fractin-positive apoptotic corpses in wild type and CX3CR1 heterozygous was similar (c). (a,b) One-way ANOVA, (n=3-6) *$p<.05$, **$p<.01$, ***$p<.005$; (c) One-way ANOVA, (n=4-6) **$p<.01$.

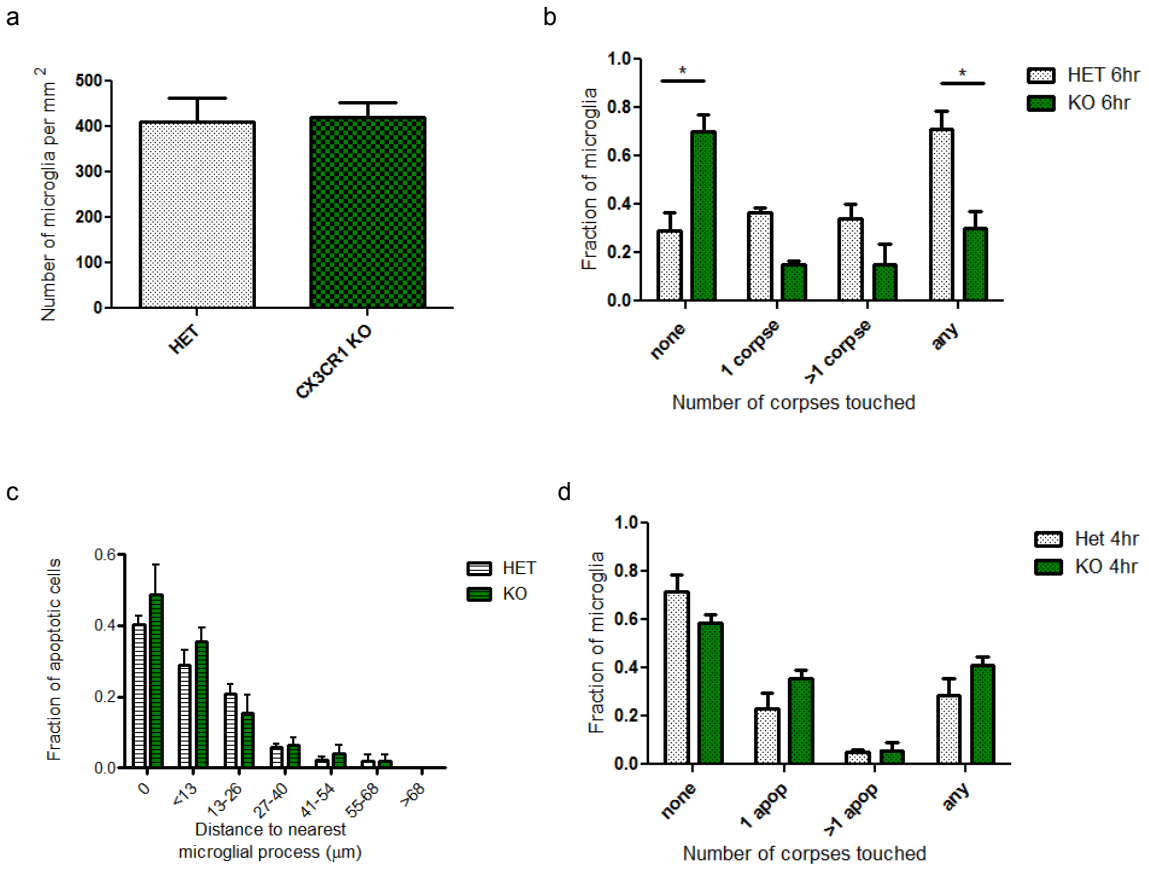
a
Number of microglia per mm 2
500
400
300
200
100
0
HET
CX3CR1 KO
b
Fraction of microglia
1.0
0.8
0.6
0.4
0.2
0.0
*
*
HET 6hr
KO 6hr
none
1 corpse
>1 corpse
any
Number of corpses touched
c
Fraction of apoptotic cells
0.6
0.4
0.2
0.0
HET
KO
0
<13
13-26
27-40
41-54
55-68
>68
Distance to nearest
microglial process (μm)
d
Fraction of microglia
1.0
0.8
0.6
0.4
0.2
0.0
Het 4hr
KO 4hr
none
1 apop
>1 apop
any
Number of corpses touched

Figure 4

Figure 4: CX3CR1-deficient microglia have a defect in association with apoptotic debris. CX3CR1-heterozygous (HET) and CX3CR1-knockout (KO) pups were injected with ethanol to induce neuronal apoptosis and tissue was harvested 4 or 6 hours later. 40μm sections were cut and confocal images of sections of the cortex were acquired. Microglia express GFP and nuclei were labeled with DAPI. Apoptotic corpses were identified via their pyknotic nuclei. The density of microglia was quantified and there was no difference between the CX3CR1-heterozygous and CX3CR1-knockout (a). An association index was determined by quantifying the fraction of microglia touching apoptotic corpses at 6 hours (b) and 4 hours (d) after injury. There was no difference at 4 hours, but by 6 hours fewer microglia from the CX3CR1-knockout had associated with apoptotic corpses as compared to the CX3CR1-heterozygous microglia. In order to confirm that there was no early defect at 4 hours, we also measured the distance from apoptotic corpses to the nearest microglial process and the values were plotted as a histogram (c). There was no difference between CX3CR1-heterozygous and CX3CR1-knockout at this early 4-hour time point. (n=3) One-way ANOVA, *$p<.05$.

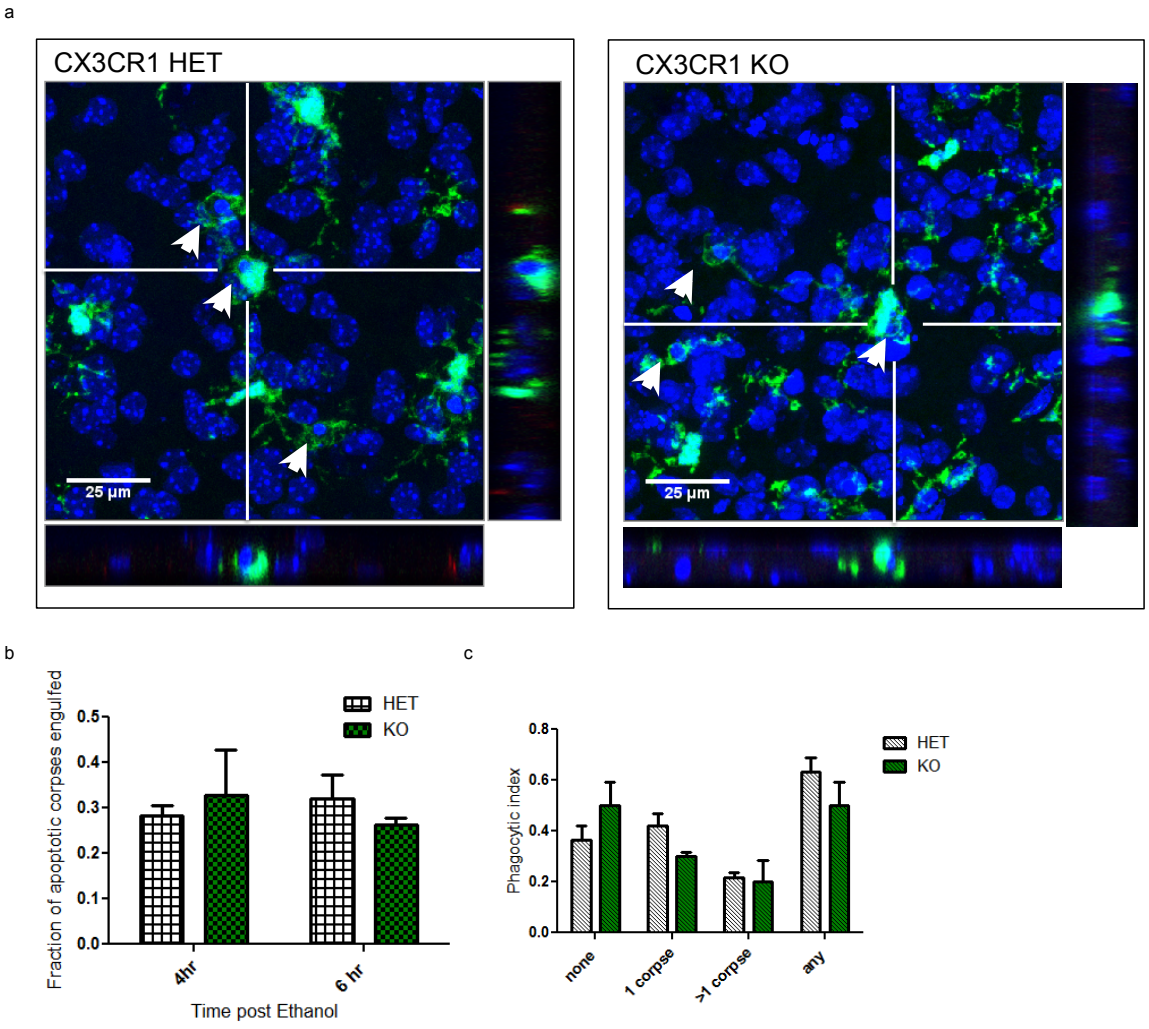
a
CX3CR1 HET
25 µm
CX3CR1 KO
25 µm
b
Fraction of apoptotic corpses engulfed
0.5
0.4
0.3
0.2
0.1
0.0
HET
KO
4hr
6 hr
Time post Ethanol
c
Phagocytic index
0.8
0.6
0.4
0.2
0.0
HET
KO
none
1 corpse
>1 corpse
any

Figure 5

Figure 5: CX3CR1 deficiency does not lead to a defect in phagocytosis *in vivo*. CX3CR1-heterozygous (HET) and CX3CR1-knockout (KO) pups were injected with ethanol to induce neuronal apoptosis. 40μm sections were cut and confocal images were acquired. Microglia express GFP (green) and nuclei were labeled with DAPI (blue). Apoptotic corpses were identified via their pyknotic nuclei (arrowheads). XZ and YZ orthogonal slices reveal DAPI-condensed pyknotic nuclei within microglia (a). The fraction of apoptotic cells that were engulfed within GFP-positive microglia was quantified at 4 and 6 hours after injury (b). A phagocytic index at 6 hours after injury was calculated by measuring the fraction of GFP-positive microglia that contained corpses (c). There was no difference in phagocytosis measures in the brain of the CX3CR1-knockout compared to the CX3CR1-heterozygous mice. (n=3) Scale=25μm.

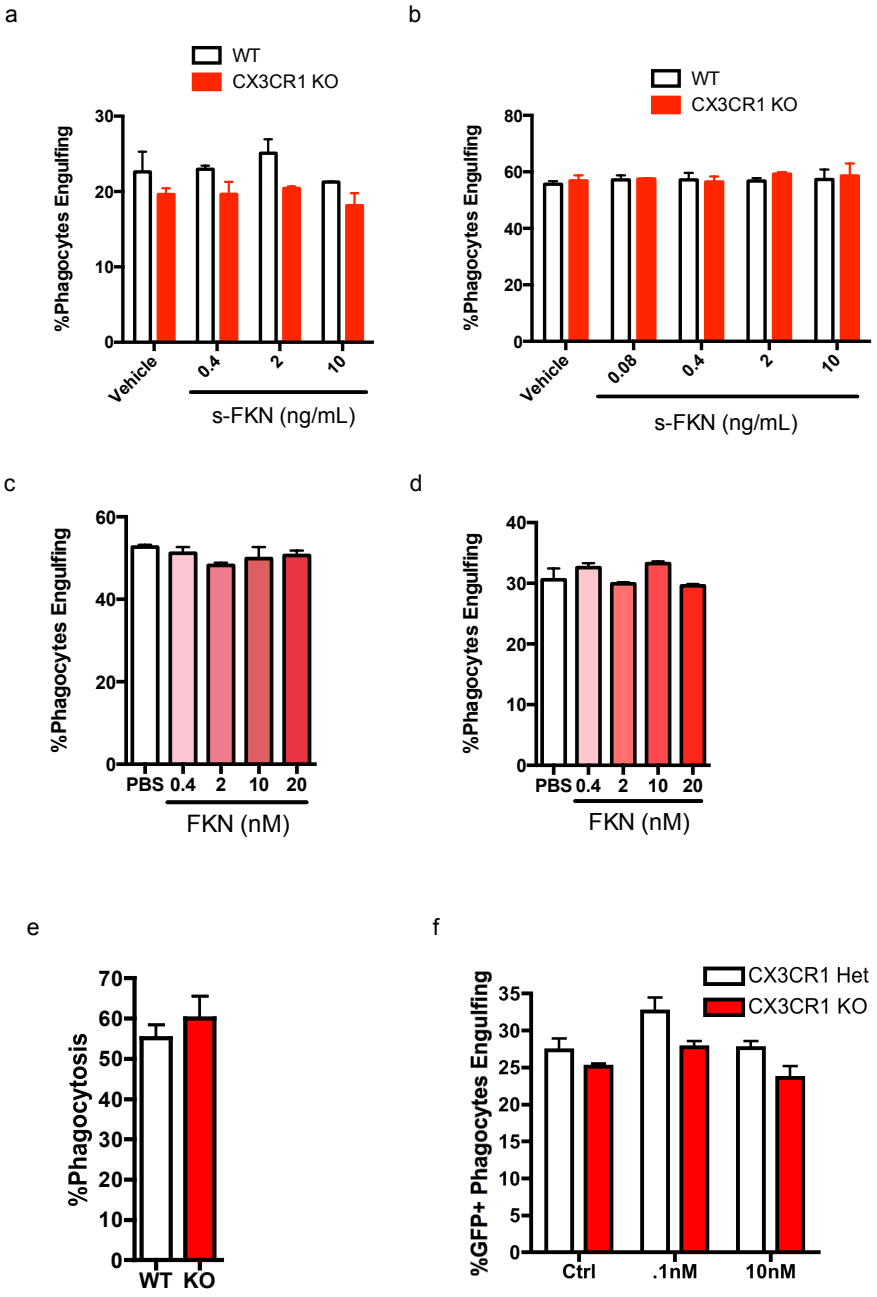
a
WT
CX3CR1 KO
%Phagocytes Engulfing
30
20
10
0
Vehicle
0.4
2
10
s-FKN (ng/mL)
b
WT
CX3CR1 KO
%Phagocytes Engulfing
80
60
40
20
0
Vehicle
0.08
0.4
2
10
s-FKN (ng/mL)
c
%Phagocytes Engulfing
60
40
20
0
PBS
0.4
2
10
20
FKN (nM)
d
%Phagocytes Engulfing
40
30
20
10
0
PBS
0.4
2
10
20
FKN (nM)
e
%Phagocytosis
70
60
50
40
30
20
10
0
WT
KO
f
CX3CR1 Het
CX3CR1 KO
%GFP+ Phagocytes Engulfing
35
30
25
20
15
10
5
0
Ctrl
.1nM
10nM

Figure 6

Figure 6: CX3CR1-deficient phagocytes do not have an overt defect in phagocytosis. Apoptotic thymocytes were used as targets, and added to either macrophages or glia and phagocytosis was allowed to proceed for 1 hour. Phagocytosis was measured via flow cytometry and the phagocytic index (fraction of cells engulfing) was calculated. Wild type (WT) and CX3CR1-knockout (KO) bone-marrow derived macrophages were treated concurrent with administration of apoptotic cells (a) or pretreated for 20 hours (b) with soluble fractalkine (s-FKN) at indicated concentrations. Wild type and CX3CR1-knockout bone-marrow derived macrophages (c) and peritoneal macrophages (d) were pretreated for 24 hours with the indicated concentrations of soluble fractalkine (FKN) before the phagocytosis assay. A phagocytosis assay was also performed on microglia isolated from wild type and CX3CR1-knockout mixed glia cultures (e). CX3CR1-heterozygous (Het) and CX3CR1-knockout mixed glial cultures were incubated with 0 (Ctrl), .1nM and 10nM of soluble fractalkine and the microglial phagocytic index was quantified by gating on GFP-positive cells (f). We detected no difference in phagocytosis with addition of exogenous fractalkine and did not detect a phagocytic defect in CX3CR1-knockout cells.

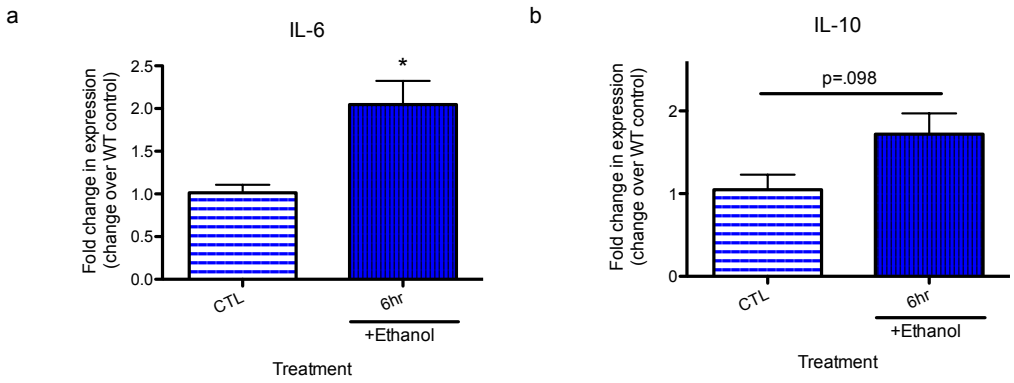
a
IL-6
Fold change in expression
(change over WT control)
2.5
2.0
1.5
1.0
0.5
0.0
*
CTL
6hr
+Ethanol
Treatment
b
IL-10
p=.098
Fold change in expression
(change over WT control)
2
1
0
CTL
6hr
+Ethanol
Treatment

Figure 7

Figure 7: Ethanol treatment leads to increased expression of IL-6. P7 animals were treated with saline (CTL) or ethanol and brain tissue was harvested 6 hours later. RNA was isolated and quantitative PCR was used to assess mRNA expression of IL-6 (a) and IL-10 (b) in control versus ethanol-treated wild type mice. Ethanol treatment led to increased expression of IL-6. (n=4-6) Students t test, *$p<.05$.

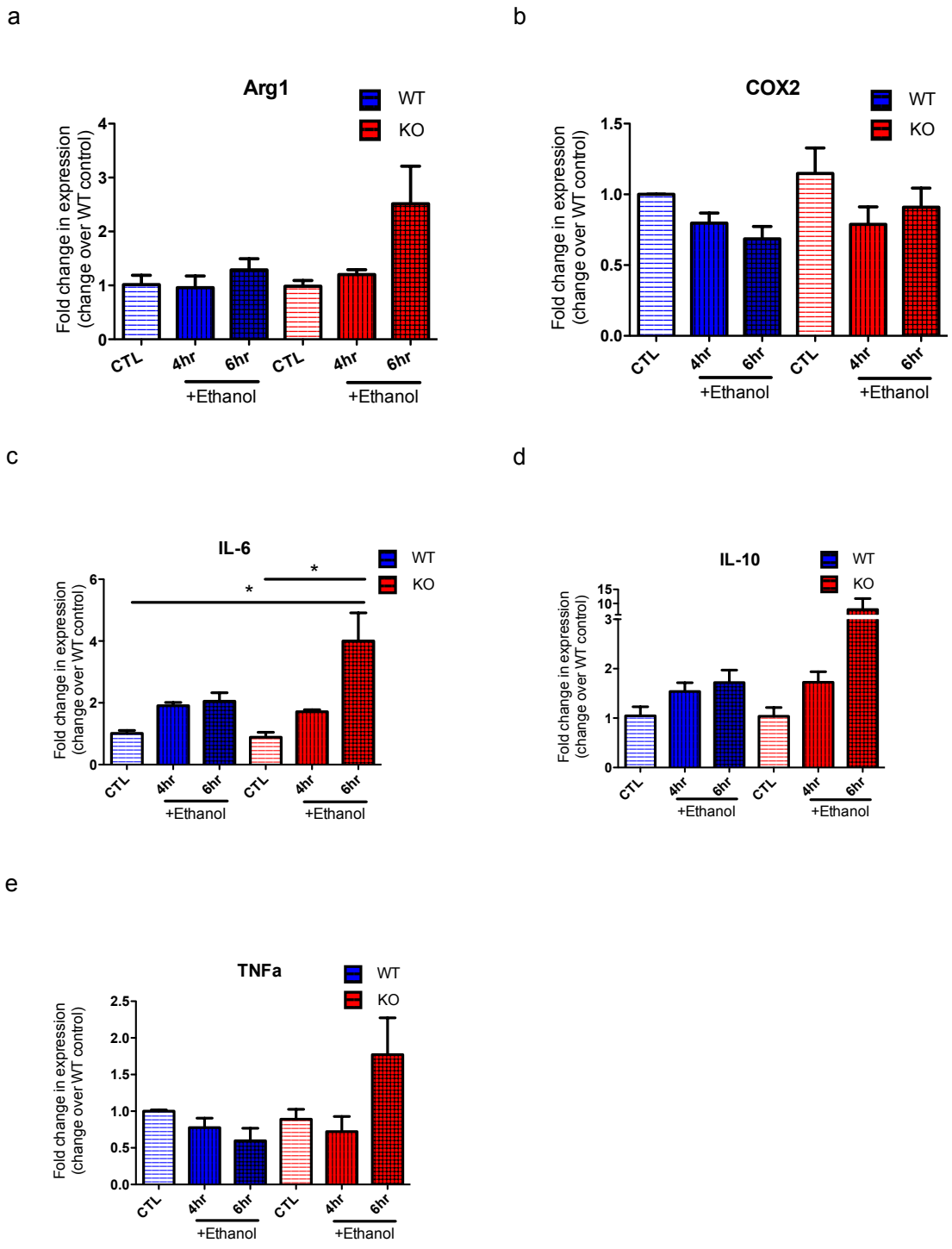
a
Arg1
WT
KO
Fold change in expression (change over WT control)
CTL
4hr
6hr
+Ethanol
b
COX2
c
IL-6
*
d
IL-10
e
TNFa

Figure 8

Figure 8: Ethanol-induced apoptosis leads to production of cytokines and fractalkine deficiency leads to an altered inflammatory response. P7 animals were treated with saline (CTL) or ethanol and brain tissue was harvested 4 or 6 hours later. RNA was isolated and quantitative PCR was used to assess mRNA expression of Arg1 (a), COX2 (b), IL-6 (c), IL-10 (d) and TNFα (e). At 6 hours after treatment, CX3CR1-knockout mice had increased IL-6 expression. (n=2-6) One-way ANOVA, *$p<.05$.

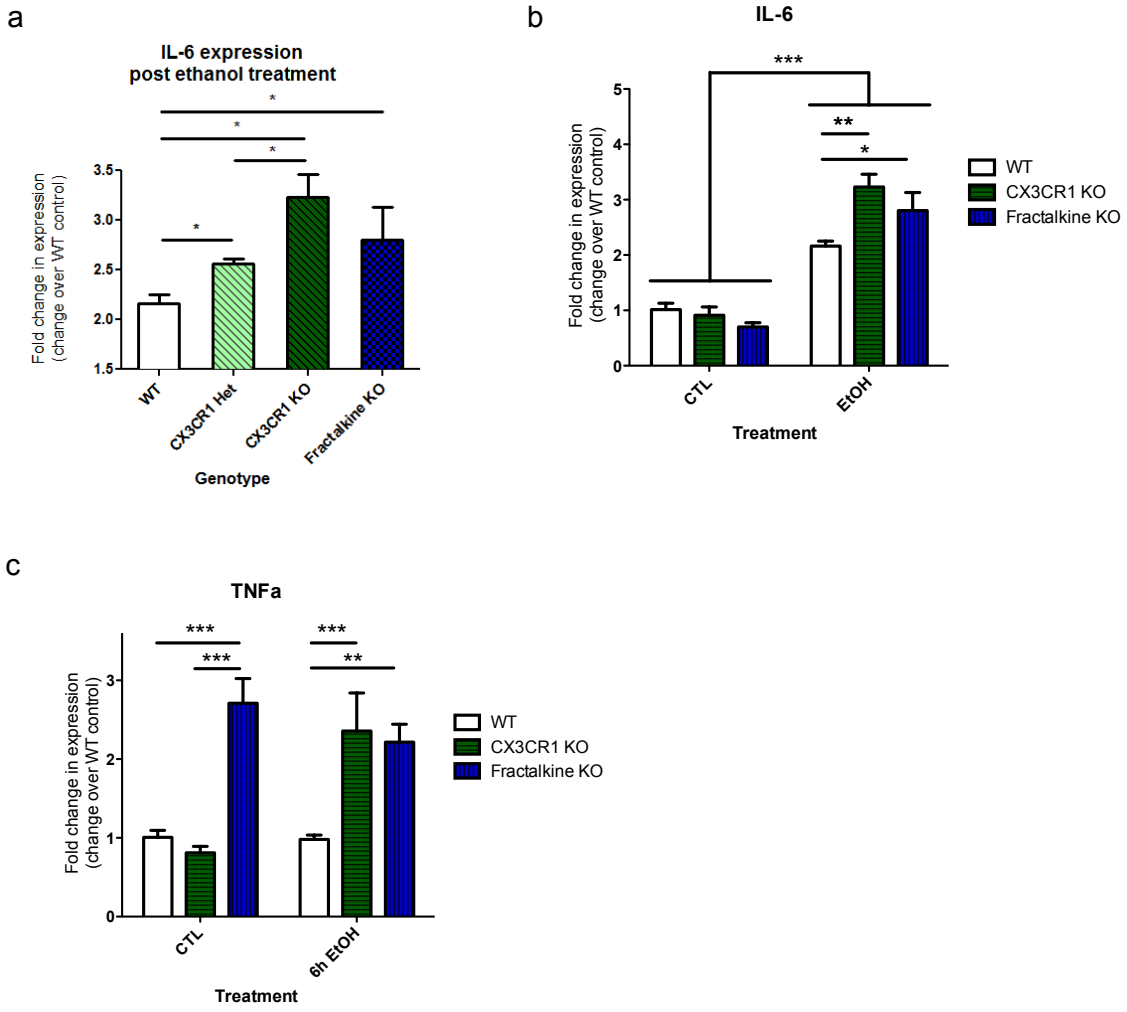
a
IL-6 expression
post ethanol treatment
Fold change in expression
(change over WT control)
3.5
3.0
2.5
2.0
1.5
*
*
*
*
WT
CX3CR1 Het
CX3CR1 KO
Fractalkine KO
Genotype
b
IL-6
***
**
*
Fold change in expression
(change over WT control)
5
4
3
2
1
0
CTL
EtOH
Treatment
WT
CX3CR1 KO
Fractalkine KO
c
TNFa
***
***
***
**
Fold change in expression
(change over WT control)
3
2
1
0
CTL
6h EtOH
Treatment
WT
CX3CR1 KO
Fractalkine KO

Figure 9

Figure 9: The inflammatory response to ethanol-induced apoptosis in fractalkine-knockout brain recapitulates some but not all of the inflammatory changes seen in the CX3CR1-knockout brain. P7 animals were treated with saline (CTL) or ethanol and brain tissue was harvested 4 or 6 hours later. Brain tissue and RNA was harvested from wild type (WT), CX3CR1-heterozygous, CX3CR1-knockout, and fractalkine-knockout at 4 or 6 hours after ethanol treatment and RNA was isolated. Quantitative PCR was used to assess mRNA expression of IL-6 (a,b) and TNAα (c). (a) is data from ethanol treated animals repeated from (b). IL-6 expression is significantly higher in the CX3CR1 knockout and the fractalkine knockout than in the wild type brain after ethanol treatment. In fractalkine knockout brain, TNFα expression is higher in control conditions as compared to wild type or CX3CR1 knockout. CX3CR1-knockout brain has increased TNFα compared to wild type after ethanol treatment. (n=3-6) (a) One-way ANOVA, *p<.05. (b,c) 2-Way ANOVA, *p<.05, **p<.01, ***p<.001

a

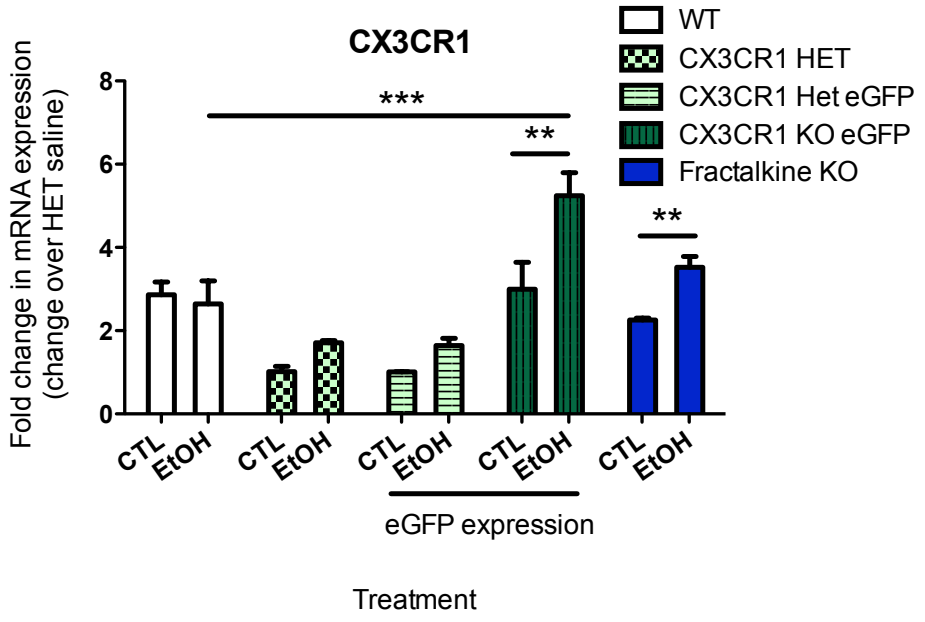
CX3CR1
WT
CX3CR1 HET
CX3CR1 Het eGFP
CX3CR1 KO eGFP
Fractalkine KO
Fold change in mRNA expression
(change over HET saline)
8
6
4
2
0
***
**
**
CTL
EtOH
eGFP expression
Treatment

b

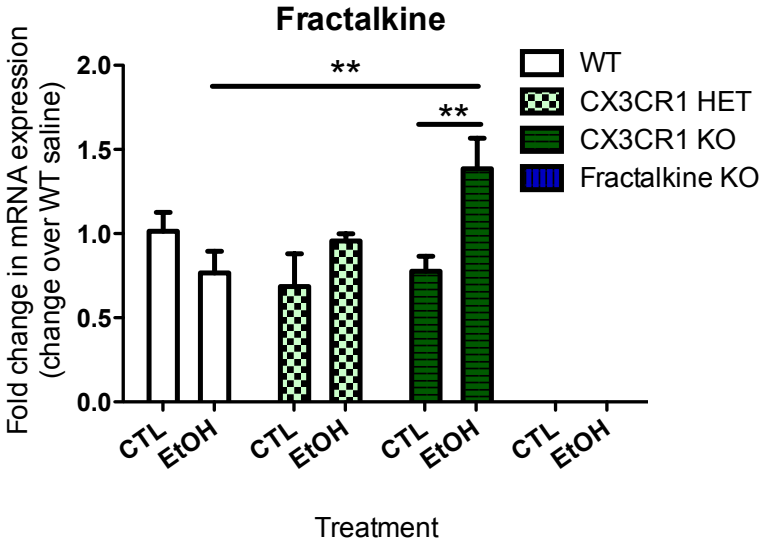
Fractalkine
WT
CX3CR1 HET
CX3CR1 KO
Fractalkine KO
Fold change in mRNA expression
(change over WT saline)
2.0
1.5
1.0
0.5
0.0
**
**
CTL
EtOH
Treatment

Figure 10

Figure 10: Fractalkine and CX3CR1eGPP mRNA is increased in CX3CR1-knockout mice after ethanol injury. P7 animals were treated with saline (CTL) or ethanol (EtOH) and brain tissue was harvested 6 hours later. RNA was isolated and quantitative PCR was used to assess mRNA expression. Wild type (WT), CX3CR1 heterozygous, CX3CR1-knockout, and fractalkine-knockout brain tissue was probed for mRNA expression of CX3CR1 (a) and fractalkine (b). Fractalkine expression was increased in the CX3CR1 knockout after ethanol treatment. In order to relate receptor expression and compare wild type to CX3CR1-deficient mice, we used two sets of primers. One set amplified CX3CR1 and the other amplified the GFP transcript expressed in place of the gene in the CX3CR1-knockout allele. Values were normalized to control-treated heterozygous mice, which have one copy of each gene. Fractalkine knockout and CX3CR1 knockout led to increased expression of the CX3CR1 gene after ethanol treatment. (a,b) (n=3-6) 2-way ANOVA, **p<.01, ***p<.001

CHAPTER 3: Brain-specific angiogenesis inhibitor-1 expression in astrocytes and neurons: implications for its dual function as an apoptotic engulfment receptor.

Brain-specific angiogenesis inhibitor-1 (BAI1) is a transmembrane protein highly expressed in normal brain that has been ascribed two apparently distinct functions: inhibition of angiogenesis and recognition and engulfment of apoptotic cells by phagocytes. In order to further understand the function of BAI1 in the central nervous system, we performed immunolocalization studies in adult mouse brain and cultured neural cells. BAI1 immunoreactivity is enriched in gray matter structures and largely excluded from myelinated axon tracts. Neuronal BAI1 expression was readily detectable in the cerebellar molecular layer as well as in primary hippocampal cultures. In some brain regions, especially olfactory bulb glomeruli, BAI1 was also expressed by GFAP-positive astrocytes. Cultured cortical astrocytes show small (~0.4μm^2) BAI1 immunoreactive membrane puncta as well as prominent focal adhesion localization in a subset of cells. In mixed neuronal-glial cultures, BAI1-expressing astrocytes frequently contained engulfed apoptotic debris. Cultured astrocytes engulfed apoptotic targets, and BAI1 accumulation occurred within the phagocytic cup. We hypothesize that glial BAI1 may subserve an engulfment function in adult brain regions such as olfactory bulb with ongoing apoptotic turnover, whereas neuronal-derived BAI1 may serve primarily as an anti-angiogenic factor in the mature neuropil. We also analyzed the BAI1-deficient mouse to look for evidence of defects in angiogenesis and engulfment. We analyzed vessel density and quantified apoptotic debris in postnatal day 8 and adult mice. In addition, we used

ethanol-induced neuronal apoptosis to test whether BAI1 function was critical for clearance after injury. BAI1 function does not appear to be critical for proper development or clearance of apoptotic cells; however, this does not rule out the possibility that it plays a role in angiogenesis and clearance under normal circumstances.

INTRODUCTION

The recognition and phagocytic clearance of apoptotic cells is a critical process in all multicellular organisms, necessary for normal morphogenesis and potentially important for the prevention of autoimmunity (Ravichandran 2003, Kinchen, Ravichandran 2007). Brain-specific angiogenesis inhibitor-1 (BAI1) is one of several recently identified phosphatidylserine receptors that functions in apoptotic cell engulfment (Bratton, Henson 2008). BAI1 serves as a phosphatidylserine receptor that binds apoptotic cell membranes and triggers activation of the best-studied apoptotic engulfment pathway, via its interaction with ELMO1 and Dock180, leading to the activation of the small GTPase Rac1 (Park, Tosello-Trampont et al. 2007). Rac1 activity is essential for the extensive actin remodeling and membrane trafficking during engulfment (Tosello-Trampont, Brugnera et al. 2001). Despite its high expression in the central nervous system, studies addressing a potential role for BAI1 in engulfment in the brain have not been done.

Characterization of the regional and cellular expression of BAI1 has been minimal, with no reports on its subcellular localization (Mori, Kanemura et al. 2002, Kaur, Brat et al. 2003). Therefore, first of all, we sought to characterize the regional, cellular and subcellular expression of BAI1 in the mature mouse brain and culture systems. Secondly, we analyzed the BAI1 knockout mouse and examined the CNS for evidence of defects in clearance, neurogenesis, or angiogenesis. We examined postnatal and adult brain to determine whether BAI1 is critical during homeostatic clearance. In addition, we used an animal model of fetal alcohol syndrome, a widely used method to induce neuronal apoptosis *in vivo* (Ikonomidou, Bittigau et al. 2000, Ghosh, Walls et al. 2009, Young, Klocke et al. 2003), in order to determine whether BAI1 is critical for clearance of apoptotic neurons after injury.

METHODS

Mice

All animal procedures were approved by the University of Virginia Animal Care and Use Committee. Mice used were C57/bl6 (Charles River) or BAI1 transgenic mice (Taconic). The BAI1 gene was targeted with a gene trap approach and homozygous transgenics have decreased BAI1 expression. BAI1 mice were initially on a 129Sv/Ev-C57/bl6 background and were backcrossed onto a C57/bl6 background for four generations.

Cell culture

Neonatal primary astrocyte cultures were prepared as previously described (Heffron, Mandell 2005). Briefly, the forebrain was dissected from newborn pups, meninges were removed, and cells were dissociated in 0.05% trypsin EDTA for 5 min at 37 °C. Following trituration, cells were pelleted and resuspended in DMEM supplemented with 10% fetal bovine serum, penicillin (50 U/ml), and streptomycin (50 μg/ml) (Gibco). Media was replaced twice per week for 2 weeks to obtain astrocyte monolayers. Mixed glial/neuronal cultures were prepared from neonatal rat hippocampus as previously described (Goodkin, Joshi et al. 2008). LR73 fibroblasts were stably transfected with a full length BAI1 construct to produce LR73-BAI1 cells, as previously described (Park, Tosello-Trampont et al. 2007).

In vitro phagocytosis assay

Mouse astrocytes were incubated with fluorescently labeled 2μm carboxylate-modified latex beads as previously described (Park, Tosello-Trampont et al. 2007). After 2 h, the cells were extensively washed with cold PBS and fixed in 4% paraformaldehyde, prior to immunofluorescence staining for BAI1 (h1570).

Ethanol-induced apoptosis

Ethanol was injected subcutaneously in postnatal day 7 pups as a 20% solution in 0.9% saline at 15.9μL/g body weight. It was administered twice, 2 hours apart (as

described by (Ghosh, Walls et al. 2009)). Brain tissue was harvested 24 hours after the first injection.

Tissue processing

Mice were anesthetized with a lethal dose of pentobarbital. For BAI1 immunolocalization studies, mice were transcardially perfused at room temperature with 10 ml PBS followed by 10 ml of PBS/4% paraformaldehyde over a period of 3–5 min. For some studies using antibody h103, mice were perfusion fixed with a high pH fixative (Berod, Hartman et al. 1981). Brains were further fixed in PBS/4% paraformaldehyde for 24 h at 4 °C. For the BAI1 transgenic tissue analysis, brains were immersion fixed in either PBS/4% paraformaldehyde for 24h at 4 °C or in 70% ethanol. Tissue was processed into paraffin by standard methods.

Western blot

LR73 parental or LR73-BAI1 cells were lysed directly in Laemmli sample buffer and separated by electrophoresis using standard procedures. Gels were transferred to nitrocellulose for 90 min with a semidry transfer apparatus and treated with blocking reagent (Li-COR block; Li-COR, Lincoln NE) overnight at 4 °C and then probed with primary antibodies (BAI1 h1570 1:10,000; alpha-tubulin, Sigma, 1:4000) for 1 h at room temperature. Secondary antibodies were goat anti-mouse InfraRed800 and goat anti-rabbit Cy5.5 (Rockland) at 1:2000 for infrared imaging. Blots were imaged on an Odyssey Li-COR Odyssey infrared scanner (Li-COR, Lincoln NE). Brain lysate was

prepared by triturating tissue in NP-40 buffer (150mM NaCl, 1% NP-40, 50mM Tris pH 8.0, protease inhibitor cocktail (Sigma)), incubating on ice for 15 minutes and sonicating. Samples were spun down at 12k rpm for 10 minutes. Supernatant was transferred to a new tube, protein assay was performed, samples were normalized, and 5X Laemmli sample buffer with DTT was added. Samples were separated by electrophoresis using standard procedures, transferred to PVDF membrane (Immobilon) for 60 min with a semidry transfer apparatus. The membrane was blocked (5% milk) for 1 hour, then incubated with primary antibody (BAI1 h1570 1:5,000; alpha-tubulin, Sigma, 1:4000 diluted in block with .1% tween) overnight. Secondary antibodies were rabbit-HRP and mouse-HRP (Sigma). Blot was developed with the Immobilon chemiluminescence kit.

Primary antibodies and immunohistochemistry/immunofluorescence

Custom polyclonal rabbit antisera against C-terminal (intracellular epitope, h1570) and N-terminal (extracellular epitope, h103) regions of BAI1 were generated by injecting rabbits with corresponding KLH-linked peptides derived from human amino acid sequences (Novus Biologicals, Littleton, CO). Antibodies were used after one round of affinity purification on peptide columns. Peptide competition experiments were used to test antibody specificity in immunohistochemistry. As an irrelevant control peptide, a 15 amino acid peptide derived from the human AMP-activated kinase-alpha-1 with no sequence similarity was used at the same concentration as the h1570 peptide (10 times molar excess). Other primary antibodies: rabbit polyclonal anti-GFAP (DAKO #Z0334; 1:4000); mouse monoclonal anti-GFAP conjugated to Cy3 (Sigma, 1:800); rabbit

polyclonal S-100beta (DAKO #Z0311; 1:500); rabbit polyclonal anti-IBA1 (Wako, 019-19741; 1:500); mouse monoclonal anti-SV2 (Developmental Studies Hybridoma Bank; 1:10); rabbit polyclonal collagen IV (chemicon, 1:750); rabbit polyclonal cleaved-caspase-3 (Cell Signaling Technnologies, 1:100); rabbit polyclonal fractin (Millipore, 1:1000), rat anti-BrDU (Abcam, 1:150). Microglia were labeled with rabbit polyclonal Iba1 (Wako, 1:500) or biotinylated *Lycopersicon esculentum* (tomato) lectin (Vector, 20 μg/ml) and visualized with streptavidin-conjugated TRITC (Jackson, 1:2000). Free floating frozen 30μm sections or 5μm paraffin sections were prepared and processed for immunohistochemistry using standard techniques. Immunoperoxidase detection was performed using the ImmPress polymeric peroxidase reagents (Vector, Burlingame, CA), according to the supplier's instructions. The chromogen used was diaminobenzidine (Dako S3000) 1 mg/ml in PBS plus 0.02% hydrogen peroxide applied for 3–5 min. Immunofluorescence detection was performed using Alexa-488 and Alexa-546 dyes (Invitrogen, Carlsbad, CA). Brightfield and immunofluorescence images were acquired with an Olympus BX40 upright microscope and a Scion Firewire CCD camera (Scion, Frederick, MD). Whole section imaging (Fig. 2) was performed using an Aperio ScanScope (Aperio, Vista, CA). Confocal microscopy was performed using a Zeiss 510 Meta microscope with a 60× or 63× oil immersion objective lens (Keck Biological Imaging Center, Department of Biology, University of Virginia).

Image analysis

The number of cleaved-caspase-3 (CC3) and BrDU positive cell bodies were manually counted and the number of bodies per area was calculated. Cell profiler (Broad Institute, (Lamprecht, Sabatini et al. 2007)) was used for automated analysis of staining. Pipelines were set up to automate detection of apoptotic debris stained with fractin and vessels stained with collagen IV. Cell profiler quantified the fraction area occupied. Data was graphed and analyzed using Graphpad Prism (La Jolla, CA).

RESULTS

I. Immunolocalization

Validation of C-terminal (intracellular) and N-terminal (extracellular) anti-BAI1 antibodies

BAI1 is a 7-pass transmembrane protein belonging to the type II adhesion type G-protein coupled receptor family. The N-terminal extracellular domain contains five thrombospondin type I repeats and an RGD (putative integrin-binding) sequence (Fig. 1A). We tested the specificity of our C-terminal (intracellular epitope, h1570) antibody using multiple approaches. First, we showed that Western blotting using h1570 detected strong bands near the expected weight (~180 kDa) in LR73 fibroblasts stably transfected with human BAI1, but not in untransfected cells (Fig. 1B). An additional immunoreactive band of lower molecular mass was present, which could be the result of proteolytic cleavage, as previously described (Kaur, Brat et al. 2005). Second, we showed that preincubation of antibody h1570 with excess immunizing peptide, but not an

irrelevant peptide, completely blocked immunohistochemical staining (Fig. 1C and D). Third, we showed that brain lysate from the BAI1-deficient mouse lacked a prominent immunoreactive band for BAI1. Also, the N-terminal anti-BAI1 antibody h103 produced qualitatively very similar staining patterns on adjacent sections as h1570 (Fig. 1E and F) (see Appendix for h103 antibody specificity tests). We found that h103 staining of tissue fixed with standard pH 7.4, 4% paraformaldehyde was weaker than that obtained with antibody h1570. However, the intensity of h103 immunostaining could be increased by using a high pH (11.0) fixation buffer as previously described (Berod, Hartman et al. 1981). The similarity in immunostaining profiles with the two antibodies suggests that in the normal adult brain there is not a large pool of cleaved and translocated extracellular fragment (referred to in the literature as vasculostatin (Kaur, Brat et al. 2005), since this pool of released protein would be detected with the h103, but not the h1570 antibody. However, we cannot exclude the possibility that vasculostatin is lost from the extracellular space due to perfusion and fixation procedures. For more on staining with h103 and other BAI1 antibodies, see Appendix 1.

BAI1 expression in the normal adult mouse brain: enrichment in neuropil and exclusion from myelinated white matter tracts

BAI1 immunoreactivity detected with antibody h1570 was widespread in all neuropil-rich zones, including spinal cord gray matter, cerebellar molecular layer, cerebral cortex, thalamic nuclei and basal ganglia (Fig. 2). Close examination of hippocampus and cortex revealed that large pyramidal neurons lacked significant

somatodendritic cytoplasmic BAI1, but that the intervening neuropil was rich in BAI1. White matter, both large tracts such as corpus callosum and anterior commissure, as well as microscopic tracts such as striatal pencil fibers, were devoid of BAI1 immunoreactivity.

Complex cellular patterns of expression in specialized neuropil zones: cerebellum, olfactory bulb, and retina

Examination of several brain regions with architecturally distinct neuropil zones revealed several interesting aspects of BAI1 localization. In the cerebellar molecular layer, strongly labeled fine branching processes were seen to emanate from interneurons, whereas Purkinje cells and their dendrites showed weaker expression (Fig. 3A). GFAP-immunoreactive Bergmann glial processes were negative for BAI1, but it was difficult to determine whether distal Bergmann glial membranous processes might account for some BAI1 immunostaining (Fig. 3B). In the olfactory bulb, glomeruli showed the highest intensity of BAI1 staining (Fig. 3C). Unlike other neuropil-rich zones, the pattern of staining in olfactory glomeruli showed stellate forms, consistent with the distal membranous processes of astrocytes. This was confirmed by co-staining with GFAP, which showed GFAP-positive process cores surrounded by BAI1-reactive distal processes (Fig. 3D). Extraglomerular astrocytes, which occupy the neuropil zones just above the glomeruli in (C) show much lower BAI1 immunoreactivity. In the retina BAI1 was highly concentrated in the two neuropil layers, the outer and inner plexiform layers (Fig. 3E). Double immunofluorescence labeling with the universal presynaptic

marker SV2 showed that not all presynaptic terminals colocalized with BAI1: in the outer plexiform layer (OPL), brightly SV2-immunoreactive photoreceptor terminals were devoid of BAI1 immunostaining, but synaptic zones in the more inner portion of the OPL, where horizontal cell and interplexiform cells synapse upon bipolar cell dendrites (Dowling 2012), did show significant BAI1 immunoreactivity (Fig. 3F).

BAI1 is expressed in cultured neurons, astrocytes, and microglia

In order to more definitively determine the cellular origin and subcellular localization of BAI1 in the brain, we performed immunofluorescence on mixed neuronal/glial cell cultures from rat hippocampus (Fig. 4). Neurons, astrocytes, and microglia, identified both by characteristic morphologies and specific markers, showed definitive punctate BAI1 immunostaining. In general, neurons and astrocytes showed the most intense labeling, with microglia showing variable and patchy staining. In older cultures, where many cells had undergone apoptosis, we observed numerous GFAP-positive astrocytes with punctate BAI1 labeling that had engulfed apoptotic nuclear debris (identified by condensed DAPI staining). Confocal microscopy with z-sectioning showed the debris to be within the confines of GFAP-positive astrocyte cytoplasm and surrounded by BAI1-positive membrane (Fig. 4C). In order to determine whether astrocytic BAI1 associates with apoptotic targets (2-μm red fluorescent carboxylate-modified beads), we performed confocal microscopy on astrocytes 2 h after addition of beads (Fig. 4D). A single confocal slice shows that some beads are surrounded by a higher concentration of BAI1 staining (h1570) than surrounding plasma membrane (see

bead at convergence of cross hairs). In addition, XZ and YZ orthogonal slices reveal BAI1 immunoreactivity surrounding a bead, indicating engulfment and not merely superficial membrane adhesion.

Punctate membrane and focal adhesion localization of BAI1 in purified cultured astrocytes

An additional pattern of astrocyte BAI1 labeling was observed in purified astrocytes, grown in serum-containing medium in the absence of neurons. In a subset (20–30% of GFAP-positive cells), BAI1 localized to focal adhesions, confirmed by double labeling with paxillin (Fig. 5A–C). Interestingly, BAI1 was not uniformly distributed through the length of the focal adhesions, but showed a speckled distribution that was sometimes polarized towards one end of the focal adhesion. All cells, whether or not they formed prominent focal adhesions, also exhibited punctate membrane BAI1 staining (Fig. 5D–F). The area of these puncta determined from single confocal sections of four different fields of astrocytes was 0.422 ± 0.387 (SD) μm^2.

II. Analysis of BAI1-deficient mouse

BAI1 has been implicated in angiogenesis as well as engulfment (Kaur, Brat et al. 2005, Park, Tosello-Trampont et al. 2007). In addition, a downstream mediator of BAI1 signaling, ELMO1, has been implicated in neurogenesis (Lu, Elliott et al. 2011).

Therefore we assessed whether BAI1 deficiency led to any differences in cellularity, vessel density, persistence of apoptotic debris, or neuronal proliferation in the brain.

Homozygous BAI1-deficient mice displayed no overt behavioral differences, for example via qualitative analysis of mobility, activity and social behavior. Of note, the weight of BAI1 homozygous mice was significantly decreased at postnatal day 7-8 (P7-P8) compared to heterozygous or wild type littermates (Fig. 6A); however, this size difference did not persist to adulthood (Fig. 7A). The cause of this early weight difference is unclear; however, it may be attributable to strain differences in body weight and growth rates, as we tested mice that were backcrossed only four generations.

Cell density and cortical thickness

BAI1 has been implicated in clearance, and because there is a significant overproliferation and pruning of neurons during development, we hypothesized that BAI1 deficiency may lead to altered development of the brain and could lead to hypercellularity. In order to test this, we quantified the cortical cell density as well as cortical thickness. Counter to our expectations, we found no difference in cellularity or cortical thickness (Fig. 6B, Fig. 7B-C), suggesting that BAI1 is not critical for clearance or pruning of cells during development.

Vessel Density

As BAI1 has been implicated as an anti-angiogenic factor, we hypothesized that BAI1-deficient mice may have an increase in vessel density in the brain. Collagen IV

staining highlights the cerebrovasculature; therefore we analyzed vessel density in both P8 pups and adults using collagen IV staining. We found no differences in area occupied by staining in brains of homozygous compared to wild type animals (Fig. 6C, Fig. 7C), suggesting BAI1 deficiency does not result in any overt change in angiogenesis.

Neurogenesis

Another member of the BAI1 pathway, ELMO1, has recently been implicated in engulfment in the brain and ELMO1 deficiency leads to defects in adult neurogenesis (Lu, Elliott et al. 2011). Based on this, we hypothesized that BAI1-deficient pups may also have a defect in neurogenesis. In order to highlight proliferating cells, pups were injected with BrDU at P7. Tissue was harvested 24 hours later and the number of BrDU positive cells in the cortex was quantified. There was no difference in the number of BrDU positive cells in the BAI1-deficient mice (Fig. 6D). Of note, we did not assess whether there was a difference in maturation or survival of newborn cells, which are other important components of neurogenesis. However, we conclude that BAI1-deficient pups have no overt defect in neuronal proliferation.

Clearance during development and after ethanol-induced neuronal apoptosis

As BAI1 has been implicated in phagocytic clearance of apoptotic cells, we hypothesized there may be increased apoptotic debris in the BAI1-deficient mice. In order to evaluate whether BAI1 is critical for clearance of apoptotic cells during physiological developmental pruning, we quantified the amount of apoptotic debris in

the cortex of P8 animals. We found no difference in the amount of debris in BAI1-deficient mice, as detected by either fractin (caspase-cleaved actin, a surrogate marker of apoptosis) or cleaved-caspase-3 (Fig. 8A-B). Next, we tested whether BAI1 deficiency impairs clearance after injury. We induced neuronal apoptosis by injecting P7 pups with ethanol. This fetal alcohol syndrome model has been widely used to study apoptosis in many genetic models, and it is known that the peak of caspase-3 activity happens at 12 hours after injury (Olney, Tenkova et al. 2002, Young, Klocke et al. 2003, Ghosh, Walls et al. 2009). We assessed the amount of apoptotic debris remaining at 24 hours after injury in order to allow time for clearance to occur. We found that there was no difference in the amount of debris in the BAI1-deficient mice, as measured by fractin (Fig. 8A) or cleaved-caspase-3 (Fig. 8B) staining remaining 24 hours after ethanol-induced apoptosis. This suggests BAI1 is not required for clearance of apoptotic debris in the brain.

Expression of BAI family proteins

The BAI1-deficient mouse was generated via a gene trap approach, and it is possible that expression of BAI1 could occur if the gene trap is not efficient. Therefore, we assessed BAI1 expression to confirm that the mice were deficient in BAI1. We looked at protein via western blot (Fig.1G) and mRNA via quantitative PCR (Fig. 9). We confirmed that expression was downregulated, however mRNA transcript was still detectable. Whether this expression is sufficient to allow translation of protein is

unclear. We can conclude from western blots that there is decreased expression of BAI1 protein (Fig. 1G).

BAI1 deficiency did not lead to an observable CNS phenotype, and it is possible that other BAI family members could be upregulated to compensate for lack of BAI1. Therefore we quantified the expression of the other BAI family members, BAI2 and BAI3, via quantitative PCR to determine whether they are increased in the BAI1 knockout mouse brain (Fig. 9). In addition, we examined whether BAI1, BAI2, or BAI3 expression was changed after injury (Fig. 10). BAI1 deficiency did not lead to upregulation of BAI2 or BAI3. Of interest, while postnatal ethanol exposure had no effect on BAI1 expression, both BAI2 and BAI3 were downregulated after injury.

DISCUSSION

Studies have attributed multiple functions to the BAI1 protein. It was originally categorized as an anti-angiogenic factor (Kaur, Brat et al. 2005), and this function is mediated by a cleaved extracellular fragment of BAI1 known as vasculostatin (Kaur, Cork et al. 2009). Our collaborators showed that BAI1 also functions in clearance of apoptotic cells and has a role in myoblast fusion (Park, Tosello-Trampont et al. 2007, Hochreiter-Hufford, Lee et al. 2013). These studies implicating BAI1 in clearance of apoptotic cells were done in the periphery. As BAI1 is most highly expressed in the brain, we hypothesized that it may play a role in clearance in the central nervous system (CNS). In order to further characterize the role of BAI1 in the brain, we performed

immunolocalization studies to determine where BAI1 is expressed. In addition, we analyzed a BAI1-deficient mouse to determine whether BAI1 is critical for CNS angiogenesis and clearance of apoptotic debris.

Our immunohistochemical and immunofluorescence labeling experiments in mouse brain and cultured neural cells reveal new information about the cellular and subcellular localization of BAI1. A previous study concluded that BAI1 expression was purely neuronal, and completely excluded from GFAP-positive astrocytes (Mori, Kanemura et al. 2002). This study was limited to human postmortem material and examined only the cerebral cortex. A subsequent paper, although focused on the downregulation of BAI1 in malignant gliomas, mentioned as unpublished data that BAI1 immunoreactivity was frequently observed in reactive astrocytes surrounding tumor, in addition to its expression in neurons and neuropil (Kaur, Brat et al. 2003). Our previous study showed relatively high levels of BAI1 in primary astrocyte cultures by Western blot and demonstrated that siRNA knockdown of BAI1 in astrocytes decreased engulfment of apoptotic targets (Park, Tosello-Trampont et al. 2007). Our current demonstration of both neuronal and astrocyte BAI1 patterns of expression is also supported by publically available *in situ* hybridization data (http://mouse.brain-map.org/brain/Bai1.html).

Astrocytes and neurons have distinct functions and it may be that the two ascribed functions of BAI1, engulfment and anti-angiogenesis, are carried out by astrocytes versus neurons, respectively. For example, it is possible that the cleavage of BAI1 to generate the released 120 kDa vasculostatin fragment is carried out primarily by

neurons to function as an anti-angiogenic factor. And on the other hand, astrocytes may use intact BAI1 as an engulfment receptor. It would be interesting to determine whether the released phosphatidylserine-binding vasculostatin fragment can compete with intact phagocytic receptor function.

Notably, we found that microglia, the well-known phagocyte in the brain, had lower levels of BAI1 than astrocytes or neurons. Microglia are capable of phagocytosis and play a central role in the response to injury and clearance of debris. The fact that microglia do not express appreciable amounts of BAI1 suggests it may not be required for these functions. BAI1 is only one of many receptors that mediate clearance (Bratton, Henson 2008), and microglia may use other receptors (Hsieh, Koike et al. 2009, Fuller, Van Eldik 2008).

The idea that there are redundant factors involved in clearance is supported by our analysis of the BAI1-deficient mouse. We found that BAI1 was not critical for clearance during developmental pruning or after injury. We did not see any defect in clearance or persistence of apoptotic debris during physiological or ethanol-injury-induced apoptosis. While making conclusions from this study, there are a couple of issues to keep in mind. As mentioned, astrocytes express BAI1; however, they may not require BAI1 for engulfment as there may be redundant pathways (Bratton, Henson 2008). Or perhaps they are not the key players in clearance of apoptotic cells in these contexts. We cannot rule out the possibility that astrocytes and BAI1 may play a role under certain circumstances. However, either other receptors and/or microglia are able to compensate

for lack of BAI1 and accomplish clearance during developmental and ethanol-induced apoptosis.

We also found that BAI1 deficiency had no overt effect on behavior or the development of the CNS, including vasculogenesis and neuronal proliferation. Again, this does not prove that BAI1 has no role in these processes; however, it suggests that BAI1 is not a critical factor required for CNS development, angiogenesis or neurogenesis.

BAI1 deficiency did not lead to an observable CNS phenotype, and it is possible that other BAI family members could be upregulated to compensate for lack of BAI1. However, we found that BAI1 deficiency did not lead to upregulation of BAI2 or BAI3. Of interest, while ethanol-induced apoptosis had no effect on BAI1 expression, both BAI2 and BAI3 were downregulated after injury. We are not the first to show modulation of BAI2 and BAI3 with injury, as the original studies describing them showed that BAI2 and BAI3 are downregulated after ischemia-induced injury (Kee, Ahn et al. 2004, Kee, Koh et al. 2002, Kee, Ahn et al. 2004). The fact that we see modulation of BAI2 and BAI3 in this additional injury model suggests that these play a role in a range of injuries; however, the potential function of this downregulation is unclear.

Many questions remain. Microglia, the professional phagocytes of the brain, are equipped with several different receptors for multiple types of clearance, including that of infectious organisms, protein aggregates, as well as for apoptotic cells. Why might microglia express only low levels of BAI1, and utilize other phagocytosis-relevant receptors? We originally hypothesized that astrocytes may have a more dedicated role in

the delicate cleanup of apoptotic neuronal debris produced during development and normal turnover, which could be carried out via BAI1. BAI1 is not required, but what redundant pathways might play a role in clearance if astrocytes are indeed involved? Finally, does BAI1 play an important role in other signaling besides angiogenesis and phagocytosis? What is the significance of BAI1 localization to astrocyte focal adhesions? It seems plausible that BAI1 could act to activate Rac1 and modulate actin dynamics in other contexts besides engulfment, and this could translate to a role at focal adhesions, which are rich in actin.

FIGURES

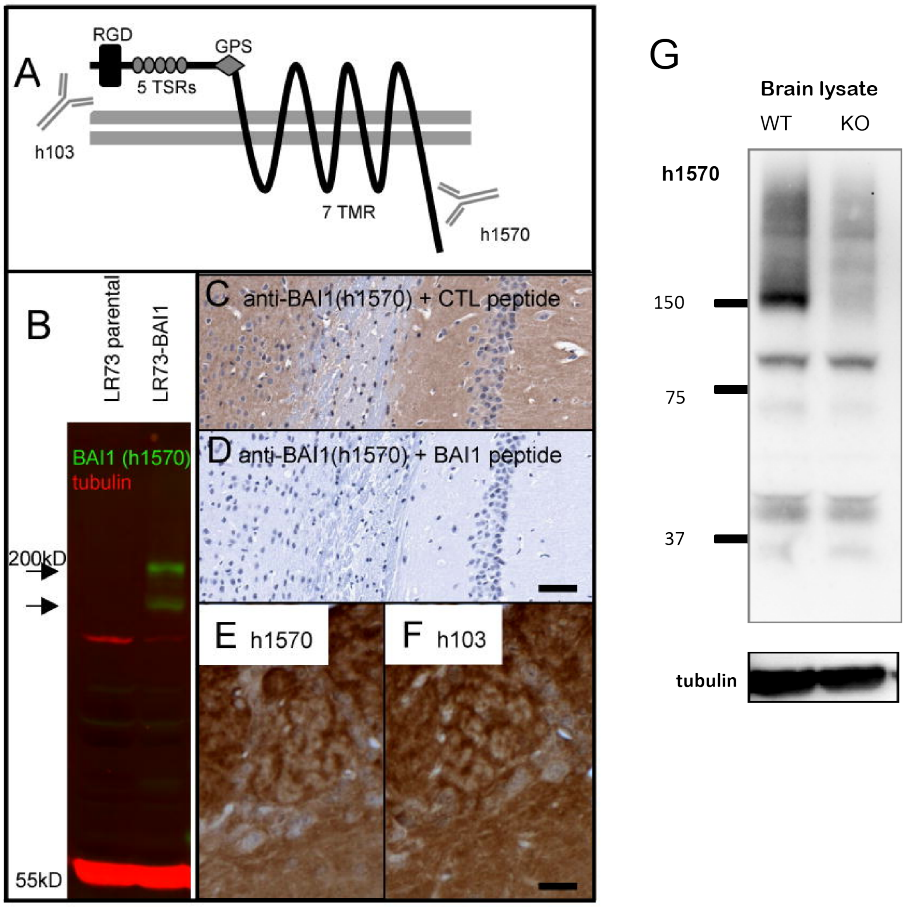
A
RGD
GPS
5 TSRs
h103
7 TMR
h1570
B
LR73 parental
LR73-BAI1
BAI1 (h1570)
tubulin
200kD
55kD
C anti-BAI1(h1570) + CTL peptide
D anti-BAI1(h1570) + BAI1 peptide
E h1570
F h103
G
Brain lysate
WT
KO
h1570
150
75
37
tubulin

Figure 1

Figure 1: Demonstration of anti-BAI1 antibody specificity. A) BAI1 is a 7-transmembrane (7 TMR) protein of the GPCR superfamily. The extracellular domain contains an RGD sequence, 5 thrombospondin type I repeats (TSRs) which are necessary for both the anti-angiogenic properties and apoptotic cell engulfment, and a G-protein coupled receptor (GPCR) proteolytic cleavage site (GPS). Antibody h103 is directed at an extracellular (N-terminal) sequence. The protein is cleaved at the GPS to release the anti-angiogenic fragment known as vasculostatin. The polyclonal h1570 antibody generated for the present study recognizes an amino acid sequence at the intracellular C-terminus. B) Western blotting of untransfected LR73 fibroblasts (parental) using h1570 shows no detectable endogenous BAI1 signal (green) at the expected molecular weight of ~180 kDa. A stably transfected line (LR73-BAI1) shows strong blotting signal at the expected molecular weight as well as in a presumed proteolytic fragment. (C, D) Preincubation of diluted h1570 antibody with an irrelevant peptide (AMP-activated kinase, alpha-1, C-terminal peptide, Santa Cruz Biotechnology) had no effect on immunostaining of mouse hippocampus (C), whereas preincubation with the immunizing peptide completely abolished immunostaining (D). Immunohistochemistry on adjacent paraffin sections using the h1570 (C-terminal) and the h103 (N-terminal-directed) antibodies gave nearly identical staining patterns, with olfactory bulb shown as an example (E, F). Western blot on brain lysate from control versus BAI1-deficient mice further shows h1570 binds BAI1 in brain lysate (G). Scale bars: D=100μm; F=25μm.

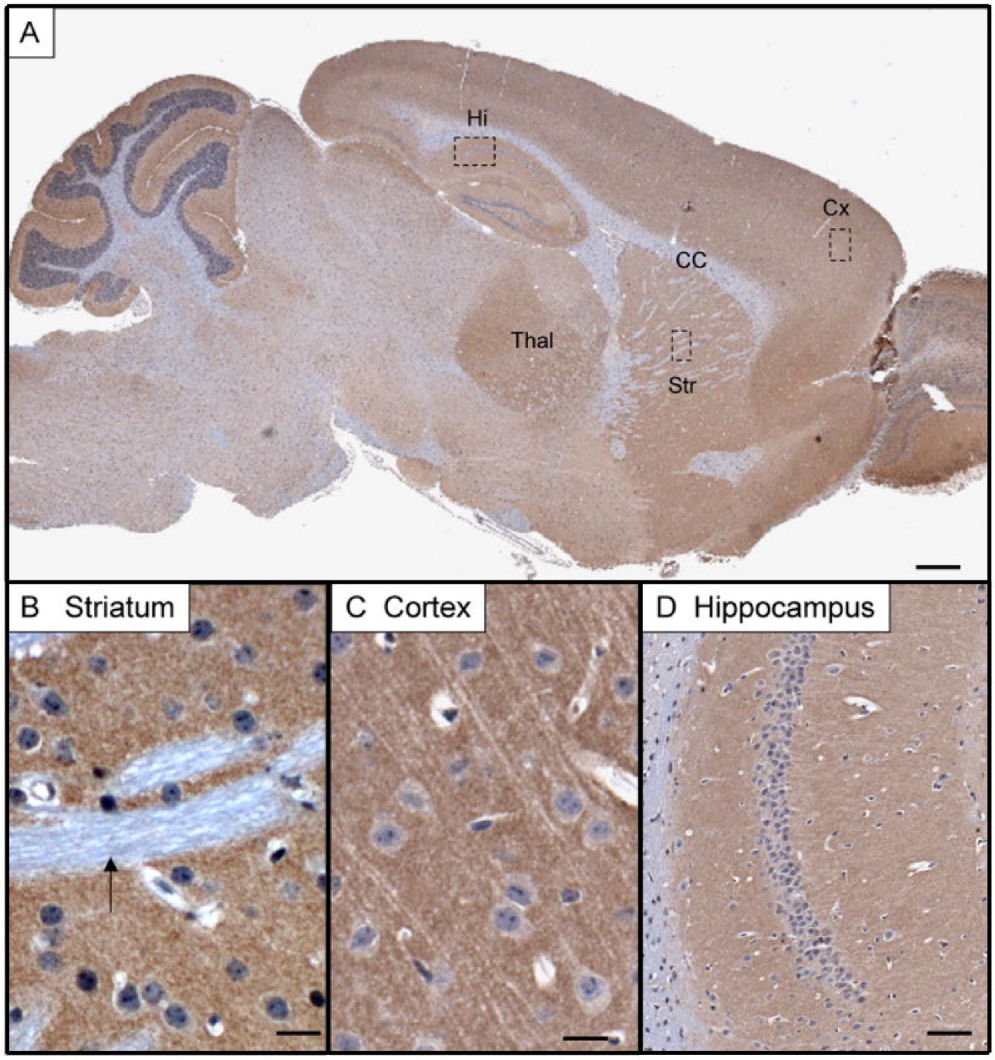

Figure 2

Figure 2: Overview of BAI1 immunoreactivity in the adult mouse brain. A) BAI1 expression detected by antibody h1570 is enriched in neuropil structures such as cortex (Cx), thalamus (Th), striatum (Str) and hippocampus (Hi), and largely absent from white matter structures such as the corpus callosum (CC). B) Striatal pencil fibers (small white matter tracts-arrow) lack BAI1 expression whereas surrounding neuropil shows finely punctate staining. C) Cortical pyramidal neurons show little somatodendritic cytoplasmic staining, but are surrounded by intense granular neuropil immunoreactivity. D) Hippocampal neurons show a neuropil pattern confined to the extent of the apical (left) and basal (right) dendritic fields of CA1. Scale bars: A=500μm; B, C=20μm; D=100μm.

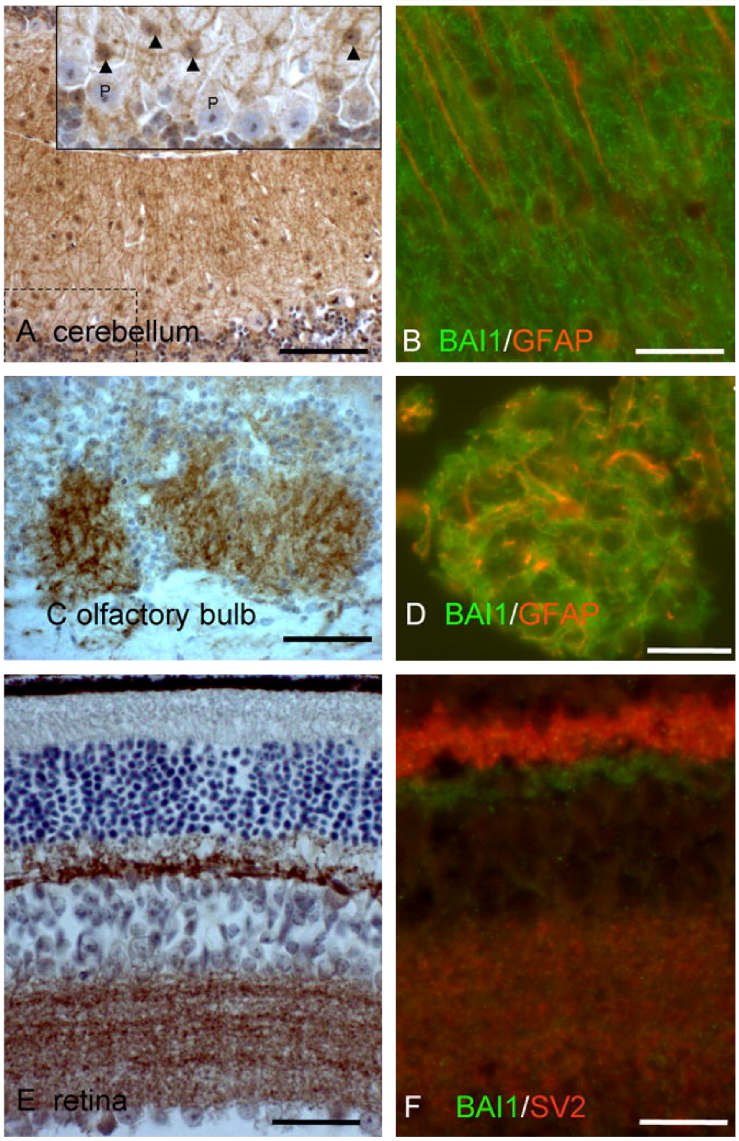
P
P
A cerebellum
B BAI1/GFAP
C olfactory bulb
D BAI1/GFAP
E retina
F BAI1/SV2

Figure 3

Figure 3: Fine patterns of neuropil BAI1 immunoreactivity in cerebellum, olfactory bulb, and retina. (A) Cerebellar staining reveals fine interlacing processes emanating primarily from small molecular layer interneurons (inset, arrowheads), not from Purkinje cells (P) or Bergmann glia. (B) BAI1 (green) fine radial processes do not colocalize with Bergmann glial fibers (GFAP, red). (C) Olfactory bulb glomeruli show intense staining in a reticular pattern coincident with distal membranes of GFAP+ astrocytes (D). Extraglomerular astrocytes, which occupy the neuropil zones just above the glomeruli in (C) show much lower BAI1 immunoreactivity. (E) Retinal BAI1 is confined to the outer (top) and inner (bottom) plexiform layers. (F) Double labeling for BAI1 and presynaptic marker SV2 reveals lack of BAI1 in large photoreceptor synaptic terminals (bright red upper portion of IPL), but strong expression in structures located beneath these terminals. In the inner plexiform layer, BAI1 is intermingled with, but does not colocalize with SV2. Scale bars: A, C=125μm; B, D, F=25μm; E=50μm.

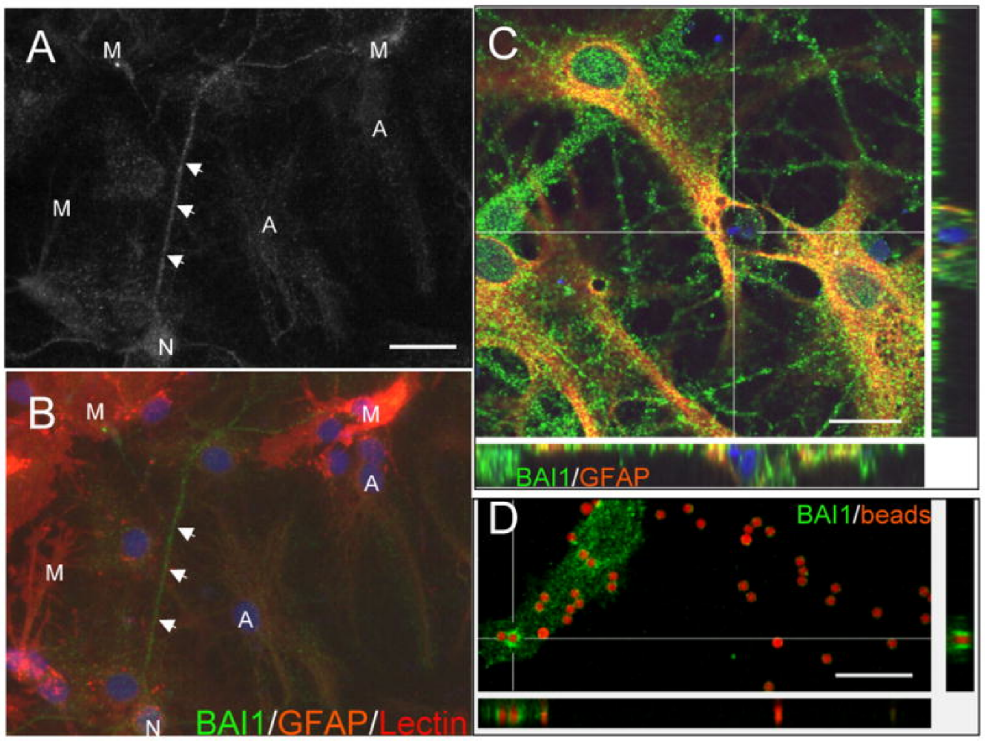

Figure 4

Figure 4: BAI1 is expressed by cultured neurons, astrocytes, and microglia. In general, neurons (N), recognized by their extensive neuritic networks, showed the strongest BAI1 immunoreactivity. Astrocytes (A), labeled lightly with GFAP-Cy3, also revealed significant punctate labeling. Microglia (M), labeled with the tomato lectin, showed variable and patchy BAI1 staining. (C) In older culture preparations in which numerous cells had undergone apoptosis, we frequently observed GFAP-positive astrocytes with punctate BAI1 labeling that had engulfed apoptotic nuclear and cytoplasmic debris. Confocal microscopy with z-sectioning showed the DAPI-positive nuclear debris to be within astrocyte cytoplasm. (D) BAI1-immunoreactive astrocyte membrane surrounds apoptotic targets (2μm carboxylate-modified red fluorescent beads) added to cultured astrocytes for 2 hours. A single confocal slice shows that some beads are surrounded by a higher concentration of BAI1 staining (h1570) than surrounding plasma membrane (see bead at convergence of cross hairs). In addition, XZ and YZ orthogonal slices reveal BAI1 immunoreactivity surrounding a bead, consistent with its engulfment. Scale bars: A=25μm, C=20μm, D=15μm.

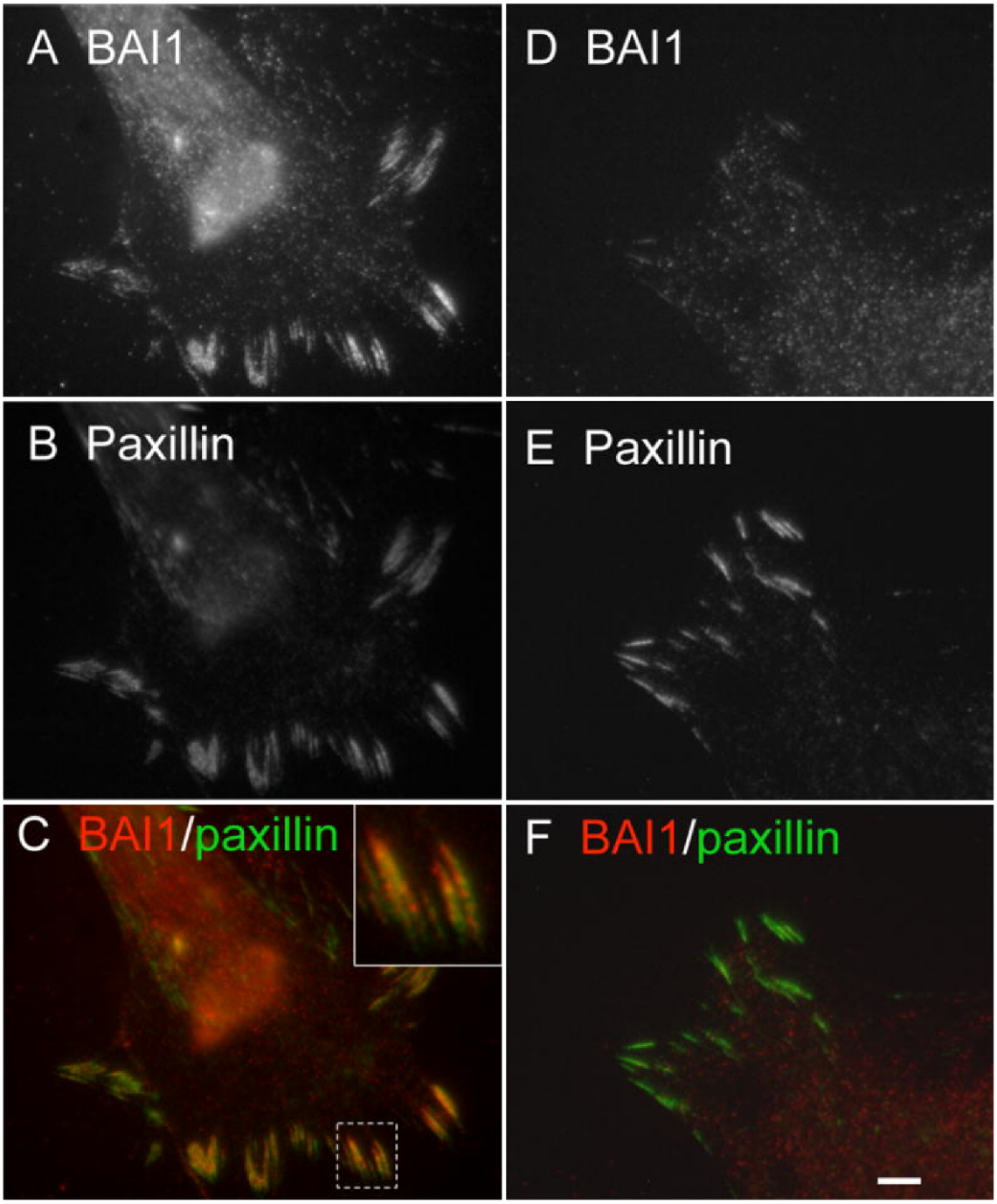
A BAI1
D BAI1
B Paxillin
E Paxillin
C BAI1/paxillin
F BAI1/paxillin

Figure 5

Figure 5: BAI1 is expressed in cultured astrocytes in two distinct patterns, membrane puncta and focal adhesions. (A-C) Some cells show prominent focal adhesion BAI1 localization, demonstrated by colocalization with paxillin, as well as membrane puncta not colocalized with paxillin. (D-F) Other cells show a predominant membrane punctate labeling with little focal adhesion localization. Scale bar=5μm.

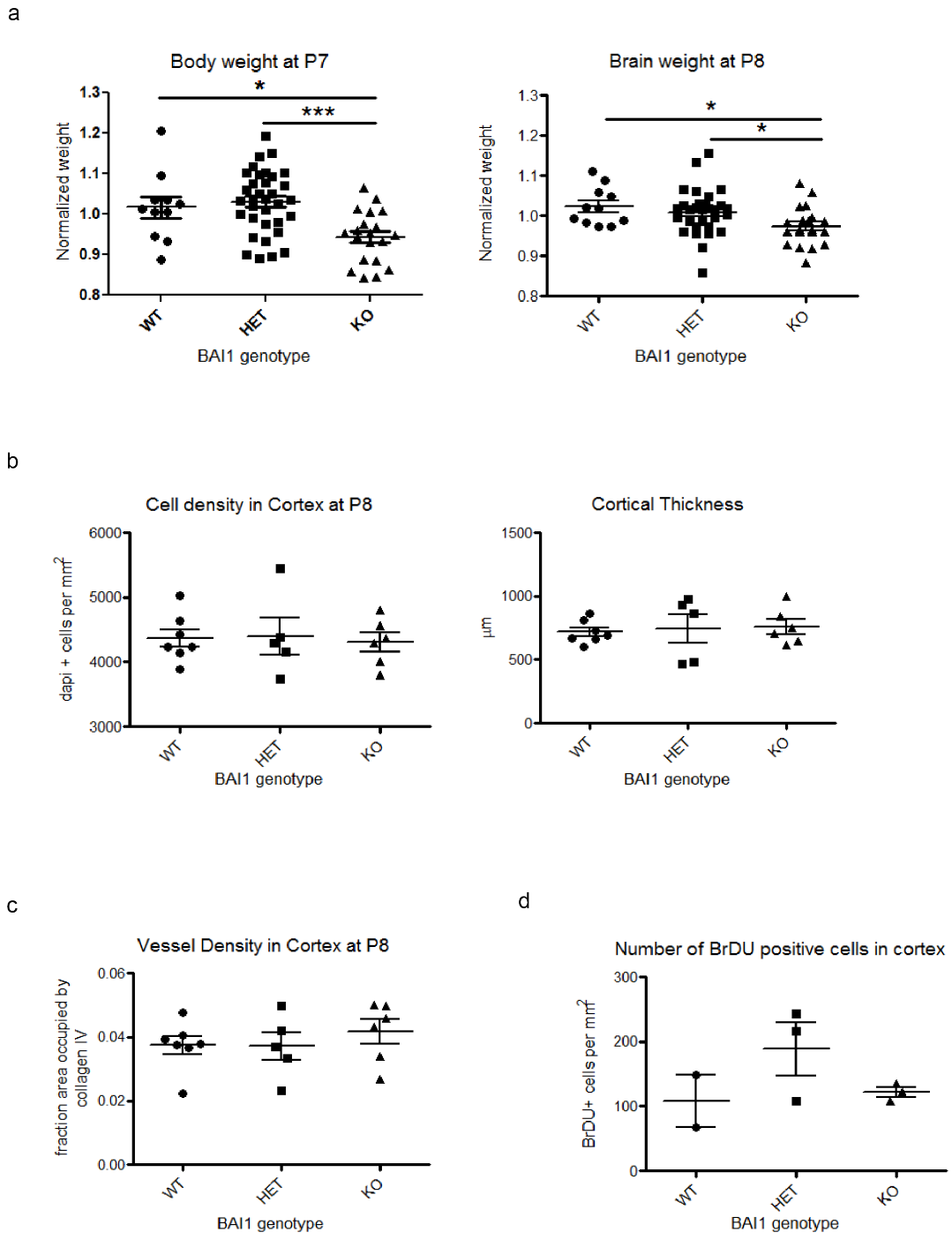
a
Body weight at P7
Normalized weight
BAI1 genotype
WT
HET
KO
Brain weight at P8
b
Cell density in Cortex at P8
dapi + cells per mm2
Cortical Thickness
µm
c
Vessel Density in Cortex at P8
fraction area occupied by collagen IV
d
Number of BrDU positive cells in cortex
BrDU+ cells per mm2

Figure 6

Figure 6: Analysis of postnatal BAI1-deficient mice. We used BAI1-knockout (KO), BAI-heterozygous (HET) and wild type (WT) animals. Body weight was measured at P7 and the brain weight and analyses were done at P8. We found that BAI1 knockout mice were smaller and had smaller brains than wild type and heterozygous mice (A). The cell density of the cortex was assessed by counting the number of DAPI positive cells per area and the cortical thickness was measured dorsal to the hippocampus from the callosum to the surface of the cortex (B). Vessel density was assessed by quantifying the fraction of area occupied by collagen IV staining in the cortex (C). Animals were injected with BrDU 24 prior to tissue harvest, and the number of BrDU positive cell bodies in the cortex with was counted. The number of BrDU-positive cells per area was calculated (D). We found BAI1 genotype had no effect on cellularity, vessel density or neuronal proliferation. Each data point represents one animal. (A,B) One-way ANOVA, *$p<.05$, ***$p<.001$.

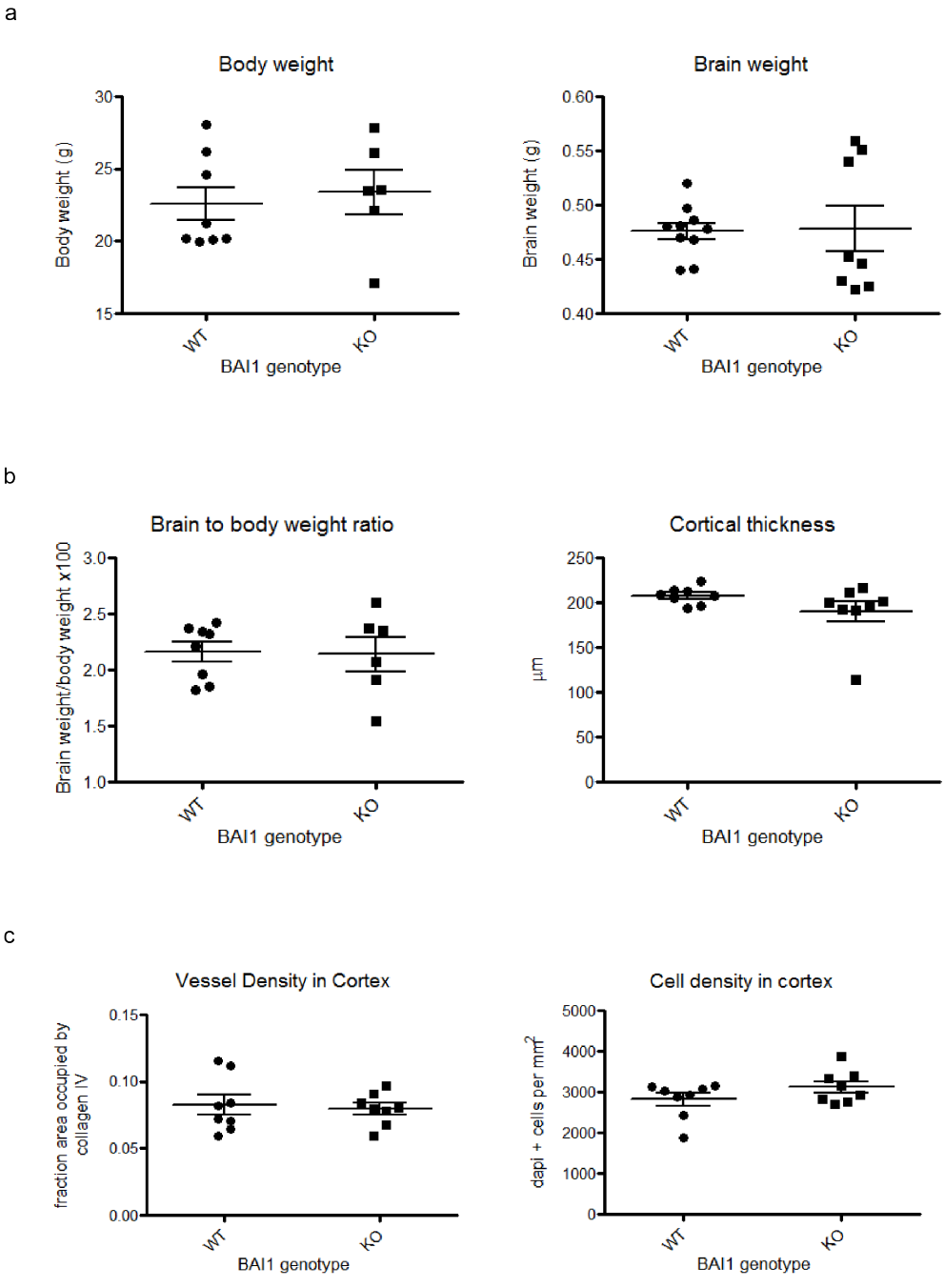
a
Body weight
Body weight (g)
30
25
20
15
WT
KO
BAI1 genotype
Brain weight
Brain weight (g)
0.60
0.55
0.50
0.45
0.40
WT
KO
BAI1 genotype
b
Brain to body weight ratio
Brain weight/body weight x100
3.0
2.5
2.0
1.5
1.0
WT
KO
BAI1 genotype
Cortical thickness
µm
250
200
150
100
50
0
WT
KO
BAI1 genotype
c
Vessel Density in Cortex
fraction area occupied by collagen IV
0.15
0.10
0.05
0.00
WT
KO
BAI1 genotype
Cell density in cortex
dapi + cells per mm2
5000
4000
3000
2000
1000
0
WT
KO
BAI1 genotype

Figure 7

Figure 7: Analysis of adult BAI1-deficient mice. Body and brain weight was measured at 10-12 weeks (A). The brain to body weight ratio was calculated by dividing brain weight by body weight and the cortical thickness was measured dorsal to the hippocampus from the callosum to the surface of the cortex (B). Vessel density was assessed by quantifying the fraction of area occupied by collagen IV staining in the cortex and the cell density of the cortex was assessed by counting the number of DAPI positive cells per area (C). Comparing wild type versus BAI1-knockout animals, we found no differences in any of these measures.

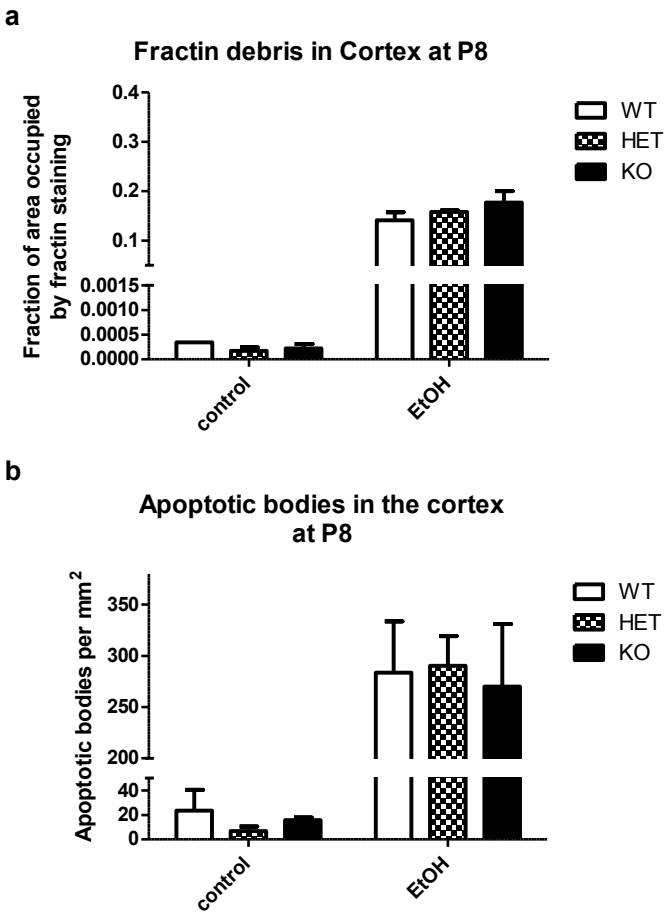
a
Fractin debris in Cortex at P8
Fraction of area occupied by fractin staining
0.4
0.3
0.2
0.1
0.0015
0.0010
0.0005
0.0000
control
EtOH
WT
HET
KO
b
Apoptotic bodies in the cortex at P8
Apoptotic bodies per mm2
350
300
250
200
40
20
0
control
EtOH
WT
HET
KO

Figure 8

Figure 8: Analysis of clearance of apoptotic cells after ethanol-induced apoptosis. We used BAI1-knockout (KO), BAI-heterozygous (HET) and wild type (WT) animals. Animals were injected at P7 with ethanol (EtOH) or saline as a control. Brain tissue was collected 24 hours later and stained for fractin (A) or CC3 (B). Images were taken in the cortex, and cell profiler was used to calculate the fraction of the area that was occupied by staining. For apoptotic body counts, the number of CC3-positive bodies was counted in 3 fields per animal and averaged. Data was graphed as the number of bodies per area (b). BAI1 genotype had no effect on the quantity of apoptotic debris observed.

a

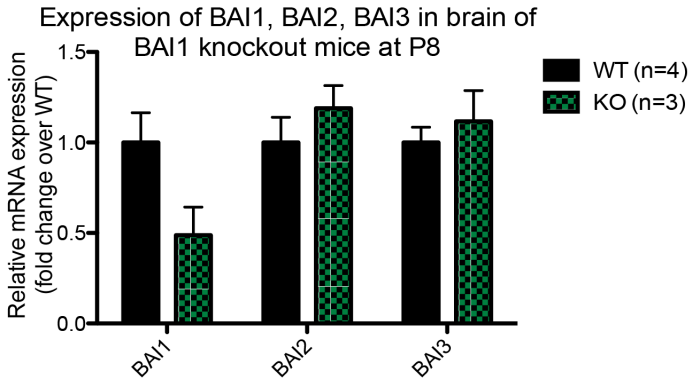
Expression of BAI1, BAI2, BAI3 in brain of BAI1 knockout mice at P8
Relative mRNA expression (fold change over WT)
1.5
1.0
0.5
0.0
BAI1
BAI2
BAI3
WT (n=4)
KO (n=3)

b

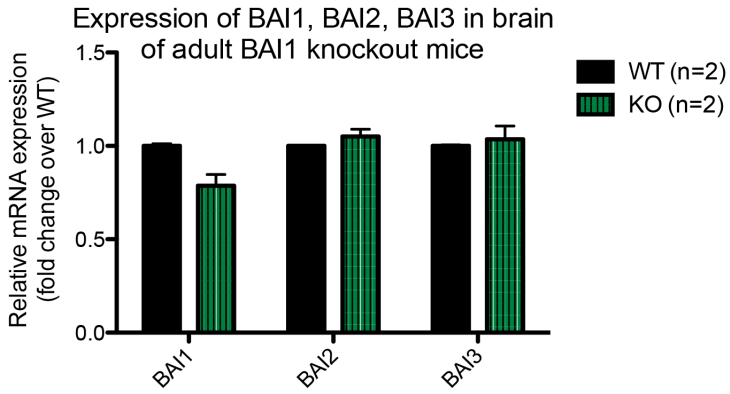
Expression of BAI1, BAI2, BAI3 in brain of adult BAI1 knockout mice
Relative mRNA expression (fold change over WT)
1.5
1.0
0.5
0.0
BAI1
BAI2
BAI3
WT (n=2)
KO (n=2)

Figure 9

Figure 9: BAI-family protein expression in BAI1-deficient mice. We harvested RNA from the brain of BAI1-knockout (KO) and wild type mice. Expression of BAI1, BAI2, and BAI3 mRNA was assessed via quantitative PCR. Analysis was done in P8 brain (A) and adult brain (B). We did not use many mice, which may explain why we did not detect any statistically significant differences in BAI1 expression in the wild type versus the knockout. We did not detect any compensatory upregulation of BAI2 or BAI3 in the BAI1 knockout mice.

a

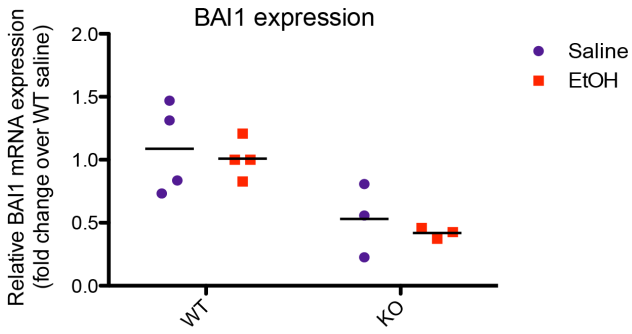
BAI1 expression
Relative BAI1 mRNA expression
(fold change over WT saline)
2.0
1.5
1.0
0.5
0.0
WT
KO
Saline
EtOH

b

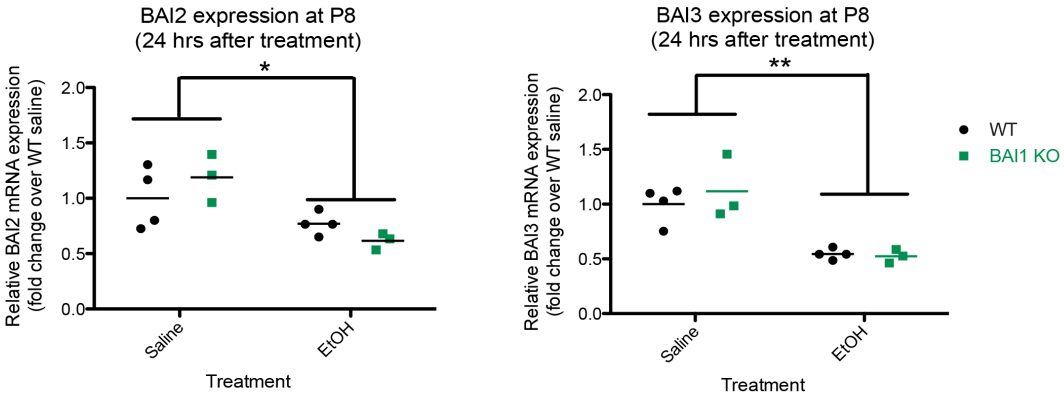
BAI2 expression at P8
(24 hrs after treatment)
*
Relative BAI2 mRNA expression
(fold change over WT saline)
2.0
1.5
1.0
0.5
0.0
Saline
EtOH
Treatment
BAI3 expression at P8
(24 hrs after treatment)
**
Relative BAI3 mRNA expression
(fold change over WT saline)
2.0
1.5
1.0
0.5
0.0
Saline
EtOH
Treatment
WT
BAI1 KO

Figure 10

Figure 10: BAI-family protein expression after ethanol-induced apoptosis. Animals were injected at P7 with ethanol (EtOH) or saline as a control. RNA was isolated from the brain and expression of BAI1 mRNA was assessed via quantitative PCR (A). Expression of BAI2, and BAI3 mRNA after ethanol injury was also quantified (B). We did not detect a change in BAI1 expression after injury, but BAI2 and BAI3 were downregulated after injury in both wild type and BAI1-knockout animals. Each data point represents one animal. (B-C) 2-way ANOVA, *p<.05, **p<01.

THOUGHTS AND FUTURE DIRECTIONS

What does our data add to the bigger picture? What are the remaining questions? What studies would we do next?

Apoptotic pathways and axon degeneration

We show that caspase-mediated cleavage of axonal cytoskeletal elements occurs in response to apoptosis and during developmental pruning. But does this cytoskeletal degradation actually underlie the ultimate axon degeneration? First of all, microtubules provide the highway used to transport factors from the cell body down to the synapse and back. Without this conduit the neuron would be deficient in signaling and trophic feedback. Second, the cytoskeletal system provides the structure that supports and gives the axon wire-like properties. Without the cytoskeleton, the axonal membranes would likely collapse and bleb. Thus it seems reasonable to speculate that disassembly of the cytoskeleton would be a catastrophic event that would lead to axon degeneration.

If cytoskeletal degradation does indeed underlie axon degeneration, it is possible that stabilization of the cytoskeleton could make axons more resistant to degeneration. Expression of caspase-resistant actin and tubulin in neurons could test this. These constructs would be designed to lack the cleavage sites recognized by caspases and thereby be resistant to apoptosis-related degradation. If this makes axons resistant to degeneration, they may be able to recover more effectively after insult.

Another relevant question is whether it is beneficial to try to prevent axon degeneration. When has a neuron passed the threshold from which it can recover? It may not be beneficial to 'rescue' an axon or degenerating neuron if it is non-functional or if it generates harmful activity. This problem is more difficult to address, as it is difficult to truly determine if a neuron is functioning 'correctly' after an insult. Ultimately an *in vivo* experiment with a functional readout is necessary.

If stabilization of the cytoskeleton makes axons more resistant to degeneration, the best way to test whether this rescue provides a benefit may be through studies using peripheral sensory or motor systems. These systems have quantifiable readouts that are directly related to axon function, such as conductance measures and pain thresholds. For example, an animal model of diabetic neuropathy may be a useful and relevant tool to study this question (Sullivan, Hayes et al. 2007). Data suggests that the injury associated with high blood glucose may be dependent on apoptotic pathways (Allen, Yaqoob et al. 2005); therefore caspases and caspase-mediated cleavage of the cytoskeleton may be involved. First we would have to confirm this. Then, we would try inducible, conditional expression of caspase-cleavage resistant actin and tubulin in

sensory neurons. We could test whether these transgenic mice are resistant to axon degeneration and sensory deficits that normally arise due to chronic high blood glucose. This would determine whether cytoskeletal stabilization is a viable treatment option for diabetic neuropathy.

There are many drugs that lead to cytoskeletal stabilization, however, they are often very toxic and can do more harm than good. Ironically, many of the microtubule stabilizing agents used in chemotherapy actually *cause* neuropathies (Jaggi, Singh 2012). An advantage of our proposed approach is that it could prevent disassembly in the context of caspase activity, but otherwise microtubule dynamics should still be intact as far as we know. We have not ruled out the possibility that caspase-cleavage of actin or tubulin could play a role in non-apoptotic cytoskeletal dynamics. However, we do not see any fractin or cleaved tubulin in normal brain (other than in neurons undergoing apoptosis such as during development and during turnover of olfactory sensory neurons).

That being said, it is possible that caspases could cleave actin and tubulin under non-apoptotic conditions in other contexts. Many interesting studies have suggested that caspases have non-apoptotic functions, including during megakarypoeisis (Kozuma, Yuki et al. 2009), microglial activation (Burguillos, Deierborg et al. 2011), and muscle differentiation (Fernando, Kelly et al. 2002), to name a few. As far as we know, caspase-substrates could be cleaved in these contexts, and actin and tubulin could be targets of the activated caspases.

Ultimately, if caspases have important homeostatic functions in other systems, caspase inhibitors may not be a viable treatment option to prevent axon degeneration. On the other hand, it may take ground-breaking research, but imagine if we could use a form of gene therapy to instill selected caspase-resistant proteins into neurons, thereby increasing their resistance to degeneration.

Apoptotic cell clearance and the 'immune response' to ethanol-induced injury

We show that acute ethanol-induced injury involves not only apoptosis but also immune responses. What do we mean when we say 'immune response'? While it may seem like a flippant question, different perspectives lead to different notions of what constitutes an immune response. Is the immune response 'good' or bad'? Ultimately functional readouts are necessary to determine whether the immune reaction has a beneficial or detrimental effect.

Some would define 'immune response' as permeation of immune cells, and look for lymphocytic infiltration in the parenchyma. However, the brain is full of immune cells during normal conditions. Microglia are often called the 'macrophages of the brain', and are distributed relatively ubiquitously by the first two postnatal weeks in mice (Alliot, Godin et al. 1999). Microglia are capable of macrophage functions such as phagocytosis and antigen presentation, and perform constant surveillance throughout the parenchyma.

Some would define an 'immune response' as the response to a foreign pathogen or injury. However the immune system does not merely function to fight off invaders

or respond to injury. Microglia, astrocytes, and other immune cells constantly perform homeostatic functions that could be considered immune-related, such as phagocytic clearance of apoptotic cells and clearance of debris, in the absence of pathogens or injury.

Measurements of 'inflammatory factors' are often used to identify an 'immune response.' Cytokines are important in immune signaling and changes in cytokine production are often taken to mean 'immune activation' or suppression. However, this is also too simplistic, as cytokine signaling has been shown to be important for more than just immune responses. For example, chemokine receptors have been shown to modulate neuronal migration and axon pathfinding during development (Stumm, Hollt 2007).

Ultimately, there are multiple ways to define an immune response, and multiple measures to characterize it. We argue that ethanol-induced apoptosis involves an immune response because a) there is a change in microglial activity that leads to altered morphology and phagocytosis of apoptotic cells b) we detect changes in production of cytokines, c) we show that fractalkine (a cytokine) signaling plays a role in modulating the amount of apoptotic debris and cytokine production after injury. Neuroimmunologists will not be surprised, but the neuroscience community has yet to appreciate that ethanol-induced apoptotic injury involves immune factors.

At face value, our data suggests that fractalkine signaling promotes a 'good' response to ethanol injury. In the absence of fractalkine or CX3CR1, there are more apoptotic neurons and the production of cytokines is exaggerated. There may be such a

thing as a 'good' and 'bad' immune response, but in reality, it is difficult to tease apart exactly what each immune factor orchestrates and which immune factors are a) protective and prevent injury, b) detrimental and worsen damage, or c) reparative (reparative factors could also be (a) or (b)). In order to really determine whether fractalkine signaling is beneficial in ethanol injury, we should have a more functional, behavioral readout.

The behavioral readouts available in mouse pups are limited. Ethanol-treated animals survive this insult but there are no blatant behavioral defects. We attempted behavioral studies using ultrasonic vocalization measurements (Scattoni, Crawley et al. 2009); however these studies are complicated and the scope of our experiments was too broad to pursue this. Still, this may be a viable tool for behavioral analysis after ethanol treatment. Alternatively, waiting until the injured pups are older would allow the use of more classic behavioral studies to measure learning or sensory alterations. If behavioral measures are established, we may be able to determine whether signaling pathways are 'good' or 'bad' for the response to ethanol injury.

Our studies point to the fact that the immune system is a critical factor in injury and suggest fractalkine signaling as a potential target for therapeutic intervention. Ultimately, we only scratch the surface and there is much more to learn about mechanisms underlying neuronal degeneration and clearance.

APPENDIX 1: Characterization of h103 antibody

Our interest in brain-specific angiogenesis inhibitor-1 (BAI1) led us to acquire many antibodies targeted against different epitopes of BAI1. We used many BAI1 antibodies through the course of experiments and have included a table indicating which antibodies appear to be useful for particular applications. While performing immunolocalization studies with an antibody directed to the C-terminus of BAI1 (h103), we unexpectedly found that staining appeared to localize to apoptotic debris and degenerating axons. This antibody allowed much superior visualization of axon degeneration compared to the markers available to us at the time, such as cleaved caspase-3. Another general goal of the lab, separate from studies of BAI1, was to identify markers that would highlight degenerating neurons and their axons; therefore we performed many experiments to characterize h103 staining. We used *in vivo* ethanol-induced apoptosis and *in vitro* NGF-deprivation induced apoptosis and showed that h103 staining was downstream of the apoptotic cascade and that caspases were sufficient to generate the epitope recognized by h103. Eventually we concluded that the apoptosis-related epitope was not BAI1, but we have yet to determine its identity. Future experiments would aim to identify the apoptosis-related epitope via pull-down and mass spectrometry.

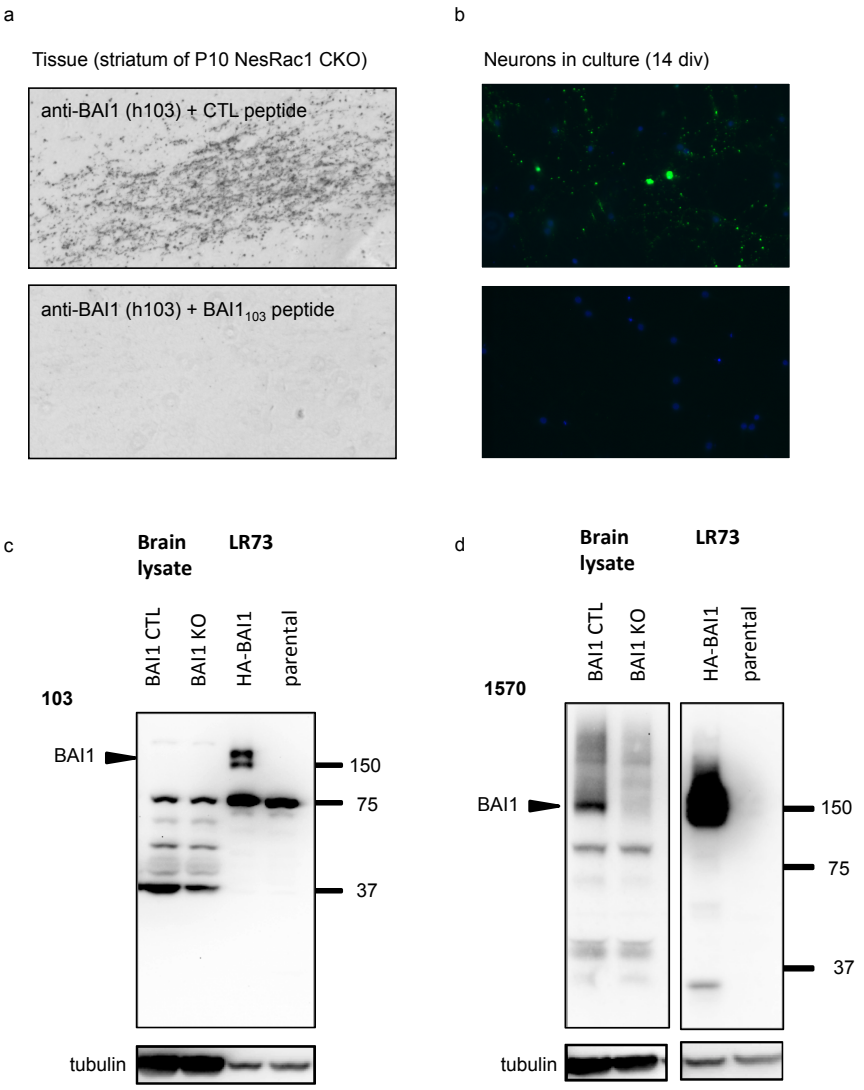
a
Tissue (striatum of P10 NesRac1 CKO)
anti-BAI1 (h103) + CTL peptide
anti-BAI1 (h103) + BAI1103 peptide
b
Neurons in culture (14 div)
c
Brain lysate
LR73
BAI1 CTL
BAI1 KO
HA-BAI1
parental
103
BAI1
150
75
37
tubulin
d
Brain lysate
LR73
BAI1 CTL
BAI1 KO
HA-BAI1
parental
1570
BAI1
150
75
37
tubulin

Figure 1

Figure 1: Peptide competition control and western blot show h103 binds the immunizing peptide and BAI1. The h103 antibody was preincubated with 20 times molar excess of either a control (CTL) peptide or the immunizing peptide and then used to stain tissue (a) or cultured degenerating neurons (b). Preincubation with the immunizing peptide prevented staining. Western blots show that h103 (103) is not sensitive enough to detect BAI1 in brain lysate, but does specifically detect BAI1 in LR73 cells stably expressing BAI1 (HA-BAI1) and not the parental cell line (c) (filled arrow indicates the expected BAI1 band). This is in contrast to another BAI1 antibody (1570), which is able to detect BAI1 in brain lysate from wild type, but not knockout animals (d). This shows that h103 does bind BAI1, albeit at a lower affinity than the 1570 antibody.

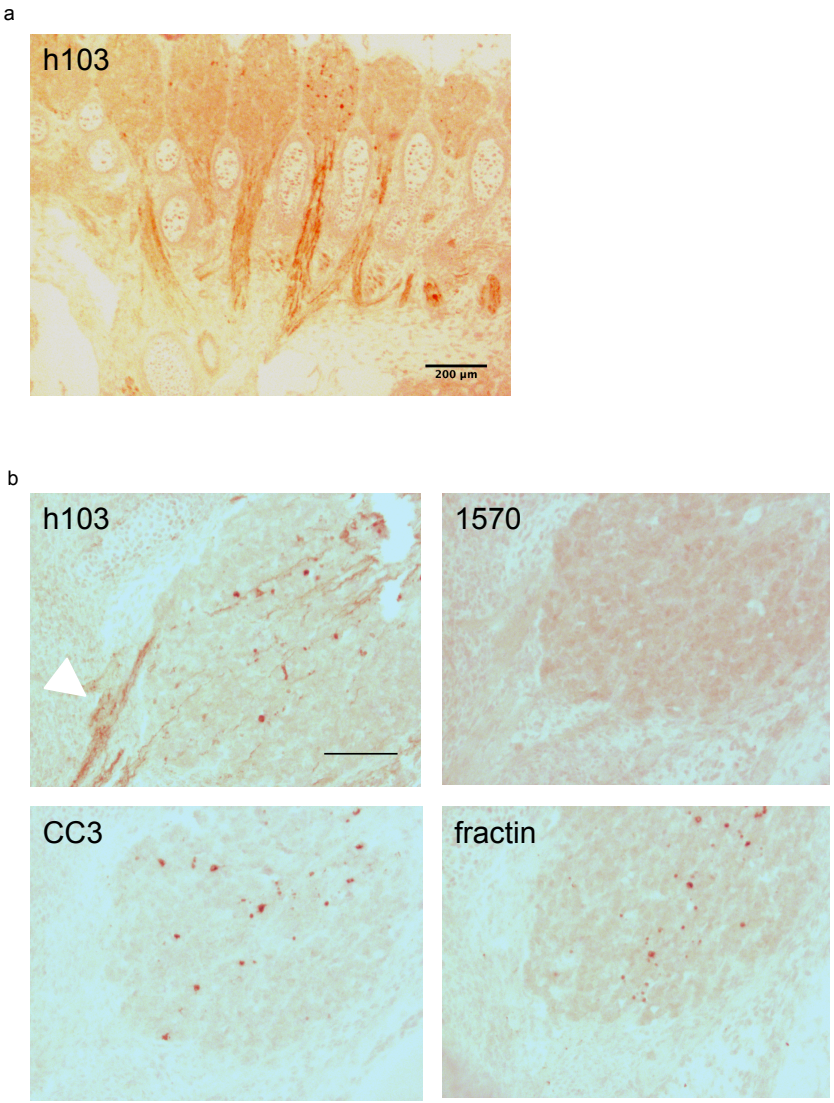

Figure 2

Figure 2: Axons undergoing developmental pruning are highlighted by h103. Immunostaining of sections from an E14.5 embryo indicate that h103 highlights neurons and their processes emanating from dorsal root ganglia (a). Adjacent sections from the trigeminal ganglion were stained for h103, 1570 (a different BAI1 antibody), cleaved caspase-3 (CC3) and fractin (caspase-cleaved actin). CC3 and fractin staining indicate that developmental apoptosis is occurring. The degenerating axons emanating from the ganglion are most effectively highlighted with h103 (arrowhead). Staining with 1570 does not match the pattern seen with h103. This hints that h103 and h1570 bind different proteins, and the h103 may preferentially label degenerating neurons. Scale in (a) is 200μm. Scale in (b) is 50μm.

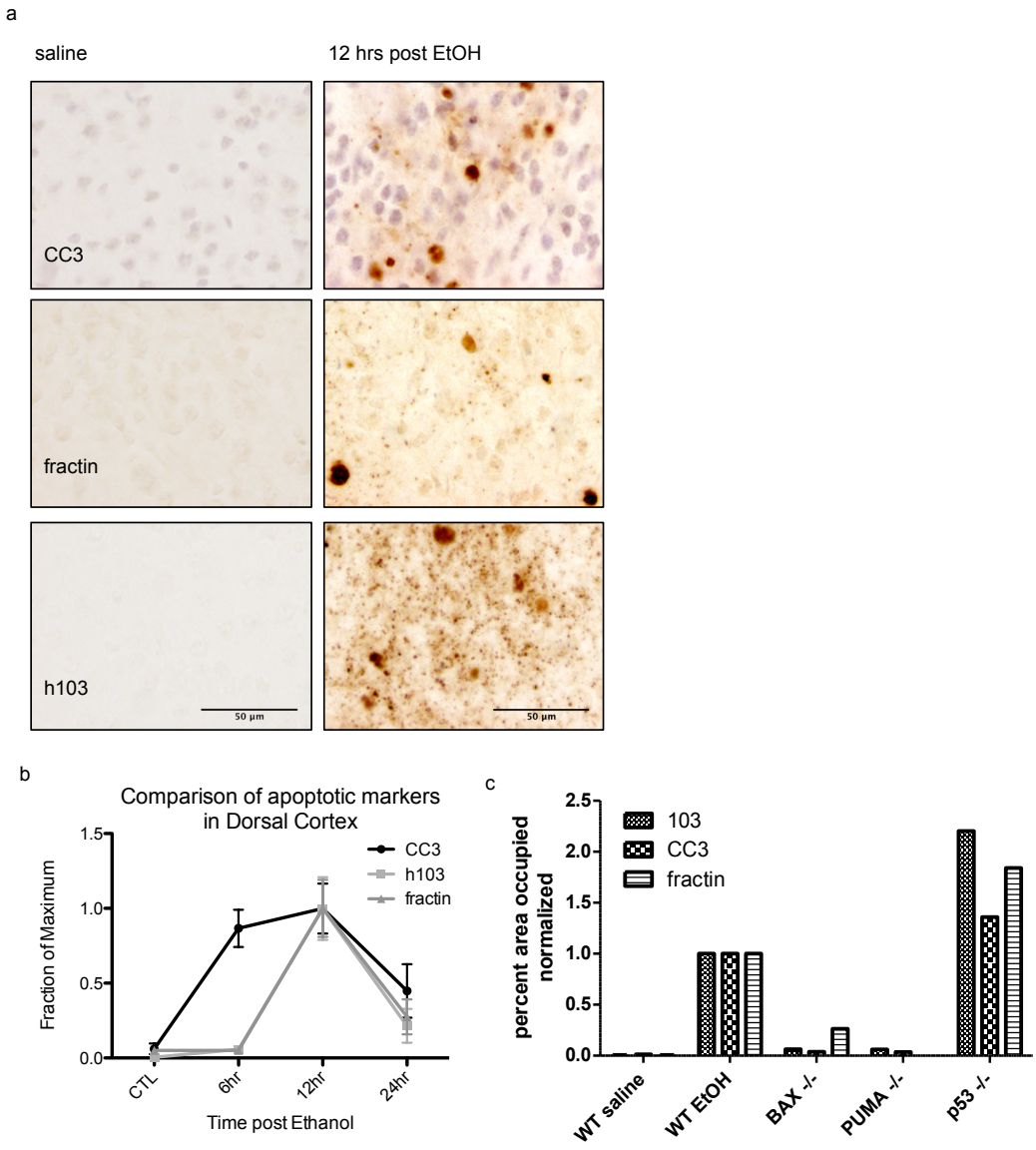
a
saline
12 hrs post EtOH
CC3
fractin
h103
50 µm
50 µm
b
Comparison of apoptotic markers in Dorsal Cortex
Fraction of Maximum
1.5
1.0
0.5
0.0
CC3
h103
fractin
CTL
6hr
12hr
24hr
Time post Ethanol
c
percent area occupied normalized
2.5
2.0
1.5
1.0
0.5
0.0
103
CC3
fractin
WT saline
WT EtOH
BAX -/-
PUMA -/-
p53 -/-

Figure 3

Figure 3: Induction of apoptosis leads to generation of the epitope labeled by the h103 antibody, which highlights degenerating neurons. Ethanol (EtOH) was injected (15.9uL/g of a 20% solution in normal saline) into pups two times, 2 hours apart in order to induce neuronal apoptosis or saline was used as a control. This led to staining with CC3, fractin and h103, indicating that h103 staining is induced by apoptosis (a). The time course of h103 staining was compared to CC3 and fractin. Increased CC3 staining preceded h103 and fractin, suggesting that CC3 becomes activated prior to generation of cleaved actin and the h103 epitope (b). PUMA and BAX-deficient pups are protected from ethanol-induced caspase activation, and staining for all the apoptotic markers, including h103, was abrogated in PUMA and BAX-knockout animals. Data for each stain is normalized to wild type ethanol. This suggests that generation of h103 is downstream of the mitochondrial-dependent pathway of apoptosis. Scale= 50μm.

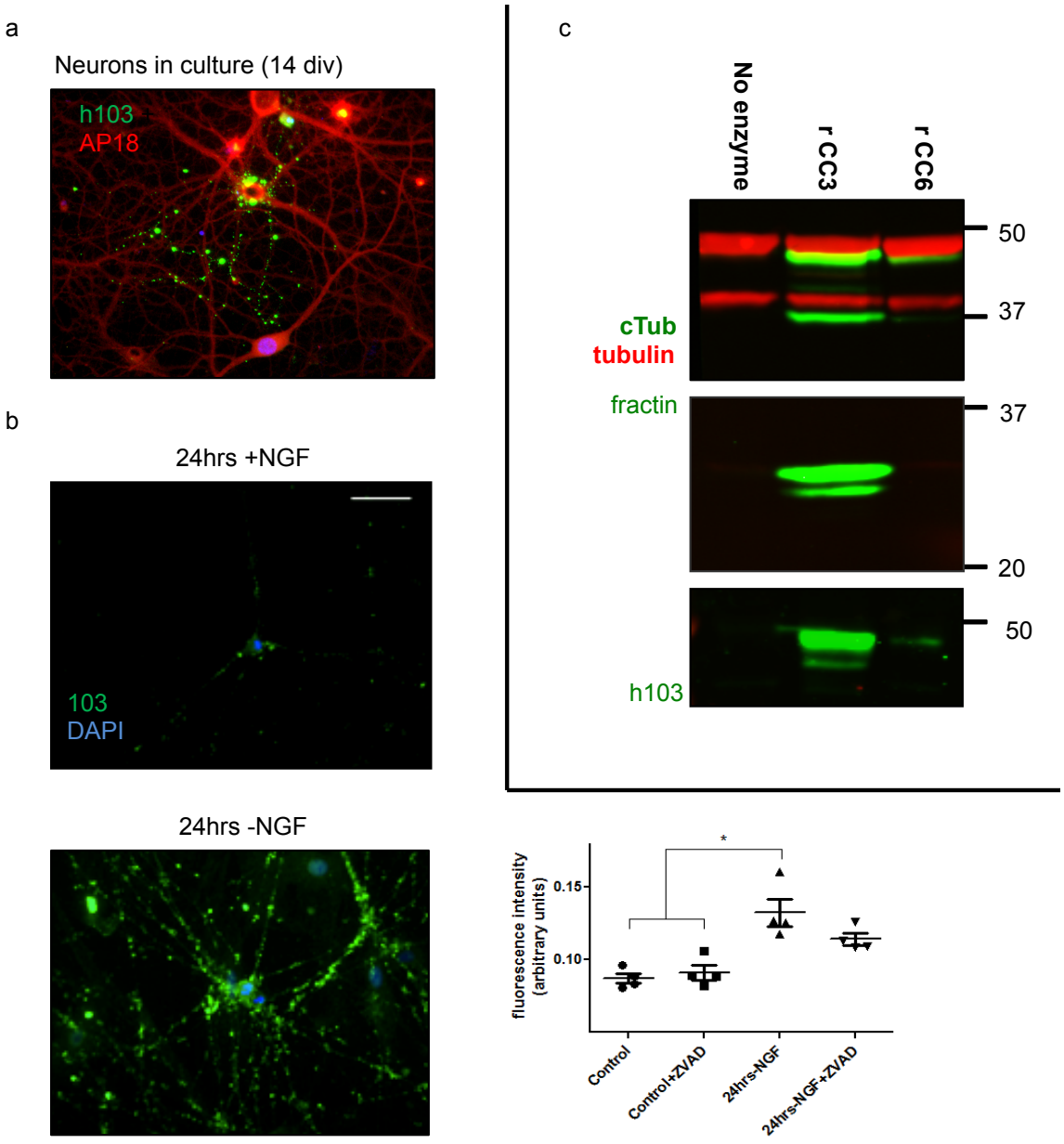
a
Neurons in culture (14 div)
h103
AP18
b
24hrs +NGF
103
DAPI
24hrs -NGF
c
No enzyme
r CC3
r CC6
50
37
cTub
tubulin
fractin
37
20
50
h103
fluorescence intensity
(arbitrary units)
0.15
0.10
*
Control
Control+ZVAD
24hrs-NGF
24hrs-NGF+ZVAD

Figure 4

Figure 4: Degenerating neurites are highlighted by h103 and caspases are sufficient to generate the epitope labeled by h103. Immunofluorescence with h103 highlighted degenerating neurons in aged primary cortical neuron cultures (a). Cultured sympathetic neurons were induced to undergo apoptosis via nerve growth factor deprivation and this led to increased staining with h103 (b). This staining seemed to be decreased when deprivation occurred in the presence of a caspase inhibitor, ZVAD (100μm) but further experiments are required before concluding whether caspase inhibition blocks production of h103. An in vitro enzymatic assay and subsequent western blot indicate that incubation of recombinant activated caspase-3 (rCC3) and activated caspase-6 (rCC6) is sufficient to generate the h103 apoptosis-related epitope (c). Fractin and cleaved tubulin (cTub) are shown as controls. (b) Scale is 50μm. One-way ANOVA with Bonferroni's multiple comparison posttest (n=4) *p<.05.

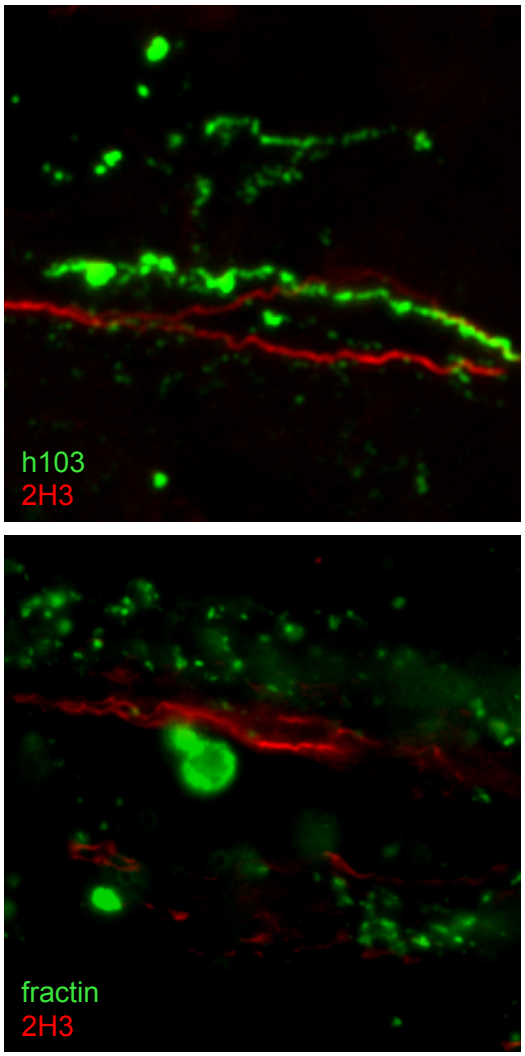

Figure 5

Figure 5: Degenerating neurites are highlighted with h103. Immunostaining of the striatum from ethanol-treated pups shows that both h103 and fractin highlight axon degeneration, but h103 does a superior job of highlighting what appear to be earlier stages in axon degeneration. This is likely early degeneration because many of the axons highlighted by h103 are relatively intact. Like fractin, h103 also highlights punctate debris that likely represents later stages of degeneration.

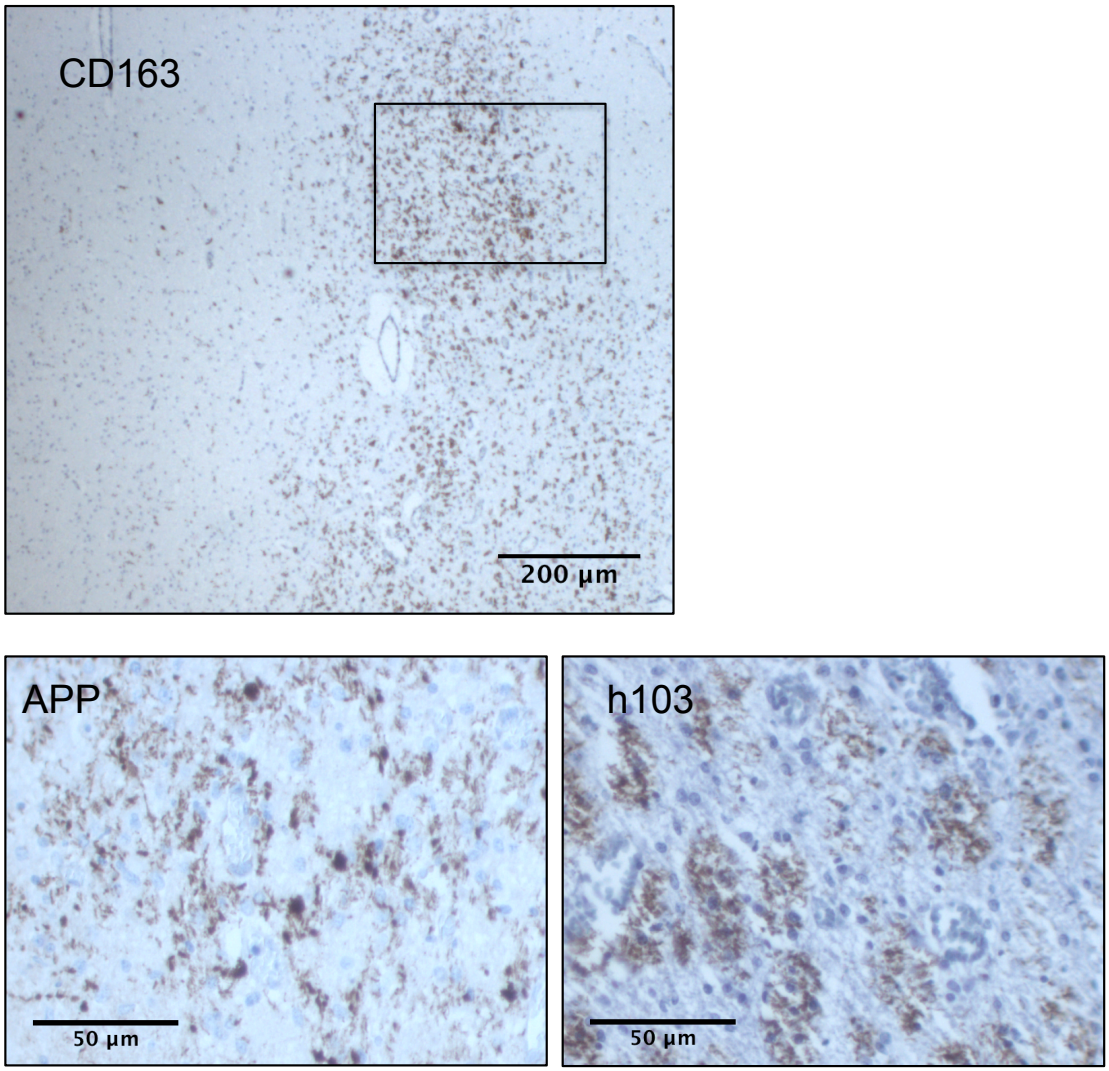

Figure 6

Figure 6: Immunostaining on adjacent sections from neonatal brain shows that h103 highlights acute infarct damage. Area of damage can be identified by infiltration of CD163+ monocytes. Boxed region was used for imaging h103 and APP. APP (amyloid precursor protein) staining is widely used as a marker of axon degeneration. Injured areas were positive for h103 staining, which correlated regionally with APP.

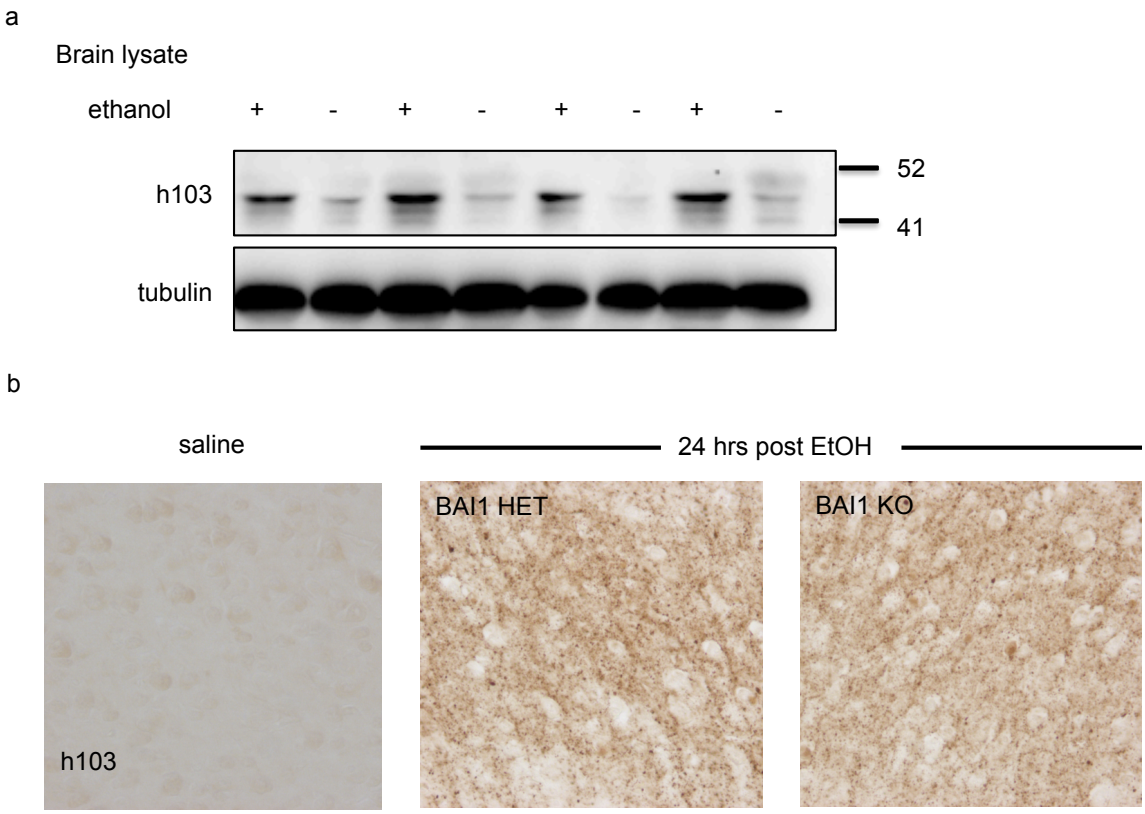
a
Brain lysate
ethanol + - + - + - + -
h103
52
41
tubulin
b
saline
24 hrs post EtOH
h103
BAI1 HET
BAI1 KO

Figure 7

Figure 7: The epitope recognized by h103 that is related to apoptosis is not BAI1. Western blot of brain tissue from control animals or animals treated with ethanol to induce neuronal apoptosis indicate that the apoptosis-related band is not seen at the expected molecular weight for BAI1 (which is 160kDa) (a). Immunostaining after ethanol-induced apoptosis shows increased h103 compared to saline control, but there is no difference in intensity in h103 in BAI1-knockout (KO) brain compared to BAI1-heterozygous brain (BAI1 HET). This suggests that the apoptosis-related staining for h103 is not representing BAI1, but some other neoepitope.

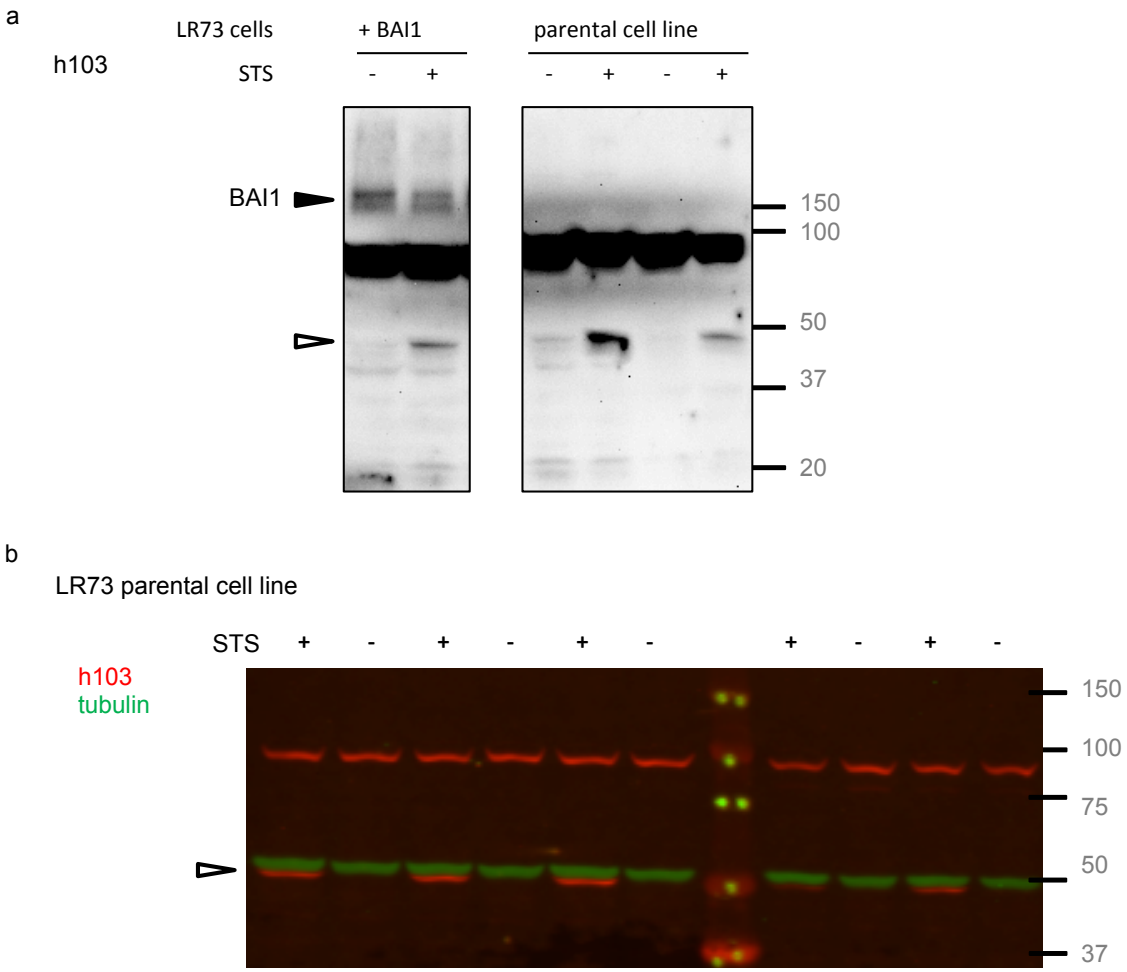
a
h103
LR73 cells
+ BAI1
parental cell line
STS
- + - +
BAI1
150
100
50
37
20
b
LR73 parental cell line
STS + - + - + - + - + -
h103
tubulin
150
100
75
50
37

Figure 8

Figure 8: The epitope recognized by h103 that is related to apoptosis is not BAI1. LR73 cells stably transfected with BAI1 and the parental line were treated with staurosporine (1μm, 3 hours) to induce apoptosis. As expected, h103 detects BAI1 (filled arrow) in the stably transfected cells, but not in the parental cell line. The h103 antibody also detects another apoptosis-related band (open arrow) that is present in both cell lines, including the parental cell line that does not express significant BAI1 (a). This was repeated in the parental cell line with multiple samples (b).

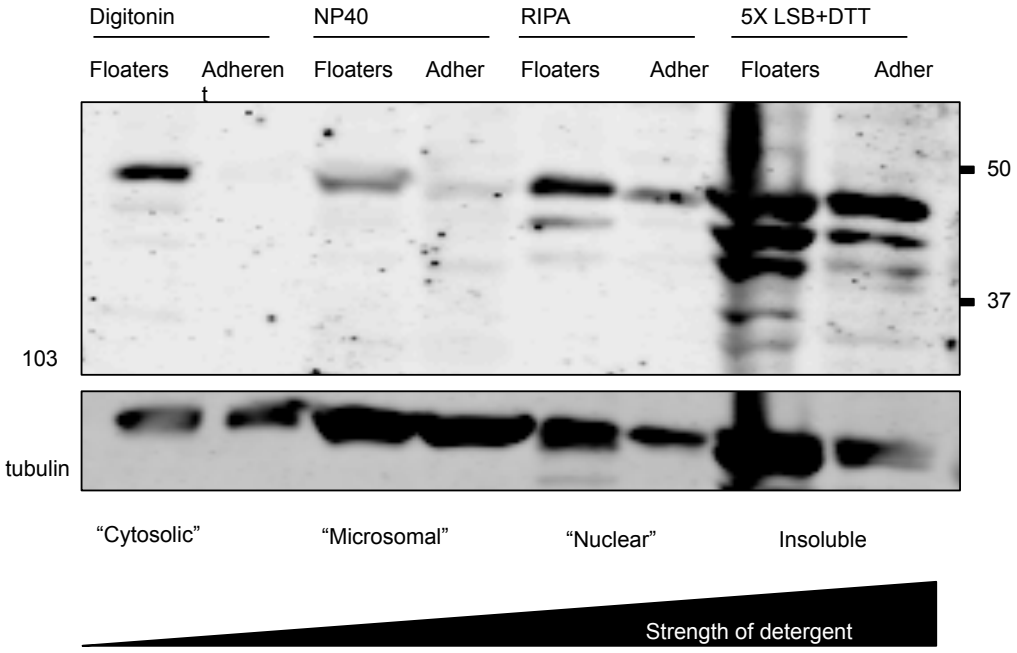
Digitonin
NP40
RIPA
5X LSB+DTT
Floaters
Adherent
Floaters
Adher
Floaters
Adher
Floaters
Adher
50
37
103
tubulin
“Cytosolic”
“Microsomal”
“Nuclear”
Insoluble
Strength of detergent

Figure 9

Figure 9: Fractionation experiments indicate that the h103 antigen can be enriched. LR73 cells were treated with staurosporine (1μm, 3 hours) and the floating cells were collected and lysed and remaining adherent cells were lysed directly on the plate. Sequential fractionation in indicated buffers was performed. This suggests that floating cells lysed in digitonin may be most amenable to pulldown and mass spectrometry.

Table 1: BAI1 antibody screen

Source	Antigen	type	IHC			Western		
			Conc	BAI1	Apo pattern	Conc	BAI1	Apo pattern
Novus h1570	C term	polyclonal	1:500	++	-	1:5000	++	-
Novus h103	N term	polyclonal	1:500	+	++	1:500	+	++
Chemicon/Millipore AB9364	C term	polyclonal	1:50	-	-	1:5000	+	-
Orbigen /Allele ABP-PAB-10421	C term	polyclonal	1:50	+	-	1:5000	+	-
Santa Cruz sc-66815	C term	polyclonal	1:20	-	-	1:400	-	-
Van Meir #14399	N term	polyclonal	1:50	-	-	1:500	-	-
R&D systems MAB4969	N term	monoclonal	1:20	-	-	1:500	-	-
Frederick National Laboratory for Cancer Research	C term Same as h103	monoclonal	Sups neat					
Clone ID:								
1A7				-	-			
1B10				-	-			
1C7				-	-			
1D1				-	-			
1D10				-	-			
1G1				-	-			
2B2				-	-			
3G3				-	-			
4B9				-	-			
4C6				-	-			
5A5				-	-			
5A6				-	-			
5A9				-	-			
5B5				-	-			
5E7				-	-			
5E8				-	-			
5G5				-	-			
5H5				+	-			
6B4				+	-			
6B9				-	-			
6C4				-	-			
6H8				-	-			

Abbreviations: Apo pattern, labeling consistent with recognition of apoptosis-related epitope; C term, carboxy terminus of BAI1; conc, concentration; monoclonal, mouse monoclonal; N term, amino terminus of BAI1; polyclonal, rabbit polyclonal; sups neat, undiluted hybridoma supernatants. (–) indicates no significant signal, (+) indicates some signal, (++) indicates robust signal.

REFERENCES

ALFONSO-LOECHES, S., PASCUAL-LUCAS, M., BLANCO, A.M., SANCHEZ-VERA, I. and GUERRI, C., 2010. Pivotal role of TLR4 receptors in alcohol-induced neuroinflammation and brain damage. *The Journal of neuroscience : the official journal of the Society for Neuroscience,* **30**(24), pp. 8285-8295.

ALLEN, D.A., YAQOOB, M.M. and HARWOOD, S.M., 2005. Mechanisms of high glucose-induced apoptosis and its relationship to diabetic complications. *The Journal of nutritional biochemistry,* **16**(12), pp. 705-713.

ALLIOT, F., GODIN, I. and PESSAC, B., 1999. Microglia derive from progenitors, originating from the yolk sac, and which proliferate in the brain. *Brain research.Developmental brain research,* **117**(2), pp. 145-152.

AWASAKI, T., TATSUMI, R., TAKAHASHI, K., ARAI, K., NAKANISHI, Y., UEDA, R. and ITO, K., 2006. Essential role of the apoptotic cell engulfment genes draper and ced-6 in programmed axon pruning during Drosophila metamorphosis. *Neuron,* **50**(6), pp. 855-867.

BAZAN, J.F., BACON, K.B., HARDIMAN, G., WANG, W., SOO, K., ROSSI, D., GREAVES, D.R., ZLOTNIK, A. and SCHALL, T.J., 1997. A new class of membrane-bound chemokine with a CX3C motif. *Nature,* **385**(6617), pp. 640-644.

BEROD, A., HARTMAN, B.K. and PUJOL, J.F., 1981. Importance of fixation in immunohistochemistry: use of formaldehyde solutions at variable pH for the localization of tyrosine hydroxylase. *The journal of histochemistry and cytochemistry : official journal of the Histochemistry Society,* **29**(7), pp. 844-850.

BISHOP, D.L., MISGELD, T., WALSH, M.K., GAN, W.B. and LICHTMAN, J.W., 2004. Axon branch removal at developing synapses by axosome shedding. *Neuron,* **44**(4), pp. 651-61.

BLANCO, A.M. and GUERRI, C., 2007. Ethanol intake enhances inflammatory mediators in brain: role of glial cells and TLR4/IL-1RI receptors. *Frontiers in bioscience : a journal and virtual library,* **12**, pp. 2616-2630.

BLASCHKE, A.J., STALEY, K. and CHUN, J., 1996. Widespread programmed cell death in proliferative and postmitotic regions of the fetal cerebral cortex. *Development (Cambridge, England),* **122**(4), pp. 1165-1174.

BRAAK, H., GHEBREMEDHIN, E., RUB, U., BRATZKE, H. and DEL TREDICI, K., 2004. Stages in the development of Parkinson's disease-related pathology. *Cell and tissue research,* **318**(1), pp. 121-134.

BRATTON, D.L. and HENSON, P.M., 2008. Apoptotic cell recognition: will the real phosphatidylserine receptor(s) please stand up? *Current biology : CB,* **18**(2), pp. R76-9.

BURGUILLOS, M.A., DEIERBORG, T., KAVANAGH, E., PERSSON, A., HAJJI, N., GARCIA-QUINTANILLA, A., CANO, J., BRUNDIN, P., ENGLUND, E., VENERO, J.L. and JOSEPH, B., 2011. Caspase signalling controls microglia activation and neurotoxicity. *Nature,* **472**(7343), pp. 319-324.

CHEN, X., SUN, C., CHEN, Q., O'NEILL, F.A., WALSH, D., FANOUS, A.H., CHOWDARI, K.V., NIMGAONKAR, V.L., SCOTT, A., SCHWAB, S.G., WILDENAUER, D.B., CHE, R., TANG, W., SHI, Y., HE, L., LUO, X.J., SU, B., EDWARDS, T.L., ZHAO, Z. and KENDLER, K.S., 2009. Apoptotic engulfment pathway and schizophrenia. *PloS one,* **4**(9), pp. e6875.

COLEMAN, M.L., SAHAI, E.A., YEO, M., BOSCH, M., DEWAR, A. and OLSON, M.F., 2001. Membrane blebbing during apoptosis results from caspase-mediated activation of ROCK I. *Nature cell biology,* **3**(4), pp. 339-345.

COOK, D.N., CHEN, S.C., SULLIVAN, L.M., MANFRA, D.J., WIEKOWSKI, M.T., PROSSER, D.M., VASSILEVA, G. and LIRA, S.A., 2001. Generation and analysis of mice lacking the chemokine fractalkine. *Molecular and cellular biology,* **21**(9), pp. 3159-3165.

CULLEN, S.P., HENRY, C.M., KEARNEY, C.J., LOGUE, S.E., FEOKTISTOVA, M., TYNAN, G.A., LAVELLE, E.C., LEVERKUS, M. and MARTIN, S.J., 2013. Fas/CD95-induced chemokines can serve as "find-me" signals for apoptotic cells. *Molecular cell,* **49**(6), pp. 1034-1048.

CUSACK, C.L., SWAHARI, V., HAMPTON HENLEY, W., MICHAEL RAMSEY, J. and DESHMUKH, M., 2013. Distinct pathways mediate axon degeneration during apoptosis and axon-specific pruning. *Nature communications,* **4**, pp. 1876.

DAVALOS, D., GRUTZENDLER, J., YANG, G., KIM, J.V., ZUO, Y., JUNG, S., LITTMAN, D.R., DUSTIN, M.L. and GAN, W.B., 2005. ATP mediates rapid microglial response to local brain injury in vivo. *Nature neuroscience,* **8**(6), pp. 752-758.

DEGTEREV, A., BOYCE, M. and YUAN, J., 2003. A decade of caspases. *Oncogene,* **22**(53), pp. 8543-8567.

DESHMUKH, M. and JOHNSON, E.M.,Jr, 1997. Programmed cell death in neurons: focus on the pathway of nerve growth factor deprivation-induced death of sympathetic neurons. *Molecular pharmacology,* **51**(6), pp. 897-906.

DOWLING, J.E., 2012. *The retina: an approachable part of the brain.* Rev edn. Cambridge, Mass.: Belknap Press of Harvard University Press.

EARNSHAW, W.C., MARTINS, L.M. and KAUFMANN, S.H., 1999. Mammalian caspases: structure, activation, substrates, and functions during apoptosis. *Annual Review of Biochemistry,* **68**, pp. 383-424.

ELLIOTT, M.R., CHEKENI, F.B., TRAMPONT, P.C., LAZAROWSKI, E.R., KADL, A., WALK, S.F., PARK, D., WOODSON, R.I., OSTANKOVICH, M., SHARMA, P., LYSIAK, J.J., HARDEN, T.K., LEITINGER, N. and RAVICHANDRAN, K.S., 2009. Nucleotides released by apoptotic cells act as a find-me signal to promote phagocytic clearance. *Nature,* **461**(7261), pp. 282-286.

FERNANDEZ-LIZARBE, S., MONTESINOS, J. and GUERRI, C., 2013. Ethanol induces TLR4/TLR2 association, triggering an inflammatory response in microglial cells. *Journal of neurochemistry,* **126**(2), pp. 261-273.

FERNANDEZ-LIZARBE, S., PASCUAL, M. and GUERRI, C., 2009. Critical role of TLR4 response in the activation of microglia induced by ethanol. *Journal of immunology (Baltimore, Md.: 1950),* **183**(7), pp. 4733-4744.

FERNANDO, P., KELLY, J.F., BALAZSI, K., SLACK, R.S. and MEGENEY, L.A., 2002. Caspase 3 activity is required for skeletal muscle differentiation. *Proceedings of the National Academy of Sciences of the United States of America,* **99**(17), pp. 11025-11030.

FINN, J.T., WEIL, M., ARCHER, F., SIMAN, R., SRINIVASAN, A. and RAFF, M.C., 2000. Evidence that Wallerian degeneration and localized axon degeneration induced by local

neurotrophin deprivation do not involve caspases. *The Journal of neuroscience : the official journal of the Society for Neuroscience,* **20**(4), pp. 1333-1341.

FOURGEAUD, L. and BOULANGER, L.M., 2007. Synapse remodeling, compliments of the complement system. *Cell,* **131**(6), pp. 1034-1036.

FULLER, A.D. and VAN ELDIK, L.J., 2008. MFG-E8 regulates microglial phagocytosis of apoptotic neurons. *Journal of neuroimmune pharmacology : the official journal of the Society on NeuroImmune Pharmacology,* **3**(4), pp. 246-256.

GEORGE, E.B., GLASS, J.D. and GRIFFIN, J.W., 1995. Axotomy-induced axonal degeneration is mediated by calcium influx through ion-specific channels. *The Journal of neuroscience : the official journal of the Society for Neuroscience,* **15**(10), pp. 6445-6452.

GHOSH, A.P., WALLS, K.C., KLOCKE, B.J., TOMS, R., STRASSER, A. and ROTH, K.A., 2009. The proapoptotic BH3-only, Bcl-2 family member, Puma is critical for acute ethanol-induced neuronal apoptosis. *Journal of neuropathology and experimental neurology,* **68**(7), pp. 747-756.

GOODKIN, H.P., JOSHI, S., MTCHEDLISHVILI, Z., BRAR, J. and KAPUR, J., 2008. Subunit-specific trafficking of GABA(A) receptors during status epilepticus. *The Journal of neuroscience : the official journal of the Society for Neuroscience,* **28**(10), pp. 2527-2538.

GRIFFITHS, M.R., GASQUE, P. and NEAL, J.W., 2009. The multiple roles of the innate immune system in the regulation of apoptosis and inflammation in the brain. *Journal of neuropathology and experimental neurology,* **68**(3), pp. 217-226.

GRONSKI, M.A., KINCHEN, J.M., JUNCADELLA, I.J., FRANC, N.C. and RAVICHANDRAN, K.S., 2009. An essential role for calcium flux in phagocytes for apoptotic

cell engulfment and the anti-inflammatory response. *Cell death and differentiation,* **16**(10), pp. 1323-1331.

HARRIS, J.A., HARDIE, N.A., BERMINGHAM-MCDONOGH, O. and RUBEL, E.W., 2005. Gene expression differences over a critical period of afferent-dependent neuron survival in the mouse auditory brainstem. *The Journal of comparative neurology,* **493**(3), pp. 460-474.

HARRISON, J.K., JIANG, Y., CHEN, S., XIA, Y., MACIEJEWSKI, D., MCNAMARA, R.K., STREIT, W.J., SALAFRANCA, M.N., ADHIKARI, S., THOMPSON, D.A., BOTTI, P., BACON, K.B. and FENG, L., 1998. Role for neuronally derived fractalkine in mediating interactions between neurons and CX3CR1-expressing microglia. *Proceedings of the National Academy of Sciences of the United States of America,* **95**(18), pp. 10896-10901.

HEFFRON, D.S. and MANDELL, J.W., 2005. Opposing roles of ERK and p38 MAP kinases in FGF2-induced astroglial process extension. *Molecular and cellular neurosciences,* **28**(4), pp. 779-790.

HOCHREITER-HUFFORD, A.E., LEE, C.S., KINCHEN, J.M., SOKOLOWSKI, J.D., ARANDJELOVIC, S., CALL, J.A., KLIBANOV, A.L., YAN, Z., MANDELL, J.W. and RAVICHANDRAN, K.S., 2013. Phosphatidylserine receptor BAI1 and apoptotic cells as new promoters of myoblast fusion. *Nature,* **497**(7448), pp. 263-267.

HOOPFER, E.D., MCLAUGHLIN, T., WATTS, R.J., SCHULDINER, O., O'LEARY, D.D. and LUO, L., 2006. Wlds protection distinguishes axon degeneration following injury from naturally occurring developmental pruning. *Neuron,* **50**(6), pp. 883-895.

HOSHIKO, M., ARNOUX, I., AVIGNONE, E., YAMAMOTO, N. and AUDINAT, E., 2012. Deficiency of the microglial receptor CX3CR1 impairs postnatal functional development of

thalamocortical synapses in the barrel cortex. *The Journal of neuroscience : the official journal of the Society for Neuroscience,* **32**(43), pp. 15106-15111.

HSIEH, C.L., KOIKE, M., SPUSTA, S.C., NIEMI, E.C., YENARI, M., NAKAMURA, M.C. and SEAMAN, W.E., 2009. A role for TREM2 ligands in the phagocytosis of apoptotic neuronal cells by microglia. *Journal of neurochemistry,* **109**(4), pp. 1144-1156.

IKONOMIDOU, C., BITTIGAU, P., ISHIMARU, M.J., WOZNIAK, D.F., KOCH, C., GENZ, K., PRICE, M.T., STEFOVSKA, V., HORSTER, F., TENKOVA, T., DIKRANIAN, K. and OLNEY, J.W., 2000. Ethanol-induced apoptotic neurodegeneration and fetal alcohol syndrome. *Science (New York, N.Y.),* **287**(5455), pp. 1056-1060.

JAGGI, A.S. and SINGH, N., 2012. Mechanisms in cancer-chemotherapeutic drugs-induced peripheral neuropathy. *Toxicology,* **291**(1-3), pp. 1-9.

JUNG, S., ALIBERTI, J., GRAEMMEL, P., SUNSHINE, M.J., KREUTZBERG, G.W., SHER, A. and LITTMAN, D.R., 2000. Analysis of fractalkine receptor CX(3)CR1 function by targeted deletion and green fluorescent protein reporter gene insertion. *Molecular and cellular biology,* **20**(11), pp. 4106-4114.

KAUR, B., BRAT, D.J., CALKINS, C.C. and VAN MEIR, E.G., 2003. Brain angiogenesis inhibitor 1 is differentially expressed in normal brain and glioblastoma independently of p53 expression. *The American journal of pathology,* **162**(1), pp. 19-27.

KAUR, B., BRAT, D.J., DEVI, N.S. and VAN MEIR, E.G., 2005. Vasculostatin, a proteolytic fragment of brain angiogenesis inhibitor 1, is an antiangiogenic and antitumorigenic factor. *Oncogene,* **24**(22), pp. 3632-3642.

KAUR, B., CORK, S.M., SANDBERG, E.M., DEVI, N.S., ZHANG, Z., KLENOTIC, P.A., FEBBRAIO, M., SHIM, H., MAO, H., TUCKER-BURDEN, C., SILVERSTEIN, R.L., BRAT, D.J., OLSON, J.J. and VAN MEIR, E.G., 2009. Vasculostatin inhibits intracranial glioma growth and negatively regulates in vivo angiogenesis through a CD36-dependent mechanism. *Cancer research,* **69**(3), pp. 1212-1220.

KEE, H.J., AHN, K.Y., CHOI, K.C., WON SONG, J., HEO, T., JUNG, S., KIM, J.K., BAE, C.S. and KIM, K.K., 2004. Expression of brain-specific angiogenesis inhibitor 3 (BAI3) in normal brain and implications for BAI3 in ischemia-induced brain angiogenesis and malignant glioma. *FEBS letters,* **569**(1-3), pp. 307-316.

KEE, H.J., KOH, J.T., KIM, M.Y., AHN, K.Y., KIM, J.K., BAE, C.S., PARK, S.S. and KIM, K.K., 2002. Expression of brain-specific angiogenesis inhibitor 2 (BAI2) in normal and ischemic brain: involvement of BAI2 in the ischemia-induced brain angiogenesis. *Journal of cerebral blood flow and metabolism : official journal of the International Society of Cerebral Blood Flow and Metabolism,* **22**(9), pp. 1054-1067.

KINCHEN, J.M. and RAVICHANDRAN, K.S., 2007. Journey to the grave: signaling events regulating removal of apoptotic cells. *J Cell Sci,* **120**(Pt 13), pp. 2143-9.

KLAIMAN, G., PETZKE, T.L., HAMMOND, J. and LEBLANC, A.C., 2008. Targets of caspase-6 activity in human neurons and Alzheimer disease. *Molecular & cellular proteomics : MCP,* **7**(8), pp. 1541-1555.

KLEIN, M.A., KAESER, P.S., SCHWARZ, P., WEYD, H., XENARIOS, I., ZINKERNAGEL, R.M., CARROLL, M.C., VERBEEK, J.S., BOTTO, M., WALPORT, M.J., MOLINA, H., KALINKE, U., ACHA-ORBEA, H. and AGUZZI, A., 2001. Complement facilitates early prion pathogenesis. *Nature medicine,* **7**(4), pp. 488-492.

KOIZUMI, S., SHIGEMOTO-MOGAMI, Y., NASU-TADA, K., SHINOZAKI, Y., OHSAWA, K., TSUDA, M., JOSHI, B.V., JACOBSON, K.A., KOHSAKA, S. and INOUE, K., 2007. UDP acting at P2Y6 receptors is a mediator of microglial phagocytosis. *Nature,* **446**(7139), pp. 1091-1095.

KOLDAMOVA, R., FITZ, N.F. and LEFTEROV, I., 2010. The role of ATP-binding cassette transporter A1 in Alzheimer's disease and neurodegeneration. *Biochimica et biophysica acta,* .

KOTILINEK, L.A., BACSKAI, B., WESTERMAN, M., KAWARABAYASHI, T., YOUNKIN, L., HYMAN, B.T., YOUNKIN, S. and ASHE, K.H., 2002. Reversible memory loss in a mouse transgenic model of Alzheimer's disease. *The Journal of neuroscience : the official journal of the Society for Neuroscience,* **22**(15), pp. 6331-6335.

KOZUMA, Y., YUKI, S., NINOMIYA, H., NAGASAWA, T. and KOJIMA, H., 2009. Caspase activation is involved in early megakaryocyte differentiation but not in platelet production from megakaryocytes. *Leukemia,* **23**(6), pp. 1080-1086.

KURUVILLA, R., ZWEIFEL, L.S., GLEBOVA, N.O., LONZE, B.E., VALDEZ, G., YE, H. and GINTY, D.D., 2004. A neurotrophin signaling cascade coordinates sympathetic neuron development through differential control of TrkA trafficking and retrograde signaling. *Cell,* **118**(2), pp. 243-255.

LAMPRECHT, M.R., SABATINI, D.M. and CARPENTER, A.E., 2007. CellProfiler: free, versatile software for automated biological image analysis. *BioTechniques,* **42**(1), pp. 71-75.

LEBLANC, A., LIU, H., GOODYER, C., BERGERON, C. and HAMMOND, J., 1999. Caspase-6 role in apoptosis of human neurons, amyloidogenesis, and Alzheimer's disease. *The Journal of biological chemistry,* **274**(33), pp. 23426-23436.

LIRK, P., HALLER, I., COLVIN, H.P., FRAUSCHER, S., KIRCHMAIR, L., GERNER, P. and KLIMASCHEWSKI, L., 2007. In vitro, lidocaine-induced axonal injury is prevented by peripheral inhibition of the p38 mitogen-activated protein kinase, but not by inhibiting caspase activity. *Anesthesia and Analgesia,* **105**(6), pp. 1657-64, table of contents.

LIRK, P., HALLER, I., COLVIN, H.P., LANG, L., TOMASELLI, B., KLIMASCHEWSKI, L. and GERNER, P., 2008. In vitro, inhibition of mitogen-activated protein kinase pathways protects against bupivacaine- and ropivacaine-induced neurotoxicity. *Anesthesia and Analgesia,* **106**(5), pp. 1456-64, table of contents.

LLEO, A., SELMI, C., INVERNIZZI, P., PODDA, M. and GERSHWIN, M.E., 2008. The consequences of apoptosis in autoimmunity. *Journal of Autoimmunity,* **31**(3), pp. 257-262.

LU, Z., ELLIOTT, M.R., CHEN, Y., WALSH, J.T., KLIBANOV, A.L., RAVICHANDRAN, K.S. and KIPNIS, J., 2011. Phagocytic activity of neuronal progenitors regulates adult neurogenesis. *Nature cell biology,* **13**(9), pp. 1076-1083.

MA, M., FERGUSON, T.A., SCHOCH, K.M., LI, J., QIAN, Y., SHOFER, F.S., SAATMAN, K.E. and NEUMAR, R.W., 2013. Calpains mediate axonal cytoskeleton disintegration during Wallerian degeneration. *Neurobiology of disease,* **56**, pp. 34-46.

MACIEJEWSKI-LENOIR, D., CHEN, S., FENG, L., MAKI, R. and BACON, K.B., 1999. Characterization of fractalkine in rat brain cells: migratory and activation signals for CX3CR-1-expressing microglia. *Journal of immunology (Baltimore, Md.: 1950),* **163**(3), pp. 1628-1635.

MADDEN, S.D. and COTTER, T.G., 2008. Cell death in brain development and degeneration: control of caspase expression may be key! *Molecular neurobiology,* **37**(1), pp. 1-6.

MASHIMA, T., NAITO, M. and TSURUO, T., 1999. Caspase-mediated cleavage of cytoskeletal actin plays a positive role in the process of morphological apoptosis. *Oncogene,* **18**(15), pp. 2423-2430.

MEVORACH, D., 2000. Opsonization of apoptotic cells. Implications for uptake and autoimmunity. *Annals of the New York Academy of Sciences,* **926**, pp. 226-235.

MIZUNO, T., KAWANOKUCHI, J., NUMATA, K. and SUZUMURA, A., 2003. Production and neuroprotective functions of fractalkine in the central nervous system. *Brain research,* **979**(1-2), pp. 65-70.

MORI, K., KANEMURA, Y., FUJIKAWA, H., NAKANO, A., IKEMOTO, H., OZAKI, I., MATSUMOTO, T., TAMURA, K., YOKOTA, M. and ARITA, N., 2002. Brain-specific angiogenesis inhibitor 1 (BAI1) is expressed in human cerebral neuronal cells. *Neuroscience research,* **43**(1), pp. 69-74.

MOURET, A., LEPOUSEZ, G., GRAS, J., GABELLEC, M.M. and LLEDO, P.M., 2009. Turnover of newborn olfactory bulb neurons optimizes olfaction. *The Journal of neuroscience : the official journal of the Society for Neuroscience,* **29**(39), pp. 12302-12314.

NIKOLAEV, A., MCLAUGHLIN, T., O'LEARY, D.D. and TESSIER-LAVIGNE, M., 2009. APP binds DR6 to trigger axon pruning and neuron death via distinct caspases. *Nature,* **457**(7232), pp. 981-989.

NODA, M., DOI, Y., LIANG, J., KAWANOKUCHI, J., SONOBE, Y., TAKEUCHI, H., MIZUNO, T. and SUZUMURA, A., 2011. Fractalkine attenuates excito-neurotoxicity via microglial clearance of damaged neurons and antioxidant enzyme heme oxygenase-1 expression. *The Journal of biological chemistry,* **286**(3), pp. 2308-2319.

OLNEY, J.W., TENKOVA, T., DIKRANIAN, K., MUGLIA, L.J., JERMAKOWICZ, W.J., D'SA, C. and ROTH, K.A., 2002. Ethanol-induced caspase-3 activation in the in vivo developing mouse brain. *Neurobiology of disease,* **9**(2), pp. 205-219.

OLNEY, J.W., WOZNIAK, D.F., JEVTOVIC-TODOROVIC, V. and IKONOMIDOU, C., 2001. Glutamate signaling and the fetal alcohol syndrome. *Mental retardation and developmental disabilities research reviews,* **7**(4), pp. 267-275.

PAOLICELLI, R.C., BOLASCO, G., PAGANI, F., MAGGI, L., SCIANNI, M., PANZANELLI, P., GIUSTETTO, M., FERREIRA, T.A., GUIDUCCI, E., DUMAS, L., RAGOZZINO, D. and GROSS, C.T., 2011. Synaptic pruning by microglia is necessary for normal brain development. *Science (New York, N.Y.),* **333**(6048), pp. 1456-1458.

PARK, D., TOSELLO-TRAMPONT, A.C., ELLIOTT, M.R., LU, M., HANEY, L.B., MA, Z., KLIBANOV, A.L., MANDELL, J.W. and RAVICHANDRAN, K.S., 2007. BAI1 is an engulfment receptor for apoptotic cells upstream of the ELMO/Dock180/Rac module. *Nature,* **450**(7168), pp. 430-434.

RANSOHOFF, R.M., LIU, L. and CARDONA, A.E., 2007. Chemokines and chemokine receptors: multipurpose players in neuroinflammation. *International review of neurobiology,* **82**, pp. 187-204.

RAVICHANDRAN, K.S., 2003. "Recruitment signals" from apoptotic cells: invitation to a quiet meal. *Cell,* **113**(7), pp. 817-820.

RAVICHANDRAN, K.S. and LORENZ, U., 2007. Engulfment of apoptotic cells: signals for a good meal. *Nature reviews.Immunology,* **7**(12), pp. 964-974.

ROBERSON, R., KUDDO, T., BENASSOU, I., ABEBE, D. and SPONG, C., 2011. Neuroprotective fractalkine in fetal alcohol syndrome. *American Journal of Obstetrics and Gynecology,* **204**(5), pp. 400.e1-400.e3.

ROSSITER, J.P., ANDERSON, L.L., YANG, F. and COLE, G.M., 2002. Caspase-3 activation and caspase-like proteolytic activity in human perinatal hypoxic-ischemic brain injury. *Acta Neuropathologica,* **103**(1), pp. 66-73.

ROSSITER, J.P., ANDERSON, L.L., YANG, F. and COLE, G.M., 2000. Caspase-cleaved actin (fractin) immunolabelling of Hirano bodies. *Neuropathology and applied neurobiology,* **26**(4), pp. 342-346.

SAXENA, S. and CARONI, P., 2007. Mechanisms of axon degeneration: from development to disease. *Progress in neurobiology,* **83**(3), pp. 174-191.

SCATTONI, M.L., CRAWLEY, J. and RICCERI, L., 2009. Ultrasonic vocalizations: a tool for behavioural phenotyping of mouse models of neurodevelopmental disorders. *Neuroscience and biobehavioral reviews,* **33**(4), pp. 508-515.

SCHAFER, D.P., LEHRMAN, E.K., KAUTZMAN, A.G., KOYAMA, R., MARDINLY, A.R., YAMASAKI, R., RANSOHOFF, R.M., GREENBERG, M.E., BARRES, B.A. and STEVENS, B., 2012. Microglia sculpt postnatal neural circuits in an activity and complement-dependent manner. *Neuron,* **74**(4), pp. 691-705.

SIMON, D.J., WEIMER, R.M., MCLAUGHLIN, T., KALLOP, D., STANGER, K., YANG, J., O'LEARY, D.D., HANNOUSH, R.N. and TESSIER-LAVIGNE, M., 2012. A caspase cascade regulating developmental axon degeneration. *The Journal of neuroscience : the official journal of the Society for Neuroscience,* **32**(49), pp. 17540-17553.

STANILAND, A.A., CLARK, A.K., WODARSKI, R., SASSO, O., MAIONE, F., D'ACQUISTO, F. and MALCANGIO, M., 2010. Reduced inflammatory and neuropathic pain and decreased spinal microglial response in fractalkine receptor (CX3CR1) knockout mice. *Journal of neurochemistry,* **114**(4), pp. 1143-1157.

STEPHAN, A.H., BARRES, B.A. and STEVENS, B., 2012. The complement system: an unexpected role in synaptic pruning during development and disease. *Annual Review of Neuroscience,* **35**, pp. 369-389.

STEVENS, B., ALLEN, N.J., VAZQUEZ, L.E., HOWELL, G.R., CHRISTOPHERSON, K.S., NOURI, N., MICHEVA, K.D., MEHALOW, A.K., HUBERMAN, A.D., STAFFORD, B., SHER, A., LITKE, A.M., LAMBRIS, J.D., SMITH, S.J., JOHN, S.W. and BARRES, B.A., 2007. The classical complement cascade mediates CNS synapse elimination. *Cell,* **131**(6), pp. 1164-1178.

STUMM, R. and HOLLT, V., 2007. CXC chemokine receptor 4 regulates neuronal migration and axonal pathfinding in the developing nervous system: implications for neuronal regeneration in the adult brain. *Journal of Molecular Endocrinology,* **38**(3), pp. 377-382.

SULLIVAN, K.A., HAYES, J.M., WIGGIN, T.D., BACKUS, C., SU OH, S., LENTZ, S.I., BROSIUS, F.,3rd and FELDMAN, E.L., 2007. Mouse models of diabetic neuropathy. *Neurobiology of disease,* **28**(3), pp. 276-285.

TOSELLO-TRAMPONT, A.C., BRUGNERA, E. and RAVICHANDRAN, K.S., 2001. Evidence for a conserved role for CRKII and Rac in engulfment of apoptotic cells. *The Journal of biological chemistry,* **276**(17), pp. 13797-13802.

TRUMAN, L.A., FORD, C.A., PASIKOWSKA, M., POUND, J.D., WILKINSON, S.J., DUMITRIU, I.E., MELVILLE, L., MELROSE, L.A., OGDEN, C.A., NIBBS, R., GRAHAM, G., COMBADIERE, C. and GREGORY, C.D., 2008. CX3CL1/fractalkine is released from apoptotic lymphocytes to stimulate macrophage chemotaxis. *Blood,* **112**(13), pp. 5026-5036.

VANDERHAEGHEN, P. and CHENG, H.J., 2010. Guidance molecules in axon pruning and cell death. *Cold Spring Harbor perspectives in biology,* **2**(6), pp. a001859.

WILLIAMS, D.W., KONDO, S., KRZYZANOWSKA, A., HIROMI, Y. and TRUMAN, J.W., 2006. Local caspase activity directs engulfment of dendrites during pruning. *Nature neuroscience,* **9**(10), pp. 1234-1236.

YANG, F., SUN, X., BEECH, W., TETER, B., WU, S., SIGEL, J., VINTERS, H.V., FRAUTSCHY, S.A. and COLE, G.M., 1998. Antibody to caspase-cleaved actin detects apoptosis in differentiated neuroblastoma and plaque-associated neurons and microglia in Alzheimer's disease. *The American journal of pathology,* **152**(2), pp. 379-389.

YOUNG, C., KLOCKE, B.J., TENKOVA, T., CHOI, J., LABRUYERE, J., QIN, Y.Q., HOLTZMAN, D.M., ROTH, K.A. and OLNEY, J.W., 2003. Ethanol-induced neuronal apoptosis in vivo requires BAX in the developing mouse brain. *Cell death and differentiation,* **10**(10), pp. 1148-1155.

YU, X., LU, N. and ZHOU, Z., 2008. Phagocytic receptor CED-1 initiates a signaling pathway for degrading engulfed apoptotic cells. *PLoS biology,* **6**(3), pp. e61.

ZIMMERMANN, H., 2000. Extracellular metabolism of ATP and other nucleotides. *Naunyn-Schmiedeberg's archives of pharmacology,* **362**(4-5), pp. 299-309.